



Georg-August University of Göttingen
Graduate School of Forest and Agricultural Sciences (GFA)

Recrystallization of pedogenic and biogenic carbonates in soil:

Environmental controls, modelling and relevance for
paleoenvironmental reconstructions and dating

Dissertation to attain the degree
Doctor of Philosophy (Ph.D.) of the Faculty of Agricultural Sciences
Georg-August University of Göttingen

Submitted by
Kazem Zamaniān
Born on February 1981 in Gonabad, Iran

Göttingen, May 2017

Betreuungsausschuss

Prof. Dr. Yakov Kuzyakov

Ökopedologie der Gemäßigten Zonen, Georg-August-Universität Göttingen

Dr. Konstantin Pustovoytov

Institut für Bodenkunde und Standortslehre (310), Universität Hohenheim

Mitglieder der Prfungskommission

1. Referee: Prof. Dr. Yakov Kuzyakov

Ökopedologie der Gemäßigten Zonen, Georg-August-Universität Göttingen

2. Referee: Prof. Dr. Daniela Sauer

Abteilung Physische Geographie, Geographisches Institut, Georg-August-Universität Göttingen

3. Referee: Prof. Dr. Joachim Reitner

Abteilung Geobiologie, Geowissenschaftliches Zentrum, Fakultät für Geowissenschaften und Geographie, Georg-August-Universität Göttingen

Date of oral examination:12.05.2017.....

To Sanaz

My beloved wife

Summary

The reliability of paleoenvironment (paleoclimate, paleovegetation etc.) interpretations and radiocarbon ages based on isotopes of carbon ($\delta^{13}\text{C}$, ^{14}C), oxygen ($\delta^{18}\text{O}$) and clumped isotopes (Δ47) in soil carbonates types e.g. mollusk shells, eggshells, fruit carbonates, rhizolith, nodules, clast coatings etc., depends on the recrystallization degree of these carbonate types after formation and/or embedding in soil. Soil CO_2 concentration and its isotopic composition is in equilibrium with CO_2 respired by roots and organisms. Dissolution of carbonate types in soil solution and further recrystallization re-equilibrate the $\delta^{13}\text{C}$ and $\Delta^{14}\text{C}$ of carbonate types with soil CO_2 . Hence, the $\delta^{13}\text{C}$ in recrystallized carbonate will save fingerprints of dominant vegetation during the recrystallization phase and $\Delta^{14}\text{C}$ will reflect the recrystallization time and most likely $\delta^{18}\text{O}$ as well as Δ47 will record the isotopic composition of oxygen in soil water and the recrystallization temperature, respectively. For example addition of only 5% modern C due to recrystallization to a 45,000-year old bone leads to more than 20,000 years underestimation of the age.

Despite the known effects of recrystallization on paleoenvironmental interpretations and radiocarbon dating, the dynamics of this process and its affecting factors remain poorly understood. This is because of low solubility of calcium carbonate and low recrystallization rates which complicate experimentally assessments. Recently, the sensitive technique of ^{14}C labeling has been shown to help understand the recrystallization process. This technique is based on $^{14}\text{CO}_2$ labeling of the soil atmosphere and subsequent tracing ^{14}C activity in a carbonate sample. ^{14}C labeling approach was used to determine the recrystallization of mollusk shells; one of the most common carbonate types in soils, sediment and cultural layers; under various environmental conditions.

Recrystallization begins soon after embedding of shells in soil and increases exponentially with time. Shell carbonate recrystallization rates ranged between $1.0 \cdot 10^{-3}$ and $1.6 \cdot 10^{-2} \% \text{ day}^{-1}$ depending on environmental conditions such as cation exchange capacity (CEC), presence of geogenic carbonates in soil i.e. loess carbonate and degree of shell fossilization i.e. degradation of organic compounds in shell structure. The recrystallization was one order of magnitude higher in soils with relatively low CEC e.g. sandy soils comparing to loamy soils with higher CEC. Presence of 30% geogenic carbonates intensifies shell carbonate recrystallization up to seven times because geogenic carbonate may also recrystallize and accumulates on shells. Recrystallization in fossils was 1.2 times higher than the fresh specimens due to higher porosity in shell structure and so more surface area contacting soil solution. Furthermore, The full recrystallization (i.e. when the whole shell materials would be recrystallized and the original isotopic signals are vanished completely) for shell particles in of 2-2.5 mm in diameter were determined as about 90 to 770 years depending on presence or absence of geogenic carbonates and fossilization stages.

Zusammenfassung

Die Zuverlässigkeit der Interpretationen von Paläo-Umgebungen (Paläoklimat-, Paläovegetation etc.) und Radiokohlenstoff datierung auf der Basis von Isotopen von Kohlenstoff ($\delta^{13}\text{C}$, ^{14}C), Sauerstoff ($\delta^{18}\text{O}$) und verklumpt Isotopen (Δ47) in Typen der Boden-Karbonat, z.B. Molluskenschalen, Eierschalen, Fruchtcarbonate, Rhizolithen, Knötchen, Clastbeschichtungen etc. hängt vom Umkristallisationsgrad dieser Karbonat-typen nach der Bildung und/oder Einbettung in den Boden ab. Die CO_2 -Konzentration des Bodens und seine Isotopenzusammensetzung liegt im Gleichgewicht mit CO_2 , das durch Wurzeln und Organismen Atmung angeregt wird. Die Auflösung von Karbonat-Typen in der Bodenlösung und die weitere Umkristallisation re-equilibrieren die $\delta^{13}\text{C}$ und $\Delta^{14}\text{C}$ der Karbonat-Typen mit dem Boden CO_2 . Daher wird das $\delta^{13}\text{C}$ in Umkristallisiertem Karbonat während der Umkristallisationsphase Fingerabdrücke dominanter Vegetation erhalten und $\Delta^{14}\text{C}$ wird die Umkristallisationszeit. Höchstwahrscheinlich reflektieren auch $\delta^{18}\text{O}$ bzw. Δ47 die Isotopenzusammensetzung von Sauerstoff in Bodenwasser und die Umkristallisationstemperatur. Zum Beispiel führt die Zugabe von nur 5% modernen C aufgrund der Umkristallisation zu einem 45.000 Jahre alten Knochen zu mehr als 20.000 Jahren Unterbewertung des Alters.

Trotz der bekannten Effekte der Umkristallisation auf Paläoumweltinterpretationen und Radiokohlenstoff-Datierung sind die Dynamik dieses Prozesses und seine beeinflussenden Faktoren schlecht verstanden. Dies liegt an der geringen Löslichkeit von Calciumcarbonat und niedrigen Umkristallisationsraten, die experimentelle Untersuchungen erschweren. In letzter Zeit wurde gezeigt, dass die empfindliche Technik der ^{14}C -Markierung dazu beiträgt, den Umkristallisationsvorgang zu verstehen. Diese Technik basiert auf der $^{14}\text{CO}_2$ -Markierung der Bodenatmosphäre und der nachfolgenden Verfolgung der ^{14}C -Aktivität in einer Karbonat Probe. ^{14}C -Markierungsansatz wurde verwendet, um die Umkristallisation von Molluskenschalen; Einer der häufigsten Karbonat-Typen in Böden, Sedimente und Kulturschichten; Unter verschiedenen Umgebungsbedingungen zu bestimmen.

Die Umkristallisation beginnt bald nach dem Einbetten von Schalen in den Boden und steigt exponentiell mit der Zeit an. Molluskenschalen Umkristallisationsraten reichten zwischen $1,0 \cdot 10^{-3}$ und $1,6 \cdot 10^{-2}\%$ pro Tag je nach Umgebungsbedingungen wie Kationenaustauschkapazität (KAK), Vorhandensein von geogenen Karbonaten im Boden (dh Lösskarbonat) und Grad der Schalenfossilisierung (dh Abbau von organischen Verbindungen in der Schalenstruktur). Die Umkristallisation war um eine Größenordnung höher in Böden mit relativ niedrigem KAK, z.B. Sandige Böden im Vergleich zu lehmigen Böden mit höherer KAK. Die Anwesenheit von 30% geogenen Karbonaten verstärkt die Schalenkarbonat-Umkristallisation bis zu siebenmal, da auch

geogenes Karbonat auch umkristallisieren und sich auf Schalen ansammeln kann. Die Umkristallisation in den Fossilien war 1,2-mal höher als die frischen Proben aufgrund der höheren Porosität in der Schalenstruktur und damit mehr Oberflächenkontaktierung der Bodenlösung. Weiterhin wurde die vollständige Umkristallisation (dh wenn die gesamten Schalenmaterialien umkristallisiert und die ursprünglichen Isotopensignale vollständig verschwunden sind) für Schalenteilchen mit einem Durchmesser von 2-2,5 mm als etwa 90 bis 770 Jahre bestimmt die in Abhängigkeit von der Anwesenheit oder Abwesenheit von geogenen Karbonaten und Schalenfossilisierungsgrad ist.

Acknowledgements

I would like to express my deepest gratitude to my supervisor Prof. Yakov Kuzyakov, for his excellent guidance, caring and patience; who fulfilled my wish by agreeing to write a DFG proposal that eventually funded. I sincerely thank my co-supervisor, Dr. Konstantin Pustovoytov for his constant support during my research and being open to all my questions.

I would like to thank herewith everyone who helped me to fulfill my work and hand in this work as my PhD thesis:

Dr. Manfred Löscher for his kind discussions in the field and his assists in loess sampling.

All the technicians in Department of Soil Science of Temperate Ecosystems, University of Göttingen especially Ingrid Ostermeyer, Karin Schmidt, Martina Gebauer, Anita Kriegel, Susann Enzmann, Heike Strutz as well as Susanne Grube for their support during my stay at University of Göttingen.

Prof. Katharine Huntington, University of Washington for supervising me to learn a new technique (carbonate clumped isotopes) and running a joint project.

Andrew Schauer, IsoLab, University of Washington for fruitful discussions about stable isotopes and kind help to analyze carbonates clumped isotopes.

My dear friends; Dr. Mohsen Zarebanadkouki, Dr. Bahar Razawi, Dr. Shibin Liu and Dr. Landon Burgener for their supports and valuable suggestions during my work.

Finally, I would like to thank specially my parents and my wife who in the first place enabled my scientific education and were always full of encouragement and love.

Table of Contents

Summary	4
Zusammenfassung.....	5
Acknowledgements.....	7
Table of Contents	8
List of Tables.....	11
List of Figures.....	12
Preface.....	15
1. Introduction: Pedogenic carbonates; forms and formation processes.....	18
Published: Earth-Science Reviews 157 (2016): 1-17	18
1.1. Abstract	18
1.2. Inorganic carbon in soil and pedogenic carbonates.....	19
1.2.1. Relevance of soil inorganic carbon.....	19
1.2.2. Soil inorganic carbon: worldwide distribution	20
1.2.3. Soil inorganic carbon pools, classification and definitions.....	21
1.2.4. Pedogenic carbonate within soil inorganic carbon pools and its relevance	22
1.3. Formation of pedogenic carbonate.....	23
1.3.1. General principle of pedogenic carbonate formation.....	23
1.3.2. Formation mechanisms of pedogenic carbonates	24
1.3.3. Morphology of pedogenic carbonates	25
1.3.4. Factors affecting pedogenic carbonate accumulation in soil.....	34
1.3.4.1. Climate.....	34
1.3.4.2. Soil parent material	36
1.3.4.3. Soil properties	37
1.3.4.4. Topography, soil position in the landscape and soil age.....	37
1.3.4.5. Local vegetation and soil organisms	38
1.4. Carbon and oxygen in pedogenic carbonates	39
1.4.1. Sources of carbon, oxygen and calcium in pedogenic carbonates	39
1.4.2. Isotopic composition of carbon ($\delta^{13}\text{C}$, $\Delta^{14}\text{C}$) and oxygen ($\delta^{18}\text{O}$) in pedogenic carbonates	39
1.5. Implications of PC in paleoenvironmental and chronological studies	41

1.6.	Recrystallization of soil carbonates.....	42
1.6.1.	Uncertainties of paleoenvironmental reconstructions based on pedogenic carbonates.....	43
1.6.2.	Evidence of pedogenic carbonate recrystallization after formation	45
1.7.	Conclusions and outlook	46
1.7.1.	Conclusions.....	46
1.8.	Acknowledgements	49
1.9.	References.....	49
2.	Recrystallization of shell carbonate in soil: ^{14}C labeling, modeling and relevance for dating and paleo-reconstructions	62
	Published: Geoderma 282 (2016): 87-95	62
2.1.	Abstract	62
2.2.	Introduction.....	63
2.3.	Material and methods.....	66
2.3.1.	Matrix materials and shells	66
2.3.2.	Experiment setup	67
2.3.3.	Labeling technique and sampling.....	68
2.3.4.	^{14}C analyses	69
2.3.5.	Calculations and statistical analyses	69
2.4.	Results	69
2.5.	Discussion.....	73
2.5.1.	Matrix carbonate recrystallization in loess and carbonate-free soil.....	73
2.5.2.	Recrystallization of shell carbonate	74
2.5.2.1.	Effects of organic compound elimination on shell carbonate recrystallization.....	74
2.5.2.2.	The effect of geogenic carbonate on shell recrystallization	75
2.5.2.3.	The combined effect of organic compounds and geogenic carbonate on shell carbonate recrystallization	76
2.5.3.	Time required for full recrystallization of shell carbonate.....	78
2.5.4.	Significance of the results for archaeology and paleoenvironmental research.....	79
2.6.	Conclusions.....	81
2.7.	Acknowledgement.....	82
2.8.	References.....	82
3.	Cation exchange retards shell carbonate recrystallization: Consequences for dating and paleoenvironmental reconstructions.....	85

Published: Catena 142 (2016): 134-138	85
3.1. Abstract	85
3.2. Introduction.....	86
3.3. Materials and methods	87
3.3.1. Matrix materials	87
3.3.2. Experimental setup and analyses.....	88
3.3.3. Statistics	90
3.3.4. Results	90
3.4. Discussion.....	93
3.5. Conclusion.....	96
3.6. Acknowledgement.....	96
3.7. References.....	96
4. Carbon sources in fruit carbonate of <i>Buglossoides arvensis</i> and consequences for ^{14}C dating.....	99
Published: Radiocarbon 59 (2017): 141-150.....	99
4.1. Abstract	99
4.2. Introduction.....	100
4.3. Material and methods.....	102
4.3.1. Experimental layout	102
4.3.2. Labeling procedure.....	103
4.3.3. ^{14}C analyses	104
4.3.4. Calculation of carbon incorporation into plant organs and age overestimation.....	104
4.3.5. Statistics	106
4.4. Results	106
4.5. Discussion.....	107
4.6. Conclusions.....	110
4.7. Acknowledgements	110
4.8. References.....	111
5. Curriculum Vita.....	113
6. Declaration	116

List of Tables

Table 1: Summary of objectives, the approaches and innovative findings of conducted studies	17
Table 2: Characteristics of the most common pedogenic carbonate features in soils ¹	25
Table 3: Chemical and physical properties of the soil	66
Table 4: Elemental composition of shell carbonates before and after organic compounds elimination by heating at 550 °C.	67
Table 5: Exchangeable cations in sand and soil and cation contents in shells	88
Table 6: Percentage of ¹⁴ C label recovered in different plant organs and soils via photosynthesis (Shoot-labeling) or taken up by roots (Root-labeling). Standard errors are shown in parentheses.	106
Table 7: Amounts of incorporated labeled carbon (mg) in plant organs after shoot or root labeling of Sand- or Loess-grown plants. Standard errors are shown in parentheses.	107

List of Figures

- Figure 1: World SIC distribution in the top meter of soils (USDA-NRCS, 2000) and its correlation with areas of lower mean annual precipitation. The iso-lines of mean annual precipitation (mm) are from (FAO, 1996). Only the iso-lines of precipitation <1000 mm are presented. Note the exponential scale of SIC content. Most SIC is located in areas with precipitation <500 mm and SIC stocks above 32 kg C m^{-2} (320 Mg C ha^{-1}) are located in areas with precipitation <250 mm. 21
- Figure 2: Earthworm biospheroliths. Left: Plain Polarized Light; PPL (Verrecchia, 2011); Right: Cross Polarized Light, XPL (courtesy O. Ehrmann). Earthworm biospheroliths are produced by earthworms' calciferous glands, which release $\sim 0.8 \text{ mg CaCO}_3 \text{ earthworm}^{-1} \text{ day}^{-1}$ (Lambkin et al., 2011). The thin section of biospherolith (right) is kindly provided by Dr. Otto Ehrmann (Bildarchiv Boden, <http://www.bildarchiv-boden.de>). 27
- Figure 3: Rhizoliths (top) and calcified roots (bottom). Top left: Rhizoliths formed in loess deposits, Nussloch, south-west Germany (© Zamanian), Top middle and right: Rhizolith formation stages by soil solution mass flow towards the roots by water uptake (top middle) leading to Ca^{2+} accumulation and CaCO_3 precipitation in the rhizosphere. Root water uptake leads to supersaturation of CaCO_3 and precipitation of carbonates, e.g. as calcite along the root. After root death and decomposition of organic tissues the rhizolith remains in soil (top right). Bottom left: Calcified roots formed in soils on alluvial deposits (© Zamanian). Bottom right: The magnification of the rectangle on bottom left; note the preserved cell structure and dissolution/re-precipitation in cells. 28
- Figure 4: Carbonate hypocoatings. Left: Hypocoatings inside the soil matrix and around the soil pores or cracks (© Kuzyakov), Center: Hypocoating formation by water evaporation or sudden decrease of CO_2 partial pressure in large pores, leading to CaCO_3 precipitation inside the soil matrix and around large pores. Right: Cross section of PC hypocoating around a pore (XPL) (Courtesy O. Ehrmann). The thin-section of calcite hypocoating around a channel (right) is kindly provided by Dr. Otto Ehrmann (Bildarchiv Boden, <http://www.bildarchiv-boden.de>). 29
- Figure 5: Carbonate nodules. Left: PC nodules at lower depths (150 cm) of Voronic Chernosem, "Stone Steppe", Russia (© Kuzyakov); Right: Cross section of PC nodule and clast coating in the topsoil (A horizon; 0-11 cm) in petric Calcisol (Zamanian, 2005). Photomicrograph is in XPL. 30
- Figure 6: Carbonate coatings on stones. Left: PC accumulation underneath stone particle (i.e. clast coating) and the chronological sequence of microlayers in PC coatings (Pustovoytov et al., 2007); Right: Coating formation by percolating water remaining underneath the coarse fragments (e.g. stones). The soluble ions (i.e. Ca^{2+} and HCO_3^-) will precipitate during soil dryness on the bottom side of the stone. In specific conditions, coatings may form on the upper side of stones (Amundson et al., 1997). The blue arrows show downward migration of water from the soil surface which may partly remain underneath stones. The orange arrows show water evaporation leading to soil dryness and supersaturation of the trapped solution and thus CaCO_3 precipitation. 30
- Figure 7: Calcrete morphology. Top: Thick calcrete formed on alluvial deposits comprised two distinct horizons: the lower calcrete contains abundant coarse fragments impregnated and cemented with PC. The upper calcrete – laminar calcrete – comprises negligible coarse fragments but horizontal layers of PC accumulation (profile depth: ca. 150 cm). Middle: PC accumulation as

microlayers in the upper calcrete. Bottom: Surrounded coarse fragments with micritic PC in the lower calcrete. Photomicrographs are in XPL (Zamanian, 2005).	32
Figure 8: Calcrete formation: Accumulation of PC by CaCO_3 redistribution within a landscape: CaCO_3 will be mainly leached from upper parts of the landscape with groundwater (inclined blue arrows) and will be moved to a lower landscape positions. Upward movement of water by capillary rise (Vertical blue arrow) will form calcrete at the middle parts of a landscape. CaCO_3 relocated from higher landscape positions cements the carbonate deposition zone (Calcic horizon) and finally form the calcrete (Knuteson et al., 1989).	33
Figure 9: Correlation between the mean annual precipitation (MAP) and the upper depth of the pedogenic carbonate horizon (B _k) (data in Heidari et al., 2004; Khormali et al., 2012, 2006, 2003; Khresat, 2001; Kovda et al., 2014; Kuzyakov, 2006; Royer, 1999, n = 1542).	35
Figure 10: The $\delta^{13}\text{C}$ values of carbonate forms in soil (changed after Nordt et al., 1996). The $\delta^{13}\text{C}$ isotopic composition of soil CO_2 and thus of pedogenic carbonates (PC) is controlled by local vegetation (C_3 or C_4 plants) (Cerling, 1984). The mean $\delta^{13}\text{C}$ value and standard deviation for biogenic carbonates (BC) are calculated from: Dettman et al., 1999; Prendergast et al., 2015; Pustovoytov et al., 2010; Regev et al., 2011; Riera et al., 2013; Stern et al., 1994. Note the different ^{13}C fractionation by rhizorespiration for C_3 and C_4 plants (Werth and Kuzyakov, 2010). The ^{13}C fractionations are presented with dashed lines and mentioned in italics.	40
Figure 11: The experiment layout and the labelling technique. $^{14}\text{CO}_2$ was released by injecting H_3PO_4 into the vial containing $\text{Na}_2^{14}\text{CO}_3$. The $^{14}\text{CO}_2$ remaining at the end of the recrystallization period (not participated in recrystallized carbonate) was trapped before each sampling by adding NaOH into the second vial. The H_3PO_4 was injected by syringe through the septa at the beginning of labelling, and NaOH injected at the end of labelling.	68
Figure 12: The distribution of measured ^{14}C activity between phases depending on time after labeling. Bar lines show standard errors.	70
Figure 13: ^{14}C activity and recrystallized amounts of CaCO_3 in loess and soil depending on recrystallization time. The filled and open symbols refer to the shells containing and free of organic compounds, respectively. Bar lines show standard errors. Note the different scales of Y axes.....	71
Figure 14: ^{14}C activity and recrystallized amounts of CaCO_3 on shells in loess and soil as a function of time (R_i). The filled and open symbols refer to the shells containing and free of organic compounds, respectively. Bar lines show standard errors. Note the different scales on Y-axes.....	72
Figure 15: (a) Percentage of shell carbonate remaining not-recrystallized after 56 days, (b, c and d) the calculated time for full recrystallization of shell carbonate containing or free of organic compounds in loess or soil (95% recrystallization assumed as full recrystallization). Circles and diamonds refer to shells in loess and loamy soil, respectively. Filled and open symbols show shells containing and free of organic compounds, respectively. The model line for each treatment is shown in different line styles.	73
Figure 16: The relation between modelled amounts of shell-carbonate recrystallization using Eq. (9) for all treatments and times with measured recrystallization. Bar lines show standard errors of measured recrystallization of each of four treatments at various dates.	78

Figure 17: Shell carbonate recrystallization depending on presence of organic compounds in shell structure and geogenic carbonates in soil. Organic compounds elimination increases shell porosity and make it vulnerable to recrystallization. Geogenic carbonates may also undergo dissolution and may recrystallize on shell surface or fill shell's structural porosities.....	80
Figure 18: (top) Carbonate recrystallization of shells in various matrixes. (middle) Carbonate recrystallization inside the matrix materials in the presence of shell particles. (bottom) Carbonate recrystallization inside the matrix materials in the absence of shell particles after 120 days. Black arrows show the time of labeling at the beginning of the experiment and at day 55.	92
Figure 19: Changes in concentrations of exchangeable Ca^{2+} (top) and exchangeable Na^+ (bottom) during the 120-day experiment period. Trend lines are shown in different styles.	92
Figure 20: Changes in concentrations of dissolved Ca^{2+} (top) and dissolved Na^+ (bottom) during the 120-day experiment period.	93
Figure 21: Shell carbonate recrystallization depending on soil cation exchange capacity and Ca^{2+} concentration: Shell carbonate recrystallization decreases as soil CEC increases (green and red lines). Shell carbonate recrystallization rates in similar time spans increase faster in soils with less CEC with increasing soil $p\text{CO}_2$ (Blue dotted lines).....	95
Figure 22: (Left) A ca. one-month-old <i>B. arvensis</i> grown in a 250 mL plastic pot; (Right, top) <i>B. arvensis</i> flower; (Right, bottom) <i>B. arvensis</i> fruits. The arrows show the openings in the pot lid, which were used for irrigation and root labelling (see 2.2. Labelling procedure).	101
Figure 23: Dilution of ^{14}C content of plant organs by dissolved inorganic C (HCO_3^-) taken from 2 sources: In carbonate-free soils, the only source of HCO_3^- is dissolution of root- and rhizomicrobially-respired CO_2 originally from the atmosphere ($^{14}\text{CO}_2$). In carbonate-containing soils, the dissolution of lithogenic carbonates ($\text{Ca}^{14}\text{CO}_3$) is a second source. The HCO_3^- from root-respired CO_2 is diluted by the HCO_3^- from lithogenic carbonates (Kuzyakov et al., 2006; Gocke et al., 2011). For shoot-labeled plants, this process leads to a reduction of the ^{14}C activity in the re-absorbed HCO_3^-	108

Preface

Carbonate-containing materials are present in soils in various morphologies which are generally classified in three groups. (1) Geogenic carbonates which are inherited from parent materials like limestone particles, loess deposits. (2) Biogenic carbonates which comprise part of organisms body for example mollusk shells, egg shells, fruit carbonates and (3) Pedogenic carbonates which are formed via pedogenesis such as nodules, coatings, etc. Isotopes of carbon ($\delta^{13}\text{C}$, ^{14}C) and oxygen ($\delta^{18}\text{O}$) in these carbonate types are valuable indicators of paleoenvironment (paleoclimate, paleovegetation etc.) and important in chronological studies (especially in Quaternary research) in soil science, geosciences, and archeological studies. The $\Delta^{14}\text{C}$ of soil carbonates is used to determine absolute ages of soils, sediments, and landscapes; $\delta^{13}\text{C}$ of soil carbonates corresponds to paleovegetation; $\delta^{18}\text{O}$ is related to carbonate formation temperatures and isotopic composition of oxygen in water ($\delta^{18}\text{O}_{\text{water}}$) that carbonates formed from and clumped isotopes of $\delta^{18}\text{O}$ and $\delta^{13}\text{C}$ (i.e. measuring of mass 47 as $^{13}\text{C}^{18}\text{O}^{16}\text{O}$) can be used as a direct indicator of carbonate formation temperatures known as $T_{\Delta 47}$.

Despite this relevance, the following issues may limit the applicability of isotopic approaches and increase the uncertainties of interpretations.

(1) The recrystallization process: all carbonate types may undergo dissolution after formation and recrystallize. The repeated cycles of dissolution and recrystallization changes the $\delta^{13}\text{C}$, $\delta^{18}\text{O}$ and $\Delta^{14}\text{C}$ of the carbonate types. Because the isotopic composition of the recrystallized carbonate controls by environmental parameters differing from the formation condition of the original carbonate type. For example the carbonate type which has been formed at relatively high temperatures may recrystallize at relatively lower temperatures. The dynamics of this process under various environmental conditions controlling the recrystallization rates are however, unknown or poorly understood.

(2) Old carbon incorporation in biogenic carbonates: The suitability of biogenic carbonates for radiocarbon dating is based on the assumption that C provides solely through organisms' respiration. That means the ^{14}C content in biogenic carbonates controls by ^{14}C content of atmospheric CO_2 . However, organisms may digest radiometrically-dead geogenic carbonates i.e. without detectable ^{14}C . The incorporation of this old C leads to overestimation of radiocarbon ages based on biogenic carbonates. So far, the effect of old C on radiocarbon ages has been examined and proved only in land snail shells.

Therefore, the main objectives of this study were:

- To analyze the effects of soil properties (presence of diffuse geogenic carbonates, cation exchange capacity) and environmental parameters (CO_2 partial pressure, temperature, soil moisture) on recrystallization rates of carbonate types using ^{14}C labeling approach
- To study the recrystallization rates of carbonate types as a function of time
- To examine the source of carbon in biogenic carbonates (i.e. fruits of *Buglossoides arvensis*) and suitability for dating purposes, and

In introduction section (chapter 1), various carbonate types in soil have been defined, the formation mechanisms and effective environmental factors leading to their formation have been mentioned and their resolution for paleoenvironment reconstruction has been argued. The problem of recrystallization and subsequent uncertainties in paleoenvironmental interpretation and dating has been discussed and simple approaches to consider recrystallization were summarized. Finally, the most important future research directions, including the anthropogenic effects i.e. fertilization and soil management have been suggested.

In chapter 2 and 3, the effects of environmental factors (i.e. soil moisture content, presence of geogenic carbonate, CEC) as well as time on carbonate recrystallization have been examined. Due to the very slow rate (around 10^{-5} day^{-1}) of recrystallization, and due to the limitations of usual approaches (mass changes, natural changes of isotopic signature, etc.), the ^{14}C labeling technique (Kuzyakov et al. 2006) has been used in both studies. The high sensitivity of the ^{14}C labeling technique enables measuring recrystallization rates even after a few days. This technique relies on the substitution of $\text{CaCO}_3\text{-C}$ with $\text{CO}_2\text{-C}$ from the soil atmosphere.

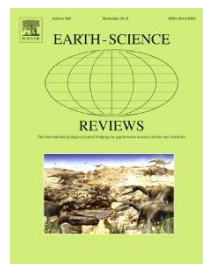
In chapter 4 the suitability of fruit carbonates of *Buglossoides arvensis* for radiocarbon dating has been argued. The seeds of *B. arvensis* have been cultivated on calcareous and non-calcareous soils. The plants have been labeled with $^{14}\text{CO}_2$ through atmosphere (shoot-labeling) or via $\text{Na}_2^{14}\text{CO}_3$ dissolved in soil solution (root-labeling) during fruit development period. Thereafter, the incorporation of dead carbon in fruit carbonate has been determined based on recovered ^{14}C and comparison between plants grown on calcareous and non-calcareous soils. The lower ^{14}C recovery in calcareous soils has been related to the incorporation of dead carbon from soil.

Table 1: Summary of objectives, the approaches and innovative findings of conducted studies

Study	Objectives	Approaches	Findings
1	<p>Summarizing available theories on:</p> <ul style="list-style-type: none"> • Pedogenic carbonates forms and formation processes • The relation of pedogenic carbonate forms to environmental factors • Implications of $\Delta^{14}\text{C}$, $\delta^{13}\text{C}$, $\delta^{18}\text{O}$ and Δ_{47} for dating and paleoenvironmental reconstructions • Discussing the uncertainties in dating and paleoenvironment reconstruction due to recrystallization 	Literature review	<ul style="list-style-type: none"> • Suggesting the most important future research directions on pedogenic carbonate, including the anthropogenic effects of fertilization and soil management
2	Determining the recrystallization rates of shell carbonate as a function of time, and presence of geogenic carbonates and organic compounds in soils and shell structure, respectively	^{14}C labeling and tracing	<ul style="list-style-type: none"> • Shell carbonate recrystallization begins very soon after embedding in soils and increases exponentially with time. • Shell recrystallization increases in the presence of geogenic carbonate. • Shell recrystallization increases after elimination of structural organic compounds and subsequently increases in shell porosity. • The ^{14}C labeling approach is sensitive in assessing recrystallization rates of biogenic carbonate within reasonably short times.
3	Determining the effect of cation exchange capacity (CEC) and elemental composition of cations on shell carbonate recrystallization to underline the consequences for radiocarbon dating and paleoenvironmental reconstructions	^{14}C labeling and tracing	<ul style="list-style-type: none"> • Shell carbonate recrystallization decreases with increasing soil CEC. • Parameters such as total CEC and the equilibria between exchangeable and dissolved cations should be included in models predicting shell diagenesis. • The ^{14}C labeling approach can be used to determine the weathering rates of soil Ca-bearing minerals.
4	Identifying the origin of C in fruit carbonate of <i>Buglossoides arvensis</i> to quantify the contribution of absorbed HCO_3^- from soil and its subsequences for radiocarbon dates.	^{14}C labeling and tracing	<ul style="list-style-type: none"> • <i>B. arvensis</i> takes up HCO_3^- from the soil via roots where the source of HCO_3^- can be dissolution of carbonate minerals (radiometrically dead, e.g. loess carbonate) and dissolution of root-respired CO_2 (recent C) in soil solution. • An age overestimation of ca. 500 years is possible due to ca. 6.0% incorporated HCO_3^-. • The age overestimation in fruit carbonate however, is insignificant in relatively old samples, approximately after two ^{14}C half-lives.

1. Introduction: Pedogenic carbonates; forms and formation processes

Published: Earth-Science Reviews 157 (2016): 1-17



Kazem Zamanian¹, Konstantin Pustovoytov², Yakov Kuzyakov^{1,3}

- ¹. Department of Soil Science of Temperate Ecosystems, University of Göttingen, Büsgenweg 2, 37077 Göttingen, Germany
². Institute of Soil Science and Land Evaluation (310), University of Hohenheim, Schloss Hohenheim 1, 70599 Stuttgart,
³. Department of Agricultural Soil Science, University of Goettingen, Buesgenweg 2, 37077, Goettingen, Germany

1.1. Abstract

Soils comprise the largest terrestrial carbon (C) pool, containing both organic and inorganic C. Soil inorganic carbon (SIC) was frequently disregarded because (1) it is partly heritage from soil parent material, (2) undergoes slow formation processes and (3) very slow exchange with atmospheric CO₂. The global importance of SIC, however, is reflected by the fact that SIC links the long-term geological C cycle with the fast biotic C cycle, and this linkage is ongoing in soils. Furthermore, the importance of SIC is at least as high as that of soil organic carbon (SOC) especially in semiarid and arid climates, where SIC comprises the largest C pool. Considering the origin, formation processes and morphology, carbonates in soils are categorized into three groups: geogenic carbonates (GC), biogenic carbonates (BC) and pedogenic carbonates (PC). In this review we summarize the available data and theories on forms and formation processes of PC and relate them to environmental factors. After describing the general formation principles of PC, we present the specific forms and formation processes for PC features and the possibilities to use them to reconstruct soil-forming factors and processes. The following PC are described in detail: earthworm biospheroliths, rhizoliths and calcified roots, hypocoatings, nodules, clast coatings, calcretes and laminar caps.

The second part of the review focuses on the isotopic composition of PC: δ¹³C, Δ¹⁴C and δ¹⁸O, as well as clumped ¹³C and ¹⁸O isotopes known as Δ₄₇. The isotopic signature of PC enables reconstructing the formation environment: the dominating vegetation (δ¹³C), temperature (δ¹⁸O and Δ₄₇), and the age of PC formation (Δ¹⁴C). The uncertainties in reconstructional and dating studies

due to PC recrystallization after formation are discussed and simple approaches to consider recrystallization are summarized.

Finally, we suggest the most important future research directions on PC, including the anthropogenic effects of fertilization and soil management. In conclusion, PC are an important part of SIC that reflect the time, periods and formation processes in soils. A mechanistic understanding of PC formation is a prerequisite to predict terrestrial C stocks and changes in the global C cycle, and to link the long-term geological with short-term biological C cycles.

Keywords: pedogenic carbonate; CaCO_3 recrystallization; diagenesis; paleoenvironment reconstructions; radiocarbon dating; inorganic carbon sequestration

1.2. Inorganic carbon in soil and pedogenic carbonates

1.2.1. Relevance of soil inorganic carbon

Soils with 1,570 Pg C (Eswaran, 1993) are the largest terrestrial C pool and are the third greatest C reservoir in the world after oceans with 38,725 Pg (IPCC, 1990) and fossil fuels with 4,000 Pg (Seigenthaler and Sarmiento, 1993) containing organic and inorganic C (Eswaran et al., 2000). Plant litter, rhizodeposits and microbial biomass are the main sources of the soil organic carbon (SOC) pool. The SOC pool comprises 697 Pg C in 0-30 cm and 1,500 Pg C in 0-100 cm depths (IPCC, 2007). Intensive exchange of organic C with the atmosphere, especially connected with anthropogenic activities, led to a very broad range of studies related to the organic C cycle in soil and these have been summarized in many reviews (e.g. IPCC, 2007; Kuzyakov, 2006).

In contrast to organic C, the exchange of soil inorganic carbon (SIC), i.e. various soil carbonate minerals (mostly calcite), with the atmosphere and the involvement of SIC in biotic C cycles is much slower (mean residence time of 78,000 years (Schlesinger, 1985)). Additionally, the distribution depth of SIC is opposite to that of SOC: most stocks are located deeper than one meter (Díaz-Hernández et al., 2003; Wang et al., 2010). These two reasons explain why much fewer studies focused on SIC than on SOC (Drees et al., 2001; Rawlins et al., 2011). Nonetheless, large stocks of SIC – 160 Pg C in 0-30 cm (Nieder and Benbi, 2008), 695-748 Pg C in 0-100 cm depth (Batjes, 1996) and 950 Pg C up to 2 m (Lal, 2012) – reflect its importance especially over the long term. The SIC content in first 2 m of soil in semi-arid regions could be 10 or even up to 17 times higher than SOC (Díaz-Hernández et al., 2003; Emmerich, 2003; Shi et al., 2012). Furthermore, a much longer

mean residence time of SIC – millennia (Schlesinger, 1985) – shows its greater role in the global C cycle compared with SOC (few hours to centuries) (Hsieh, 1993; Qualls and Bridgman, 2005). SIC also links SOC with short residence times to the long-term geological C cycle (Liu et al., 2010). Soils of arid and semi-arid regions with usually alkaline pH (> 8.5) and richness in Ca and/or Mg ($> 0.1\%$) may enhance the SIC content following organic fertilization and increase the respired CO₂ (Bughio et al., 2016; Wang et al., 2015).

Changes in environmental properties such as soil acidification because of N fertilization, N fixation by legumes or intensification of re-wetting cycles due to irrigation could release great amounts of SIC and increase CO₂ emissions (Eswaran et al., 2000; Shi et al., 2012). Such effects, though driven by natural processes, are well known in our planet's history, e.g. between the Pleistocene and Holocene, when around 400-500 Pg C were released from SIC and strongly intensified global warming over a short period (Adams and Post, 1999). The formation and accumulation of carbonate minerals in soils, in contrast, can directly mitigate the increase of atmospheric CO₂ (Landi et al., 2003; Xie et al., 2008) if calcium (Ca²⁺) ions have been released to the soil via sources other than carbonate-containing minerals, for instance from weathering of igneous rocks, decomposition of organic matter or dissolved Ca²⁺ in rainwater (Boettinger and Southard, 1991; Emmerich, 2003; Monger et al., 2015). This calls for investigating SIC stocks, forms and their dynamics to understand the role of SIC in the C cycle at regional and global scales, the fast and slow processes of C cycling, as well as the link between biotic and abiotic parts of the C cycle.

1.2.2. Soil inorganic carbon: worldwide distribution

Large SIC stocks are mostly found in regions with low water availability (i.e. arid, semi-arid and sub-humid regions) (Fig. 1) (Eswaran et al., 2000). Low precipitation and high potential evapotranspiration strongly limit the dissolution and leaching of carbonates from soil (Eswaran et al., 2000; Royer, 1999). Accordingly, the highest SIC content – around 320 to 1280 Mg C ha⁻¹ – is accumulated in soils of arid regions with mean annual precipitation (MAP) below 250 mm such as middle east, African Sahara and west USA (Fig. 1). As MAP increases, the SIC content decreases and less than 40 Mg C ha⁻¹ may accumulate at MAP exceeding 1000 mm for example in Amazonian forests and monsoonal forests in south-east Asia. However, partial eluviation and redistribution of carbonates may concentrate SIC deeper in the soil profile (Díaz-Hernández et al., 2003; Wang et al., 2010).

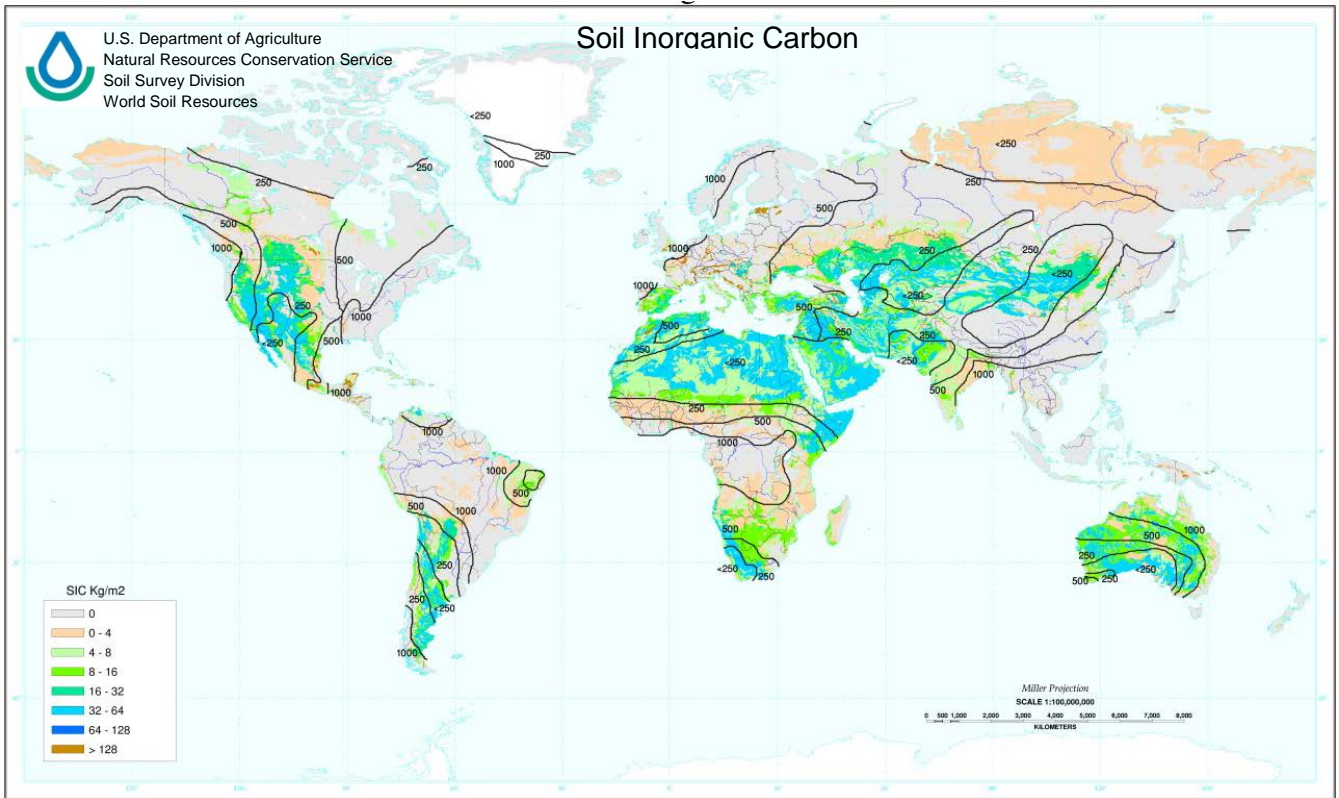


Figure 1: World SIC distribution in the top meter of soils (USDA-NRCS, 2000) and its correlation with areas of lower mean annual precipitation. The iso-lines of mean annual precipitation (mm) are from (FAO, 1996). Only the iso-lines of precipitation <1000 mm are presented. Note the exponential scale of SIC content. Most SIC is located in areas with precipitation <500 mm and SIC stocks above 32 kg C m^{-2} (320 Mg C ha^{-1}) are located in areas with precipitation <250 mm.

1.2.3. Soil inorganic carbon pools, classification and definitions

Based on origin, formation processes and morphology, the SIC can be subdivided into three large groups:

1. Geogenic carbonates (GC)¹: carbonates which have remained or are inherited from soil parent materials such as limestone particles or allocated onto the soil from other locations by calcareous dust or landslides etc.

¹ Here we do not review the forms and formation of geogenic and biogenic carbonates in soil.

2. Biogenic carbonates (BC)¹: carbonates formed within terrestrial or aquatic animals and plants as part of their skeleton, for example shells, bones and calcified seeds, or released from or within certain organs such as the esophageal glands of earthworms.

3. Pedogenic carbonates (PC): carbonates formed and redistributed in soils via dissolution of the SIC pool (i.e. geogenic, biogenic or previously formed pedogenic carbonates) and reprecipitation of dissolved ions in various morphologies such as carbonate nodules.

This review focuses solely on the origin, morphology and processes of PC formation. The GC and BC are mentioned only if relevant for PC formation.

1.2.4. Pedogenic carbonate within soil inorganic carbon pools and its relevance

PC originates during soil formation from GC or BC and/or former PC by recrystallization and redistribution in soil (see section 2). PC accumulation affects the physical, chemical and biological properties of soil (Nordt et al., 1998) and thus affects plant growth and soil productivity.

PC accumulation can plug soil pores (Baumhardt and Lascano, 1993; Gile, 1961), increasing bulk density and reducing root penetration, water migration and oxygen supply (Baumhardt and Lascano, 1993; Georgen et al., 1991).

Fine PC crystals (i.e. micrite < 4 µm) are more active in chemical reactions than large particles of GC (such as for example limestone). The availability of phosphorus and some micro-nutrients such as iron, zinc and copper for plants is therefore extremely reduced in the presence of PC (Becze-Deák et al., 1997). Accordingly, the presence of PC, their localization and forms in soil modify the water budget and fertilizer management.

Considering the effect of PC on plant growth and soil productivity, the layers or horizons containing PC have been defined quantitatively (e.g. amounts of carbonate, layer thickness) as diagnostic materials, diagnostic properties or diagnostic horizons in many soil classification systems such as World Reference Base, Soil Taxonomy, Russian and German systems especially in higher levels, i.e. major soil groups (WRB, 2014) orders and sub-orders (Soil Survey Staff, 2010).

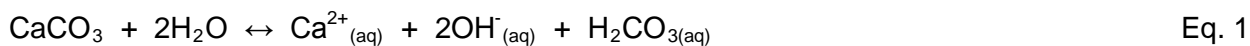
In this review we focus on 1) the general mechanisms of PC formation, 2) the most common morphological forms of PC and their specific formation processes and 3) environmental factors affecting the rate of PC accumulation in soils. We then discuss 4) the importance and applications of PC in environmental sciences and mention 5) the uncertainties because of recrystallization and 6) evidence of PC recrystallization. Finally, we suggest 7) directions of further studies.

1.3. Formation of pedogenic carbonate

1.3.1. General principle of pedogenic carbonate formation

The general process of PC formation consists of three steps: 1) dissolution of SIC pools², 2) movement of dissolved ions within pores, through soil profiles as well as landscapes and 3) reprecipitation.

(1) **Dissolution of SIC pools:** The dissolution of SIC – mostly of CaCO_3 – considering the solubility product ($K_{\text{sp}} \approx 10^{-6} - 10^{-9}$) in distilled water (Robbins, 1985) is comparatively low (Eq. 1). The dissolution rate is strongly controlled by soil pH and dissolved CO_2 . The dissolution rate of CO_2 and concentration of dissolved inorganic carbon (DIC) species (i.e. HCO_3^- , CO_3^{2-} , $\text{H}_2\text{CO}_3^\circ$ and CO_2), however, is controlled by the partial pressure of CO_2 ($p\text{CO}_2$) in the soil atmosphere (Andrews and Schlesinger, 2001; Karberg et al., 2005). CaCO_3 solubility in pure H_2O at 25 °C is 0.013 g L⁻¹, whereas in weak acids such as carbonic acid, the solubility increases up to five times (Aylward, 2007). The acidity produced by CO_2 dissolution removes OH^- ions and shifts the Eq. 1 to the right, leading to further dissolution of CaCO_3 . The increase of $p\text{CO}_2$ in the soil air increases the solubility of CaCO_3 , otherwise the pH will drop.



(2) **Movement of dissolved ions:** the dissolved Ca^{2+} ions and DIC species are translocated by water movement in various directions: i.e. diffusion, capillary rise (unidirectional), water percolation (mainly downwards) or evaporation (upward). The transportation occurs over multiple spatial scales from mm to km: within and between microaggregates, macroaggregates, soil horizons, landscapes and even from terrestrial to aquatic ecosystems. The dissolved ions, however, may remain without significant translocation if soil permeability is very low, e.g. at the top of hard bedrock. Despite downward and upward migration of water, the upward migration of Ca^{2+} ions and DIC species is strongly restricted. Because $p\text{CO}_2$ in the soil air strongly decreases close to the surface, CaCO_3 solubility declines, the solution becomes supersaturated and CaCO_3 precipitates. The rare cases of

² This is the general formation mechanism of PC. If Ca ions are provided by sources other than SIC, such as weathering of Ca-bearing silicates, PC may also form (See section 2.4., parent material).

upward CaCO_3 migration are possible only from continuously evaporating groundwater (e.g. in calcretes, see section 2.3.), or in the case of a higher CO_2 concentration in the topsoil versus subsoil, e.g. due to high microbial and root respiratory activities.

(3) **Re-precipitation:** if soil solution becomes supersaturated with CaCO_3 , the solutes precipitate. Supersaturation of soil solution in respect to CaCO_3 may take place for two reasons: 1) decreasing soil water content mainly connected with evapotranspiration and 2) decreasing $p\text{CO}_2$ (Robbins, 1985; Salomons and Mook, 1976). Considering changes in precipitation rates due to environmental properties (see section 2.4) however, various morphologies may form.

1.3.2. Formation mechanisms of pedogenic carbonates

Considering the water movement during PC formation and the morphology of accumulated PC, various theories and mechanisms have been proposed for PC formation. These can be classified into four groups (adapted from (Monger, 2002)):

1. Perdescendum models: dissolution of GC, BC or PC in the topsoil, downward leaching and re-precipitation in subsoil because of water consumption. This is the main process of PC redistribution and accumulation in soil horizons (Gile et al., 1966; Machette, 1985; Royer, 1999). Lateral movement of solutes in this model also explains PC formation in various positions of a landscape (Monger, 2002).

2. Perascendum models: PC forms by upward water movement due to capillary rise or fluctuations of shallow groundwater. Dissolution occurs in the subsoil, and upward movement of the solution (after soil dryness because of evaporation, or drop in CO_2 concentration) accumulates PC near or even at the soil surface (Khadkikar et al., 1998; Knuteson et al., 1989; Miller et al., 1987; Monger and Adams, 1996; Suchý, 2002). This model also includes the dissolution of SIC in higher landscape elevations and carbonate migration with groundwater with subsequent evaporation in soils at lower landscape elevations.

3. In situ models: dissolution of SIC pool and re-precipitation of dissolved CaCO_3 take place without significant movement through the soil profile (Monger and Adams, 1996; Rabenhorst and Wilding, 1986; West et al., 1988). This process commonly redistributes carbonates within the soil aggregates and pores of one horizon.

4. Biological models: biological activities increase the concentration of Ca^{2+} ions inside the organisms (e.g. plant cell-walls, plant vacuoles, fungi hyphae) or close to the organisms (e.g. along

roots due to water mass flow towards the root, below termite nests because of their characteristic residual collectivity). Further calcification of Ca-bearing organs or supersaturation of soil solution at such sites forms PC (Alonso-Zarza, 1999; Becze-Deàk et al., 1997; Elis, 2002; Monger and Gallegos, 2000; Verrecchia et al., 1995).

Depending on the prevalence of one or more of these mechanisms and their localization, the accumulation of re-precipitated carbonate generates various morphological forms of PC.

1.3.3. Morphology of pedogenic carbonates

Around 10 main PC forms are differentiated based on their morphology, properties and formation mechanisms (Table 2). These PC forms are classified based on the contribution of biotic and abiotic processes to their formation as well as PC formation rates.

Table 2: Characteristics of the most common pedogenic carbonate features in soils¹

PC features	Characteristics					Formation ⁵ category	Formation time scale
	Shape	Size	Density ²	Porosity ³	Impurities ⁴		
PC features mostly related to biotic controls							
Earthworm biospheroliths ^A	Spheroidal	Few mm	High	Moderate	Moderate	4	Days
Calcified root cells ^B	Branch shape structures	Less than mm in diameter and up to few cm length	Low	High	Low	4	Weeks to months
Rhizoliths ^B	Cylindrical structures	Up to several cm in diameter and up to several meters length	High	Moderate	Low to high outward root center	4	Months to years
Needle fiber calcite	Microscopic needle shape crystals	Some µm	Very high	Very low	Very low to pure calcite	4 or could be even not pedogenic	Days
Pseudomorph calcite after gypsum	Microscopic lenticular crystals	Some µm	Very high	Very low	Very low to pure calcite	Not clear, probably 4	Not clear

Table 2: continue

PC features	Characteristics					Formation ⁵ category	Formation time scale
	Shape	Size	Density ²	Porosity ³	Impurities ⁴		
PC features mostly related to abiotic controls							
Soft masses	Diffuse powder	Visible powder	Low	High	Low	probably 3	Weeks
Hypocoatings ^C	Laminated carbonate inside soil matrix and along soil pores	Few mm thickness with diffuse boundary into soil matrix	High	Low	High	2	Weeks to months
Nodules ^D	Spheroidal	Few mm to few cm in diameter	Low to very high	Low to very high	High	3	Decades
Clast Coatings ^E	Laminated carbonate beneath (or at the top of) clasts	Few mm to few cm thickness, the same length as related clast	High	Low	Moderate	1, (2) ⁶	Centuries to millennia
Calcretes ^F	Cemented horizon ⁷	At least 10 cm	Very high	Very low	High	2, (1, 3, 4)	Millennia

¹. The information for pedogenic carbonate features were inferred considering data in: Alonso-Zarza, 1999; Amundson et al., 1997; Barta, 2011; Becze-Deák et al., 1997; Brock and Buck, 2005; Candy et al., 2005; Durand et al., 2010; Gile et al., 1966; Gocke et al., 2011a; Khormali et al., 2006; Klappa, 1980; Kovda et al., 2003; Pustovoytov and Leisten, 2002; Rabenhorst and Wilding, 1986; Verrecchia and Verrecchia, 1994; Versteegh et al., 2013; Villagran and Poch, 2014; Wieder and Yaalon, 1982.

². Low: 1.5-1.6, moderate: 1.6-1.7, high: 1.7-1.8, very high: 1.8->2 g cm⁻³

³. Very low: <5, low: 5-20, moderate: 20-30, high: >30 %

⁴. Very low: <10, low: 10-30, moderate: 30-50, high: >50 % (minerals or particles other than calcite)

⁵. See section 1.3.2. (Formation mechanisms of pedogenic carbonate).

⁶. In parentheses: probable mechanism(s) other than the main one.

⁷. Calcretes and laminar caps are new soil horizons which are formed by cementation.

A) Earthworm biospheroliths: Calciferous glands or esophageal glands of earthworms produce carbonate features, which are excreted in earthworm casts (Fig. 2) (Becze-Deák et al., 1997). Despite the primary biogenic origin of earthworm biospheroliths, they frequently provide an initial nucleus for further spherical accumulation of other forms of PC. The presence of earthworm biospheroliths in soils is an indication of stable conditions, i.e. absence of erosion or deposition (Becze-Deák et al., 1997). Earthworm biospheroliths occur frequently in loess-paleosol sequences (Becze-Deák et al., 1997) and can be used for ¹⁴C dating (Pustovoytov et al., 2004). The formation rate of earthworm biospheroliths is fast – within a few days (Lambkin et al., 2011).

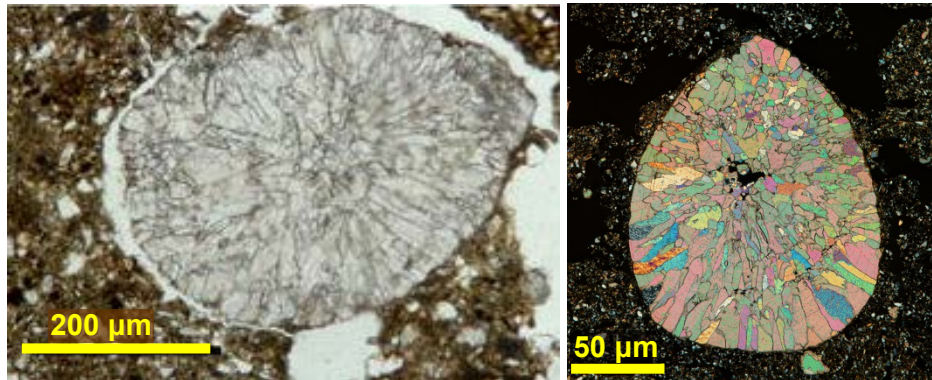


Figure 2: Earthworm biospheroliths. Left: Plain Polarized Light; PPL (Verrecchia, 2011); Right: Cross Polarized Light, XPL (courtesy O. Ehrmann). Earthworm biospheroliths are produced by earthworms' calciferous glands, which release $\sim 0.8 \text{ mg CaCO}_3 \text{ earthworm}^{-1} \text{ day}^{-1}$ (Lambkin et al., 2011). The thin section of biospherolith (right) is kindly provided by Dr. Otto Ehrmann (Bildarchiv Boden, <http://www.bildarchiv-boden.de>).

B) Rhizoliths are formed by mass flow of water with soluble Ca^{2+} towards the root and precipitation of CaCO_3 along the root (Fig. 3 top). Because Ca^{2+} uptake is much lower than the water uptake, the remaining Ca^{2+} ions precipitate with CO_2 from rhizomicrobial respiration as CaCO_3 , thus forming the rhizoliths (Callot et al., 1982; Hinsinger, 1998; Lambers et al., 2009). The other but rare possibility is the release of HCO_3^- instead of H^+ by roots to compensate for the uptake of anions such as NO_3^- . Increasing soil pH by released HCO_3^- induces CaCO_3 precipitation around the root (Klappa, 1980). Rhizolith formation is common for shrubs and trees, but is not relevant for grasses because of their short life cycle. CaCO_3 accumulation increases with root age over decades to centuries (Gocke et al., 2011a) and may form huge rhizolith landscapes, e.g. in Western Australia. In strongly calcareous soils, plants may reduce Ca^{2+} toxicity by CaCO_3 precipitation in vacuoles of root cortical cells. This leads to calcification of the root cortex and formation of another type of rhizoliths termed calcified roots (Jaillard, 1987) (Fig. 3 bottom).

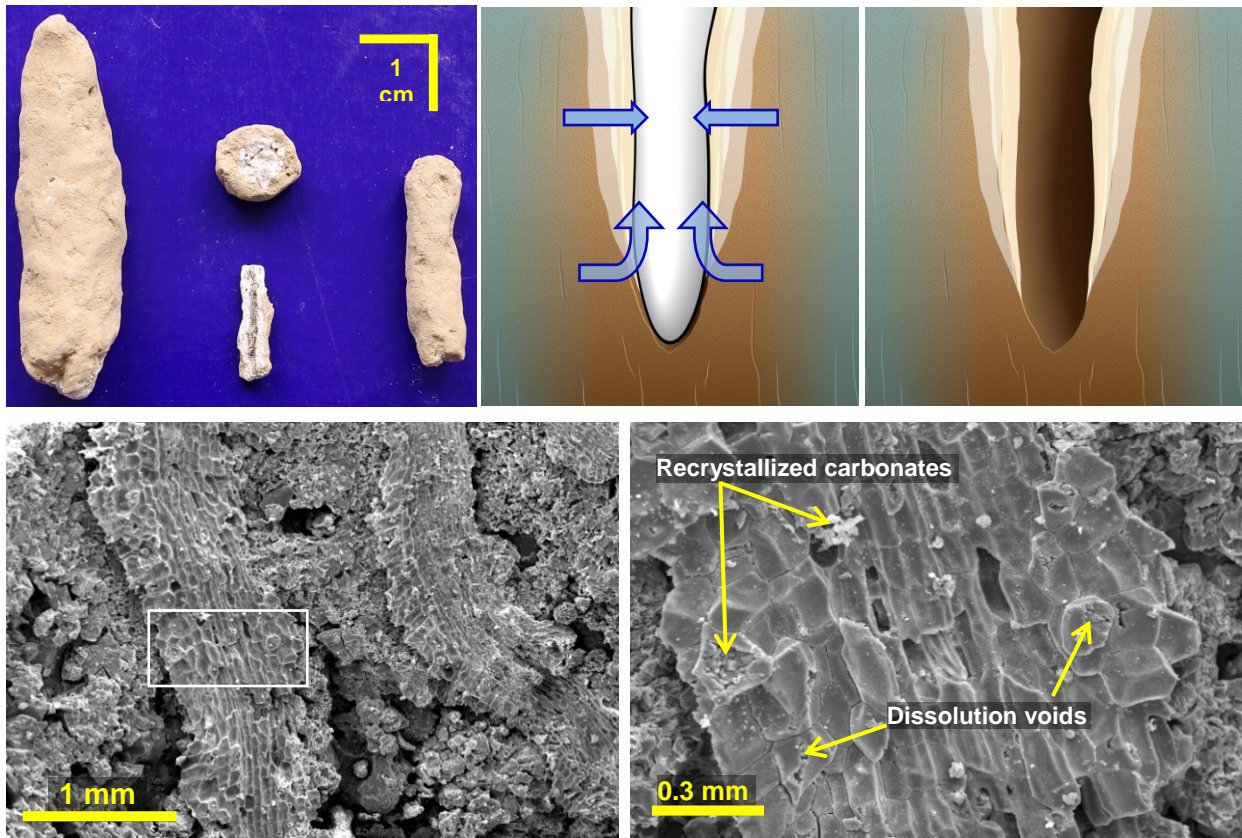


Figure 3: Rhizoliths (top) and calcified roots (bottom). Top left: Rhizoliths formed in loess deposits, Nussloch, south-west Germany (© Zamanian). Top middle and right: Rhizolith formation stages by soil solution mass flow towards the roots by water uptake (top middle) leading to Ca^{2+} accumulation and CaCO_3 precipitation in the rhizosphere. Root water uptake leads to supersaturation of CaCO_3 and precipitation of carbonates, e.g. as calcite along the root. After root death and decomposition of organic tissues the rhizolith remains in soil (top right). Bottom left: Calcified roots formed in soils on alluvial deposits (© Zamanian). Bottom right: The magnification of the rectangle on bottom left; note the preserved cell structure and dissolution/re-precipitation in cells.

C) Hypocoatings or Pseudomycels are formed by penetration of percolating water through the soil matrix and rapid precipitation of CaCO_3 around large and medium soil pores (Fig. 4). Rapid precipitation is common because of the strong $p\text{CO}_2$ decrease in these pores compared to the micro-pores. Hypocoatings may also be formed by a fluctuating water table (Durand et al., 2010). Because of fast precipitation, this form of CaCO_3 is young, potentially forming within weeks to months.

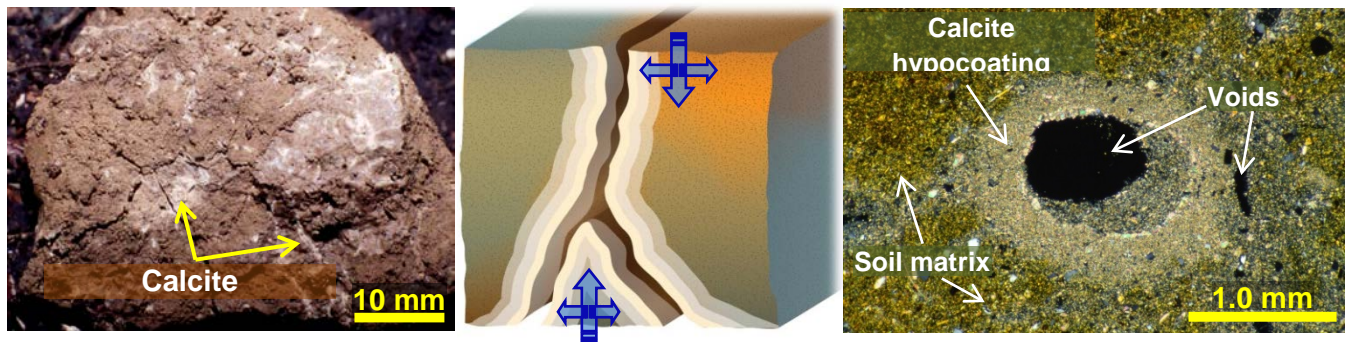


Figure 4: Carbonate hypocoatings. Left: Hypocoatings inside the soil matrix and around the soil pores or cracks (© Kuzyakov), Center: Hypocoating formation by water evaporation or sudden decrease of CO₂ partial pressure in large pores, leading to CaCO₃ precipitation inside the soil matrix and around large pores. Right: Cross section of PC hypocoating around a pore (XPL) (Courtesy O. Ehrmann). The thin-section of calcite hypocoating around a channel (right) is kindly provided by Dr. Otto Ehrmann (Bildarchiv Boden, <http://www.bildarchiv-boden.de>).

D) Nodules (Fig. 5) are formed *in situ* by impregnation of soil matrix with CaCO₃ at specific locations (Durand et al., 2010). This impregnation creates the diffuse and gradual outer boundaries of the nodules, and the internal fabric of the nodules remains similar to the host soil (Durand et al., 2010). Although nodules are one of the most common forms of PC, the formation processes and localization of nodules remain unclear. The CaCO₃ accumulation probably initially begins around a nucleus, e.g. mineral particles, organic remnants, particles of GC or biospheroliths. Sometimes, nodules have a sharp outer boundary as well as a dissimilar fabric as does the host soil (Fig. 5). This probably reflects soil turbation or translocation of nodules from other horizons or other parts of the landscape by means of deposition (Kovda et al., 2003).

E) Coatings on clasts are formed by slowly percolating water becoming trapped on the bottom of clasts such as stone particles. Subsequent desiccation by evaporation or water uptake by roots supersaturates the trapped water with CaCO₃. CaCO₃ then precipitates in microlayers on the bottom of clasts (Fig. 6). The microlayers usually have light and dark colors, reflecting the presence of impurities. The light-colored microlayers are mostly comprised pure calcite, but the darker one may contain organic compounds and/or minerals other than CaCO₃ (Courty et al., 1994; Durand et al., 2010). The formation period of coatings is centuries to millennia. Therefore, radiocarbon dating and the stable isotope composition ($\delta^{13}\text{C}$ and $\delta^{18}\text{O}$) of microlayers represent an informative chronological and paleoenvironmental proxy (Fig. 6 left) (Pustovoytov, 2002).

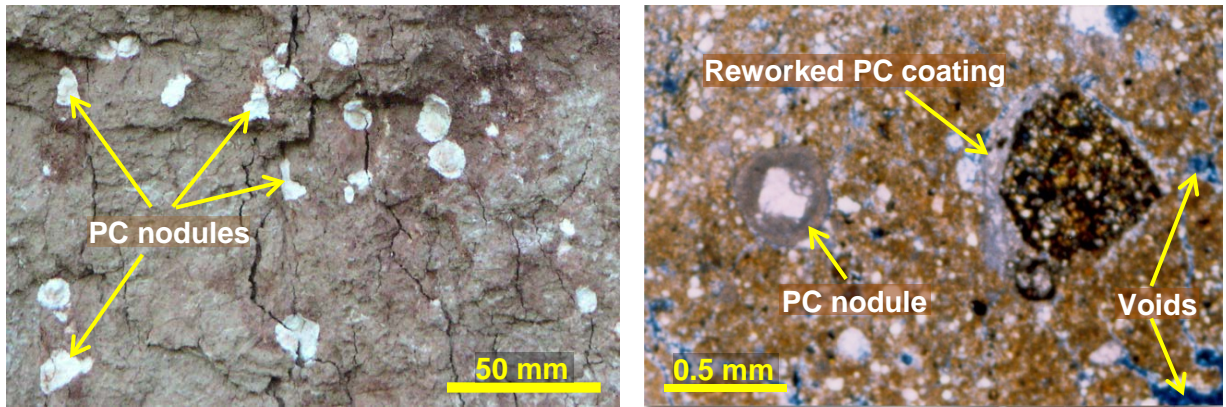


Figure 5: Carbonate nodules. Left: PC nodules at lower depths (150 cm) of Voronic Chernosem, "Stone Steppe", Russia (© Kuzyakov); Right: Cross section of PC nodule and clast coating in the topsoil (A horizon; 0-11 cm) in petric Calcisol (Zamanian, 2005). Photomicrograph is in XPL.

The formation mechanism of clast coatings, however, is not always similar to that of stalactites. The presence of cracks between the coating and the clast surface creates free space for precipitation of new carbonates (Brock and Buck, 2005). Coatings may also form at the top of clasts in regions with summer/fall precipitation. In wet summers, the stone surface will be warmer than the soil solution, leading to supersaturation of bicarbonate on the stone top and consequently CaCO_3 precipitation (Amundson et al., 1997). The alteration in clast coating orientation (i.e. mostly at the bottom of clast), however, is an indicator of soil disturbance (Fig. 5 right).

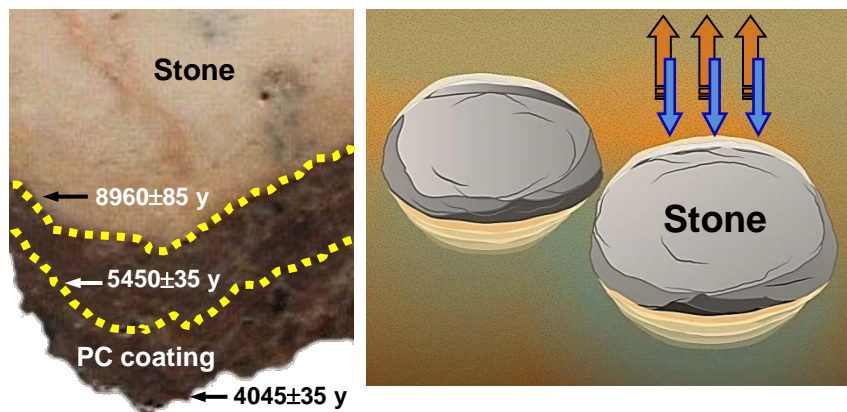


Figure 6: Carbonate coatings on stones. Left: PC accumulation underneath stone particle (i.e. clast coating) and the chronological sequence of microlayers in PC coatings (Pustovoytov et al., 2007); Right: Coating formation by percolating water remaining underneath the coarse fragments (e.g. coarse sand or gravel).

stones). The soluble ions (i.e. Ca^{2+} and HCO_3^-) will precipitate during soil dryness on the bottom side of the stone. In specific conditions, coatings may form on the upper side of stones (Amundson et al., 1997). The blue arrows show downward migration of water from the soil surface which may partly remain underneath stones. The orange arrows show water evaporation leading to soil dryness and supersaturation of the trapped solution and thus CaCO_3 precipitation.

F) Calcrete: The soil horizon impregnated and cemented with PC is termed calcrete (Goudie, 1972; Reeves, 1970) (Fig. 7). Calcrete reflects the recent or past existence of a shallow groundwater table. Fluctuating groundwater levels accompanied with intensive evapotranspiration accumulate carbonates in soil horizons (Khadkikar et al., 1998; Knuteson et al., 1989), leading to their cementation and the formation of calcrete (Fig. 8). Cementation by CaCO_3 may occur also by 1) leaching of dissolved Ca^{2+} and HCO_3^- ions from upper horizons (Fig. 8) (Gile et al., 1966; Machette, 1985), or 2) dissolution of Ca^{2+} containing rock (i.e. limestone) and carbonate precipitation without translocation of dissolved ions (Rabenhorst and Wilding, 1986; West et al., 1988). Biological activities such as bio-mineralization of roots lead to the formation of laminar crusts known as rootcretes in soil (Verrecchia et al., 1993; Wright et al., 1996). Nonetheless, huge CaCO_3 amounts accumulated as calcrete cannot be explained by the translocation of dissolved ions within the soil profile. They clearly reflect the Ca^{2+} relocation from higher landscape positions (Sauer et al., 2015). Considering the formation mechanisms, the properties of calcretes, however, will be different: for instance, the presence of high Mg-calcite is an indication of groundwater calcrete (Miller et al., 1985).

The necessary time span for calcrete formation is millennia or longer. Soil erosion or deposition may change the depth of maximum PC accumulation (Alonso-Zarza, 2003; Gile, 1999) and prolong or shorten the formation period of calcrete (See section 2.4. Topography and soil position in the landscape and soil age). The thickness of calcrete, its location, micromorphology and formation stages are useful indicators of development and age of soils and landscapes (Adamson et al., 2015; Gile et al., 1966).

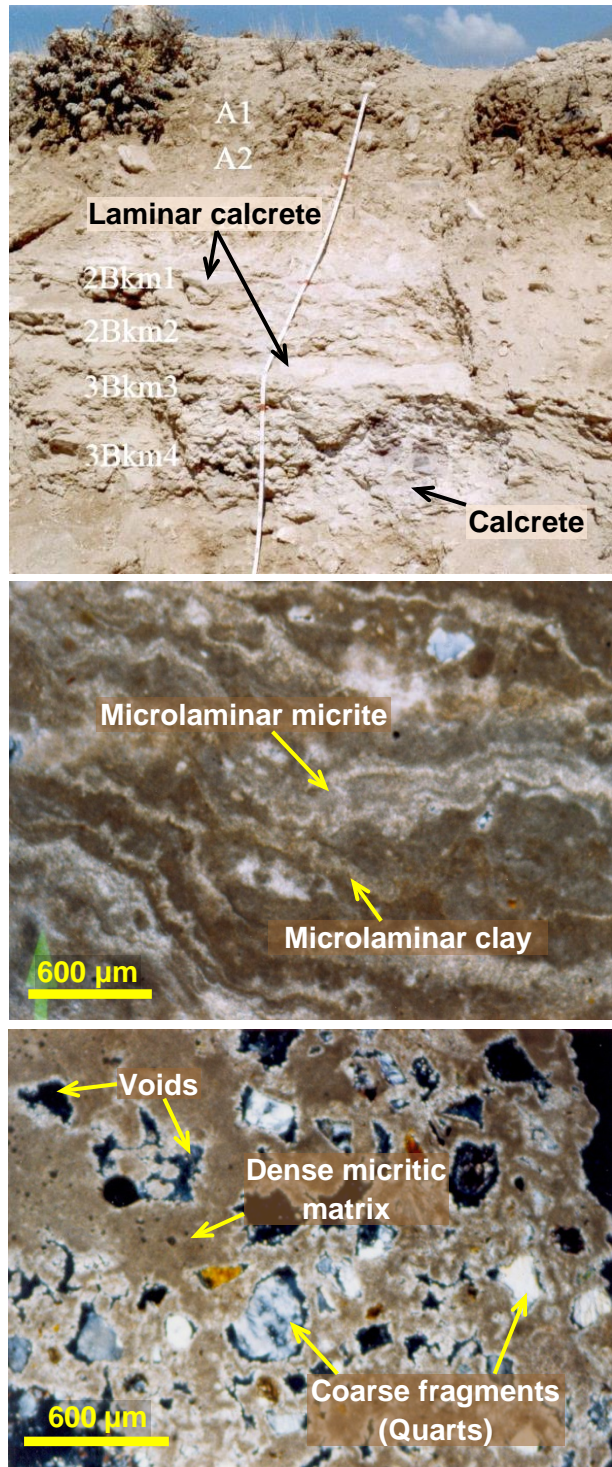


Figure 7: Calcrete morphology. Top: Thick calcrete formed on alluvial deposits comprised two distinct horizons: the lower calcrete contains abundant coarse fragments impregnated and cemented with PC. The upper calcrete – laminar calcrete – comprises negligible coarse fragments but horizontal layers of PC accumulation (profile depth: ca. 150 cm). Middle: PC accumulation as

microlayers in the upper calcrete. Bottom: Surrounded coarse fragments with micritic PC in the lower calcrete. Photomicrographs are in XPL (Zamanian, 2005).

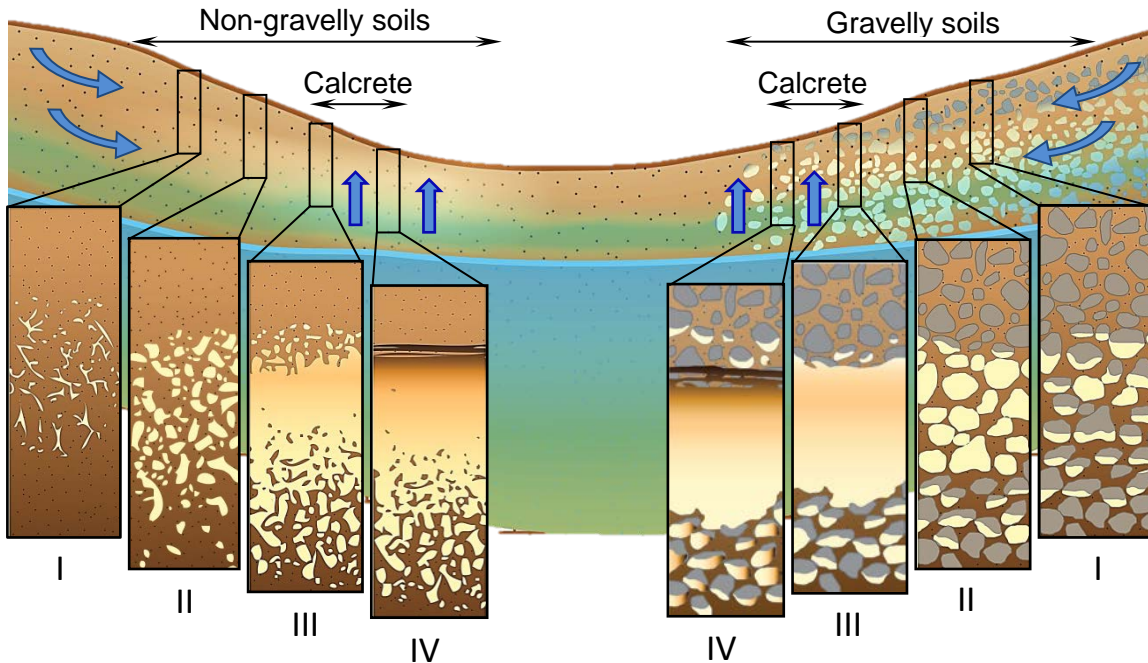


Figure 8: Calcrete formation: Accumulation of PC by CaCO_3 redistribution within a landscape: CaCO_3 will be mainly leached from upper parts of the landscape with groundwater (inclined blue arrows) and will be moved to a lower landscape positions. Upward movement of water by capillary rise (Vertical blue arrow) will form calcrete at the middle parts of a landscape. CaCO_3 relocated from higher landscape positions cements the carbonate deposition zone (Calcic horizon) and finally form the calcrete (Knuteson et al., 1989).

Considering the four steps of Gile et al.'s (1966) model, formation of coatings on clasts is the initial stages of PC accumulation in gravelly soils (right), while in non-gravelly soils (left) nodules would be formed. Connection of coatings as well as nodules by the gradual CaCO_3 accumulation will plug the soil horizon (stage III) and forms calcrete. Water stagnation at the top of calcrete and subsequent gently drying soil will generate a laminar cap at the top of calcrete in the same way in gravelly and non-gravelly soils (stage IV).

G) Laminar caps are formed in the presence of several restrictions for vertical water percolation and the subsequent formation of a perched water table (Alonso-Zarza, 2003; Gile et al., 1966).

Restricted water permeability leads to lateral water movement at the top of the low permeable zone. Such low permeable zones can for example be an existing calcrete or hard bedrock (Rabenhorst and Wilding, 1986). When the soil becomes dry, PC will precipitate in microlayers at the top of the low permeable zone and further decrease the permeability. A laminar cap forms a new horizon in the soil, which is nearly entirely occupied with PC and is impermeable to roots. Clay minerals and organic matter comprise non-calcareous materials in this horizon, and soil skeletal particles and coarse fragments such as pebbles and gravels are present in minor amounts and lower than 1% (Fig. 7) (Brock and Buck, 2009; Gile et al., 1966). The formation of a laminar cap may also be controlled by biological activity (e.g. Cyanobacteria, fungi or horizontal plant roots) (Verrecchia et al., 1995) in the same manner as calcrete formation.

1.3.4. Factors affecting pedogenic carbonate accumulation in soil

A large complex of several external and internal as well as biotic and abiotic factors affects the formation processes, accumulation rates and total amounts of PC. The external factors such as climate, topography and organisms mainly affect PC localization and PC formation rates. These factors mainly affect the water balance and CO₂ content in the soil air. The internal soil factors such as parent material and physical and chemical properties are mainly responsible for the total amount of PC, its morphology and impurities.

1.3.4.1. Climate

Climate, i.e. precipitation and temperature, is suggested as the main controlling factor for PC formation and localization (Borchardt and Lienkaemper, 1999; Eswaran et al., 2000). The amount and seasonal distribution of mean annual precipitation controls the depth of carbonate leaching and accumulation (Egli and Fitze, 2001) (see section 1.2) (Fig. 9). Therefore, accumulation of PC near the soil surface is common for precipitation less than 500 mm (Landi et al., 2003; Retallack, 2005). Moreover, MAP controls the soil moisture regime and so, affects the morphology of PC features. For instance, drier conditions may lead to formation of euhedral or well-shaped CaCO₃ crystals, whereas anhedral crystals with irregular and broken boundaries are formed at more humid periods (Kuznetsova and Khokhlova, 2012).

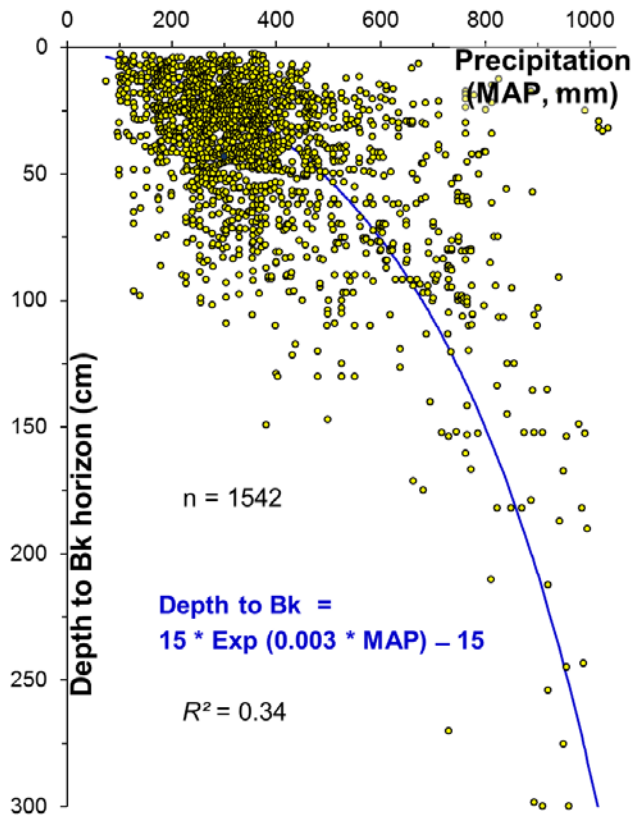


Figure 9: Correlation between the mean annual precipitation (MAP) and the upper depth of the pedogenic carbonate horizon (Bk) (data in Heidari et al., 2004; Khormali et al., 2012, 2006, 2003; Khresat, 2001; Kovda et al., 2014; Kuzyakov, 2006; Royer, 1999, n = 1542).

The effect of temperature on PC formation, accumulation and localization is complicated. PC can accumulate in soils in a wide range of temperatures from very hot conditions in hot deserts (Amit et al., 2011; Thomas, 2011) to cold climatic zones such as tundra (Courty et al., 1994; Pustovoytov, 1998). Increasing temperature decreases CO₂ solubility (Krauskopf and Bird, 1994), which directly affects the supersaturation of soil solution with CaCO₃ (Barker and Cox, 2011). Increasing temperature, however, boosts microbial respiration and thus increases the CO₂ concentration in soil air (Lal and Kimble, 2000). This biotic effect of temperature overwhelms the abiotic effect of CO₂ solubility (Gocke and Kuzyakov, 2011). Accordingly, higher temperatures increase the PC accumulation rates (Candy and Black, 2009; Gocke and Kuzyakov, 2011). Faster rates (due to warmer conditions) lead to more impurities such as rare earth elements in the PC structure (Gabitov et al., 2008; Violette et al., 2010). The presence of such co-precipitates affects the dissolution rate of PC after formation as well as its morphology and crystal size (Eisenlohr et al., 1999) (see section 4.3.2).

The temperature controls PC morphology and the formation of CaCO_3 polymorphs (Ma et al., 2010). Increase of temperature decreases the $[\text{CO}_3^{2-}]/[\text{Ca}^{2+}]$ ratio and so, aragonite formation is favored instead of calcite or vaterite (Ma et al., 2010).

In conclusion, the balance between MAP (total amount and seasonality) and evapotranspiration (driven by temperature and wind speed) determines the rates and the amounts of PC as well as the depth of PC accumulation. Hence PC are formed during soil drying when evapotranspiration exceeds precipitation (Birkeland, 1999; Gile et al., 1966; Hough et al., 2014; Rawlins et al., 2011).

1.3.4.2. Soil parent material

Soil parent material and the Ca source for CaCO_3 precipitation affect the total amount, formation rates, mineralogical and isotopic composition of PC. There is more PC in soils formed on calcareous parent materials (Díaz-Hernández et al., 2003; Schlesinger et al., 1989). Moreover, thicker PC coatings form under limestone particles (i.e. particles larger than 1 cm) compared to sandstones (Pustovoytov, 2002; Treadwell-Steitz and McFadden, 2000). The source of Ca for PC formation can be examined by pursuing trace elements in the PC structure as well as examining the isotopic composition, e.g. Ca originated from atmospheric deposition is evident by similar $^{87}\text{Sr}/^{86}\text{Sr}$ ratios in aerosols and accumulated PC (Chiquet et al., 1999). $\delta^{13}\text{C}$ of PC on calcareous vs. non-calcareous parent materials usually shows a higher heterogeneity i.e. wider range of $\delta^{13}\text{C}$, because GC such as limestone particles remain inside the PC structure (Kraimer and Monger, 2009). In aeolian deposits, however, the finer particle size distribution of calcareous dust may lead to complete dissolution of GC and thus less $\delta^{13}\text{C}$ heterogeneity in PC features (Kraimer and Monger, 2009). The weathering of non-calcareous parent materials contributes to the localization of cations such as rare earth elements (REE), uranium, barium etc. as impurities in PC structure (Violette et al., 2010; Yang et al., 2014).

The weathering of non-calcareous parent materials such as igneous rocks in some old soils may provide nearly the total Ca available for PC formation (Landi et al., 2003; Naiman et al., 2000; Whipkey et al., 2000). However, it usually supplies less than 2% of Ca in precipitated PC (Capo and Chadwick, 1999). The presence of co-precipitated cations from parent material in the PC structure changes the crystallographic parameters of CaCO_3 and controls the crystal morphology (Klein, 2002). For instance, impurities decrease the crystal size (Catoni et al., 2012). Elongated and needle-shaped crystals are formed in solution at higher concentrations (100 ppb) of $(\text{REE}^{3+})/(\text{Ca}^{2+})$, while rhombohedral and prismatic crystals are common at lower concentrations (10 ppb) (Barker

and Cox, 2011). The impurities also inhibit PC dissolution because they remain on the crystal surface and decrease ion exchange (Eisenlohr et al., 1999).

Aluminosilicates as well as organic compounds such as fulvic and humic acids are additional impurities (Gabitov et al., 2008; Stumm and Morgan, 1996). The presence of aluminosilicates and organic compounds in PC structure affects crystal growth. For instance, binding of carboxyl groups at or near crystal growth sites inhibits the growth rate of CaCO_3 crystals (Reddy, 2012).

1.3.4.3. Soil properties

Soil texture, structure, pH, ion strength and composition of soil solution can affect PC formation (Chadwick et al., 1989; Finneran and Morse, 2009; Ma et al., 2010; Reddy, 2012). Soil properties such as texture and structure control the accumulation depth of PC because they affect water holding capacity, water penetration and movement (Chadwick et al., 1989). The pH affects carbonate crystal size and morphology by controlling the supersaturation state of soil solution with CaCO_3 (Ma et al., 2010). The ratio of bicarbonate/carbonate decreases as the soil pH becomes alkaline (e.g. pH > 8.5). This favors higher nucleation rates and faster precipitation of smaller CaCO_3 crystals (Ma et al., 2010). Ionic strength controls the mole fraction of free water during CaCO_3 dissolution (Finneran and Morse, 2009). Therefore, CaCO_3 dissolution in saline soils takes longer and precipitation occurs earlier compared to salt-free soils.

1.3.4.4. Topography, soil position in the landscape and soil age

The topography and soil position in a landscape affect the total amounts, the accumulation rate and the accumulation depth of PC. The upper parts of a hillslope may contain no or few PC features, while thick calcretes may form at downslope positions because of groundwater presence or downslope flow of soil solution (Jacks and Sharma, 1995; Khadkikar et al., 1998). Stable land surfaces in a landscape usually show the greatest PC accumulation compared to the other positions. On unstable land surfaces the depth of PC accumulation and the total amount of PC in soil changes due to erosion and deposition.

Erosion increases the PC exposure into the percolating water front, and rewetting cycles promotes carbonate dissolution. PC dissolution followed by the translocation of ions leads to less PC accumulation in the soil profile or their deeper localization. It can lead to complex profiles with overprinting over multiple formation phases that have been formed during various climate cycles.

Deposition also changes the depth of water percolation, reducing the PC accumulation in a particular depth of the soil profile (Alonso-Zarza, 2003; Candy and Black, 2009; Gile, 1999). On stable land surfaces, total PC is positively correlated with soil age. Increasing amounts over time also creates various PC morphologies (Adamson et al., 2015; Badía et al., 2009; Bockheim and Douglass, 2006; Díaz-Hernández et al., 2003). Disperse PC accumulations increase with soil age, will be connected to each other and finally plug soil pores, forming calcrete (Fig.8). Therefore, various morphologies and stages for PC accumulation are used as an indicator of soil development (Fig. 8) (Amoroso, 2006; Gile et al., 1966; Machette, 1985; Pustovoytov, 2003).

1.3.4.5. Local vegetation and soil organisms

In the presence of active roots, carbonate dissolution increases by 5 to 10 times. Carbonate solubility increases near roots because of (1) up to 100 times higher CO₂ concentration in the rhizosphere versus atmosphere and (2) up to two units lower local pH because of H⁺ and carboxylic acid release by roots (Andrews and Schlesinger, 2001; Berthelin, 1988; Gocke et al., 2011b). The higher ions concentration leads to two-orders-of-magnitude-faster PC accumulation close to the roots compared to root-free soil (Gocke et al., 2011b; Kuzyakov et al., 2006), e.g. to rhizolith formation (Fig. 3). Note, however, differences in root distribution and thickness as well as variation in root respiration and exudation (Hamada and Tanaka, 2001; Kuzyakov and Domanski, 2002) change the PC formation rates under various plant species. For example, carbonate dissolution and re-precipitation under maize is higher than in soils covered by ryegrass because the root growing rates and exudation are higher under maize.

Soil microorganisms, i.e. bacteria and fungi, are also active in PC formation. If Ca²⁺ ions are available in solution, bacteria can produce a visible accumulation of carbonates within a few days (Monger et al., 1991). Extracellular polymers such as polysaccharides and amino acids may also control the morphology of CaCO₃ (Braissant et al., 2003). For example the presence of aspartic acids favors the formation of needle shape crystals (Braissant et al., 2003). However, even components of bacterial cells such as cell walls may act as nuclei of carbonate precipitation (Perito et al., 2014).

1.4. Carbon and oxygen in pedogenic carbonates

1.4.1. Sources of carbon, oxygen and calcium in pedogenic carbonates

Carbon in PC originates from dissolved CO₂ in soil solution (Eq. 1, 2). Respiration of roots and microorganisms and the decomposition of litter and SOM are the sole CO₂ sources in the soil air during the growing season (Karberg et al., 2005). However, in frozen soils or soils with very low respiration rates (e.g. dry hot deserts), the CO₂ concentration is partly controlled by the diffusion of atmospheric CO₂ into the soil (Cerling, 1984).

The source of oxygen in PC is related more to the soil water than to soil CO₂. This is confirmed by the close correlation between $\delta^{18}\text{O}$ of PC and mean $\delta^{18}\text{O}$ of local meteoric water (Cerling, 1984; Cerling and Quade, 1993).

Calcium in PC can originate from three sources: (1) dissolution of GC as limestone (and/or to a lesser extent dolostone) (Kelly et al., 1991; Rabenhorst and Wilding, 1986), (2) atmospheric deposition, which is the main source of Ca especially in non-calcareous soils (Naiman et al., 2000) and (3) weathering of Ca-bearing minerals other than carbonates (Landi et al., 2003; Naiman et al., 2000; Whipkey et al., 2000) such as augite, apatite, hornblende, gypsum, oligoclase and plagioclase.

1.4.2. Isotopic composition of carbon ($\delta^{13}\text{C}$, $\Delta^{14}\text{C}$) and oxygen ($\delta^{18}\text{O}$) in pedogenic carbonates

The isotopic signature of PC - $\delta^{13}\text{C}$ and $\delta^{18}\text{O}$ - is controlled by the isotopic composition of soil CO₂ and of water, respectively (Cerling, 1984). During the growing season, root and microorganism respiration is high and represents the only CO₂ source in soil (Cerling, 1984); the relative abundance of C₃ and C₄ plants in the local vegetation controls the $\delta^{13}\text{C}$ value of PC (Fig. 10). Due to isotopic discrimination by photosynthetic pathways, the $\delta^{13}\text{C}$ of CO₂ under C₃ plant species (-27‰ on average) differs from that under C₄ species (-13‰ on average) (Cerling et al., 1997). Further isotopic discrimination results from CO₂ diffusion in soil (ca. +4.4‰) and carbonate precipitation (ca. +11‰). Consequently, PC are ¹³C enriched by about 15‰ compared to the respired CO₂. The values are ca. -12‰ under pure C₃ and +2‰ under pure C₄ vegetation (Fig. 10).

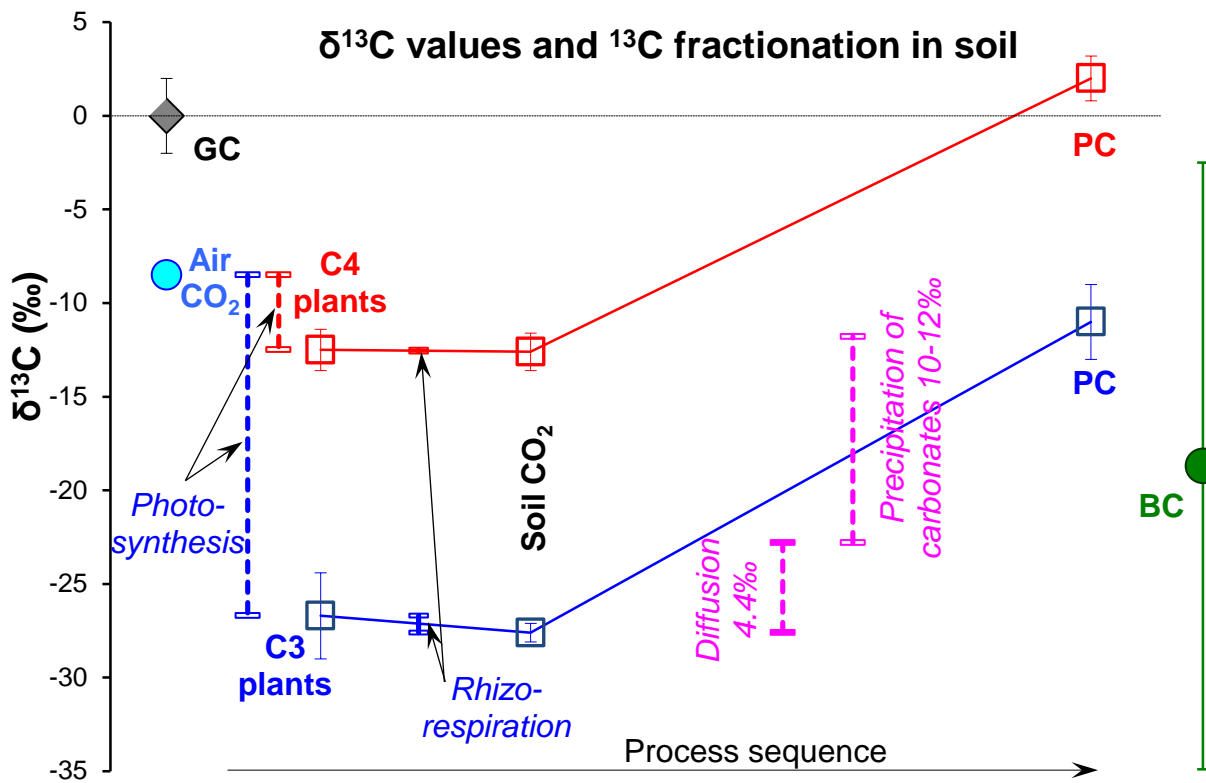


Figure 10: The $\delta^{13}\text{C}$ values of carbonate forms in soil (changed after Nordt et al., 1996). The $\delta^{13}\text{C}$ isotopic composition of soil CO_2 and thus of pedogenic carbonates (PC) is controlled by local vegetation (C_3 or C_4 plants) (Cerling, 1984). The mean $\delta^{13}\text{C}$ value and standard deviation for biogenic carbonates (BC) are calculated from: Dettman et al., 1999; Prendergast et al., 2015; Pustovoytov et al., 2010; Regev et al., 2011; Riera et al., 2013; Stern et al., 1994. Note the different ^{13}C fractionation by rhizorespiration for C_3 and C_4 plants (Werth and Kuzyakov, 2010). The ^{13}C fractionations are presented with dashed lines and mentioned in italics.

Since root and rhizomicrobial respiration are the dominant CO_2 sources in soils (Kuzyakov, 2006), SOM decomposition has a minor effect on ^{13}C of PC (Ueda et al., 2005). Diffusion of atmospheric CO_2 (global average $\delta^{13}\text{C} = -8.5\text{\textperthousand}$ in 2015) can further enrich ^{13}C in PC. Nonetheless, the effect of diffused atmospheric CO_2 is restricted maximally to the upper 50 cm of the soil (Cerling, 1984) and is negligible in the presence of vegetation.

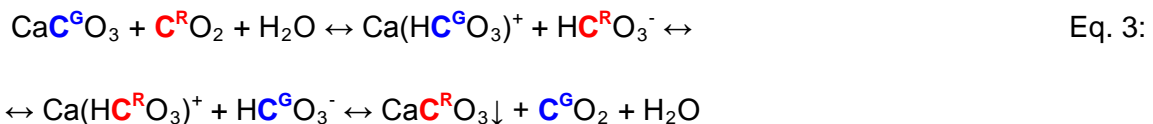
The $\Delta^{14}\text{C}$ of PC is determined by biological activities in soil. In contrast to $\delta^{13}\text{C}$, SOM decomposition affects $\Delta^{14}\text{C}$ in PC. Therefore, the relative proportion of CO_2 respired by the rhizosphere and the CO_2 released from SOM decomposition determine the ^{14}C abundance in PC.

The contribution of SOM decomposition to ^{14}C abundance in PC, however, is more important in deeper horizons. This is because the SOM age mostly increases with soil depth (i.e. the older the SOM, the more depleted the ^{14}C abundance) (Amundson et al., 1994).

The $\delta^{18}\text{O}$ of PC is controlled by the oxygen isotopic composition of meteoric water, from which carbonates originate (Cerling, 1984). Increasing evaporation leads to higher $\delta^{18}\text{O}$ depletion in PC (Liu et al., 1996; Zhou and Chafetz, 2010). Since the temperature controls the amount of evaporation, changes in the isotopic composition of meteoric water corresponds to mean annual air temperature (MAAT) (Cerling, 1984; Hsieh et al., 1998a, 1998b).

1.5. Implications of PC in paleoenvironmental and chronological studies

$\delta^{13}\text{C}$ and $\delta^{18}\text{O}$ as well as $\Delta^{14}\text{C}$ of PC are valuable proxies for paleoenvironmental and chronological investigations (Feeakins et al., 2013; Levin et al., 2011; Monger et al., 2009; Konstantin Pustovoytov et al., 2007; Wang et al., 1996). Dissolution of SIC and re-precipitation of dissolved ions (i.e. Ca^{2+} and DIC species) takes place under complete equilibrium with soil air CO_2 (Eq. 3) (Cerling, 1984; Nordt et al., 1996).



where the index ^G reflects the origin of carbon from geogenic carbonate present in soil before dissolution and ^R reflects the carbon origin from CO_2 respired by roots and microorganisms. Therefore, substituting $\text{HC}^{\text{G}}\text{O}_3^-$ by $\text{HC}^{\text{R}}\text{O}_3^-$ will conserve the $\delta^{13}\text{C}$ fingerprints of dominant vegetation within accumulated PC (Fig. 10) (Amundson et al., 1989; Cerling et al., 1989).

The $\Delta^{14}\text{C}$ of PC is applied to determine the absolute age of soils, sediments, cultural layers and late-Quaternary geomorphological units (Amundson et al., 1994; Chen and Polach, 1986; Gile, 1993; Pustovoytov et al., 2007; Pustovoytov and Leisten, 2002; Wang et al., 1996). The radiocarbon ages help to distinguish between individual stages of PC formation and correlate them to past environmental changes (Fig. 6) (Candy and Black, 2009; Pustovoytov et al., 2007).

Along with radiocarbon dating (age limit up to 60,000 years), the Th/U-technique allows estimation of crystal growth within longer time intervals during soil formation (age determination up to over 500,000 y) (Ku et al., 1979; Sharp et al., 2003; Candy et al., 2005; Durand et al., 2007;

Blisniuk et al., 2012). Uranium may be incorporated into the PC structure as impurities during crystal growth (see section 3.3, parent material). The broader age range that can be determined is the major advantage of application of the U/Th-dating to Quaternary carbonate materials. Some sedimentological settings have been suggested to be favorable for diagenetic contamination of carbonate by environmental uranium, which may result in younger measured ages (McLaren and Rowe, 1996). However, the U/Th ages of different carbonate samples usually show a good match with independently estimated ages of their contexts. Such inter comparisons are based on archaeological age estimations (Magnani et al., 2007), OSL and radiocarbon dating (Magee et al., 2009) or their combinations (Clark-Balzan et al., 2012). Although the sample quantities required for U/Th dating are larger compared to the ^{14}C AMS procedure, substantial reduction in sample size can be achieved through the use of multi-collector inductively coupled plasma mass spectrometry (Seth et al., 2003) and laser ablation techniques (Spooner et al., 2016).

Since the $\delta^{13}\text{C}$ of PC reflects that of soil CO_2 and is related to the $p\text{CO}_2$ in soil air and in the atmosphere, the $\delta^{13}\text{C}$ of PC can be used as a CO_2 paleobarometer to estimate the atmospheric CO_2 concentration during the formation time of PC (Huang et al., 2012; Retallack, 2009). This CO_2 paleobarometer shows a high potential for paleosols covered with pure C_3 vegetation (presumably most pre-Miocene soils) or if the proportion of C_4 biomass can be estimated (for example, if the humus horizons are preserved) (Ekart et al., 1999; Royer et al., 2001).

The $\delta^{13}\text{C}$ and $\delta^{18}\text{O}$ in the lattice of PC crystals enable estimating the temperature of PC formation (Ghosh et al., 2006a). The combination of ^{13}C and ^{18}O in CaCO_3 crystals, known as Δ_{47} or clumped isotopes, is the measuring $\delta^{18}\text{O}$ and $\delta^{13}\text{C}$ connected in one molecule simultaneously, for instance as $^{13}\text{C}^{18}\text{O}^{16}\text{O}$. The Δ_{47} value in a crystal lattice depends only on the environmental temperature: increasing the temperature will decrease the Δ_{47} in that crystal (Eiler, 2007). Therefore, the Δ_{47} value in PC can be used as a paleothermometer to estimate the temperature during PC formation (Ghosh et al., 2006a; Versteegh et al., 2013). The estimated PC formation temperature and the relation between environmental temperature and elevation enable drawing conclusions about the uplift range of geological surfaces (Ghosh et al., 2006b). Accordingly, the PC features now located at higher elevations with cooler temperature may have been formed in warmer environments (Peters et al., 2013).

1.6. Recrystallization of soil carbonates

All the above-mentioned applications of $\delta^{13}\text{C}$, $\Delta^{14}\text{C}$, $\delta^{18}\text{O}$ and clumped isotopes in PC are based on two assumptions:

- (1) The formed PC feature is completely free of GC admixtures.

(2) The formed PC feature represents a geochemically closed system. This means PC experiences no further cycle(s) of dissolution and re-precipitation (= recrystallization) after initial formation.

Deviations from these assumptions reveal uncertainties in chronological and re-constructional studies based on PC (Cerling, 1991; Pustovoytov and Leisten, 2002; Quast et al., 2006). Because recrystallization rates depend on various biotic and abiotic factors (Gocke et al., 2011b; Gocke and Kuzyakov, 2011), the resulting errors will differ, especially where recrystallization is relatively fast, e.g. in the presence of high root and microbial respiration (Gocke et al., 2011b; Kuzyakov et al., 2006).

The low solubility of carbonates ($K_{sp} = 10^{-6}$ - 10^{-9}) (Robbins, 1985) and consequently low recrystallization rates lead to difficulties in measuring these rates over short periods. Recently, however, it has been shown that the sensitive ^{14}C labeling approach (Gocke et al., 2011b, 2010; Kuzyakov et al., 2006) can contribute to a better understanding of the recrystallization dynamics and their effects on the isotopic composition of C in PC. This technique labels soil air with $^{14}\text{CO}_2$. By tracing the ^{14}C activity of a carbonate sample and knowing the amounts of added C as CO_2 , the amounts of recrystallized carbonates can be calculated. This approach was used to show the dependence of CaCO_3 recrystallization rates on (i) CO_2 concentration in soil (Gocke et al., 2010), (ii) presence of plants with various root systems (Gocke et al., 2011b), (iii) temperature (Gocke and Kuzyakov, 2011), and (iv) migration of recrystallized CaCO_3 along soil profile (Gocke et al., 2012). The very slow rates assessed by the ^{14}C labeling approach (about 0.00003 day^{-1}) demonstrated that at least centuries or probably even several millennia are necessary for full recrystallization and thus for complete formation of PC (Kuzyakov et al., 2006). This means that the first assumption may not be achieved even after a long time, at least in PC features formed in loess deposits. Furthermore, the exponential nature of recrystallization (Kuzyakov et al., 2006) – partial re-dissolution and recrystallization of formed PC – may also make the second assumption questionable.

1.6.1. Uncertainties of paleoenvironmental reconstructions based on pedogenic carbonates

The recrystallization of PC under conditions different from the environment during PC formation (e.g. changes in local vegetation or environmental temperature) will strongly complicate the application of the isotopic signature of PC for paleo-reconstruction studies. The new isotopic signals of a PC feature will reflect the altered and not the original environmental conditions (Pendall et al., 1994). Considering the first assumption, mixing of old PC as well as "dead" (i.e. not applicable for radiocarbon dating) limestone particles with newly formed PC overestimates the absolute ages of

soils, landscape or geomorphological surfaces (Pendall et al., 1994; Pustovoytov and Terhorst, 2004). For instance, if only 1% dead limestone particle remain in the structure of a given PC specimen (i.e. not full recrystallization of GC), the age of PC will be overestimated by more than two times. If the amount of remaining GC is 5%, the age overestimation will increase to about 10 times (Kuzyakov et al., 2006). Moreover, the difference of $\delta^{13}\text{C}$ values of the remaining GC to that of PC (Fig. 10) leads to a less negative $\delta^{13}\text{C}$ of PC (Pendall et al., 1994; Quast et al., 2006) and consequently to doubtful paleoecological interpretations.

Recrystallization will also affect the stable isotopic signature and interpretations for paleoenvironmental studies and PC-based radiocarbon dating. If only 1% of modern ^{14}C is mixed with a dead limestone specimen, the age estimation will be 36,500 years. Increasing the contamination with modern ^{14}C to 10% alters the age of that limestone to about 18,500 years (Williams and Polach, 1969).

PC recrystallization also affects $\delta^{18}\text{O}$ (Cerling, 1991) and may thus overestimate PC formation temperature by up to 20 °C (Ghosh et al., 2006b). Therefore, interpretation of the $\delta^{13}\text{C}$, $\Delta^{14}\text{C}$, $\delta^{18}\text{O}$ and Δ_{47} signatures in PC for paleoenvironmental reconstructions and dating should consider possible deviations from the above-mentioned assumptions.

Formation of PC following BC dissolution will also affect the chronological and paleoecological interpretations based on BC. In archeological sites, various BC types preserved in soils are frequently used to interpret their isotopic signatures. This includes:

- Shells (i.e. mollusk shells) (Xu et al., 2010; Yanes et al., 2013)
- Bone pieces (Berna et al., 2004; Krueger, 1991; Zazzo et al., 2009)
- Eggshell particles (Janz et al., 2009; Kandel and Conard, 2005; Long et al., 1983; Vogel et al., 2001)
- Tooth enamel and dentin (Feakins et al., 2013; Hedges et al., 1995; Hoppe et al., 2004)
- Old wood ashes (Regev et al., 2011) and calcified fossil seeds (Pustovoytov et al., 2004; Regev et al., 2011).

BC features are used to recognize the settlements or habitats, diet regimes and extinction periods of ancient humans, animals and plants (Hoppe et al., 2004; Janz et al., 2009; Kandel and Conard, 2005) as well as to reconstruct the environmental conditions during their lifetimes (Villagrán

and Poch, 2014; Xu et al., 2010; Yanes et al., 2013). PC formation and mixing with fossil BC will complicate the results of such paleo-reconstruction studies, e.g. the age of a 45,000 y-old bone will be estimated 20,000 y if only 5% contamination with modern C took place (Zazzo and Saliège, 2011). Paleoenvironmental reconstructions and dating based on PC as well as BC should consider possible recrystallization and isotopic exchange.

1.6.2. Evidence of pedogenic carbonate recrystallization after formation

The recrystallization of PC features after formation can be recognized in isotopic composition as well as morphology. The following evidence confirms the recrystallization of PC features in different environmental conditions as the dominant process during their formation.

(a) Relatively young radiocarbon ages of PC features compared to geological periods are usually explained by admixtures of modern ^{14}C during recrystallization (Pustovoytov and Terhorst, 2004). A correspondence between measured $\Delta^{14}\text{C}$ ages of PC with other chronological data is therefore used to evaluate the PC contamination and the reliability of achieved dates. The other chronological data include stratigraphy of the sampling context or the ages of accompanying datable compounds such as organic C and artefacts (Pustovoytov and Terhorst, 2004; Vogel et al., 2001).

(b) Large $\delta^{13}\text{C}$ variation in PC from paleosols with similar ages (and probable similar vegetation and $p\text{CO}_2$ in the respective geological period) is referred to recrystallization. In contrast, fewer $\delta^{13}\text{C}$ differences in PC from contrasting geological time spans are also introduced as recrystallization evidence (Quast et al., 2006).

(c) The size of PC features is positively correlated to the $\delta^{13}\text{C}$ signature of recently recrystallized carbonates (Kraimer and Monger, 2009). The smaller the PC size, the more $\delta^{13}\text{C}$ changes due to recrystallization is expected.

(d) The microscopic indications of PC dissolution under a polarized microscope can be recognized as follows (Durand et al., 2010):

1. PC grains with well-rounded shapes.
2. Presence of crystals with pronounced serration.
3. Formation of mouldic voids (e.g. preferential dissolution of shell fragments leaves empty spaces previously occupied by carbonates).

4. Clay-coating networks without carbonate crystals (formed after partial dissolution of carbonate grains and further clay illuviation with pore filling).
5. Depletion of hypocoatings (i.e. soil carbonate-free matrix around voids such as channels).
 - (e) The dissolved ions may recrystallize on the former PC feature. The microscopic evidence of such recrystallization is (Durand et al., 2010):
 1. Irregular distribution of crystal size and mottled crystal mosaics of different sizes (i.e. replacement of finer crystals with coarser ones).
 2. Star-like masses of elongated and radially arranged sparite crystals around a central zone of microsparite crystals.
 3. Curved contacts between neighboring sparitic ($> 20 \mu\text{m}$) carbonate crystals.

1.7. Conclusions and outlook

1.7.1. Conclusions

Various formation mechanisms and environmental factors result in distinct morphological features of PC such as nodules and coatings, which form in various time spans – from a few weeks (e.g. hypocoatings) and decades (e.g. rhizoliths) to hundreds of thousands or even millions of years (e.g. calcrete). PC forms therefore reflect soil genesis processes and record the effects of soil-forming factors. $\delta^{13}\text{C}$, $\Delta^{14}\text{C}$ and $\delta^{18}\text{O}$ as well as Δ_{47} in PC are valuable tools for paleoenvironmental reconstructions and soil age estimation. PC features, however, have variable physical and chemical properties including various CaCO_3 contents and impurities. This reflects the response of PC features to environmental conditions such as changes in local vegetation or climatic properties. Furthermore, depending on the duration of PC formation period, the isotopic inventory of individual PC features will reveal different resolutions in paleo-reconstruction and chronological studies.

PC can undergo recrystallization after formation. This complicates the interpretations of paleoenvironment records and chronological studies based on PC isotopic composition. Every recrystallization cycle may occur under new environmental conditions – i.e. climate or local vegetation – differing from the previous one. Full or even partial re-equilibration to the new environment will insert new signals into the isotopic inventory of PC. Recrystallization therefore resets the radiometric clock by adding modern ^{14}C to the isotopic inventory of PC. It can therefore lead to a strongly biased assessment of air $p\text{CO}_2$ or temperature (as well as vegetation or

precipitation) for the period of PC formation. The result is misleading paleoenvironmental reconstructions. Nonetheless, incorporating the variety of PC features (with corresponding formation mechanisms and time, as well as physical and chemical properties and microscopic indications) enables considering how recrystallization may have altered the isotopic composition of PC features.

Future research directions

Based on the overview of the mechanisms and rates of PC formation and of their applications for reconstructing soil genesis and paleoenvironment, as well as considering the huge SIC stocks in soil, the following research directions can be grouped into three issues:

(1) Mechanisms and rates of PC formation

- The effects of biotic processes such as respiration (CO_2 concentration), carboxylic acid excretion (pH changes) or water uptake (Ca concentration in rhizosphere) by plants and microorganisms on PC formation were shown in a few studies (Kuzyakov et al., 2006; Monger et al., 1991). However, the biotic activities are frequently disregarded with respect to PC formation. This calls for demonstrating the importance of biota for PC formation under a broad range of environmental conditions. It remains unclear whether PC can be formed in the absence of biological activity at all.
- Both roots and microorganisms may have similar functions in PC formation: respiration, acid release, etc. We are not aware of any study comparing the importance of roots or microorganisms for PC formation. This should be done for individual PC forms.
- Various plant species such as shrubs, grasses and herbs have different root systems, rooting depth and resistance to higher pH due to CaCO_3 accumulation. How various plant species affect PC formation rates as well as the depth of PC accumulation should be clarified.
- Formation mechanisms of various PC features and the budget of the elements (e.g. Ca) remain unclear. More studies such as comparisons of the Ca content in parent material as well as in soil layers with PC are needed to identify the Ca source(s) in PC.

(2) Implications for paleoenvironment reconstructions and soil genesis

- The reliability of PC features as proxies for paleoenvironment reconstructions and dating purposes is still questionable because of recrystallization. This calls for quantifying how the environmental factors such as soil moisture, temperature, initial GC content, and the depth of PC

formation affect PC recrystallization. In this respect, ^{14}C labeling of soil CO_2 showed high potential for understanding the dynamics of carbonate recrystallization in soils (Kuzyakov et al., 2006). The radiometric ages of PC features should be compared with independently estimated ages of their contexts, such as archeological sites or geomorphic landscape elements. Furthermore, long-term experimental observation of CaCO_3 alteration with time in native soils can serve as a good complimentary approach.

- Individual PC features, considering variations in their physical and chemical properties, should respond differently to changes in environmental conditions, i.e. will have different recrystallization rates. Therefore, the recrystallization rates of various PC features should be compared under identical environmental conditions.

- A part of ^{13}C enrichment in PC comparing to the respiration CO_2 is because of soil CO_2 diffusion (Cerling, 1984). The CO_2 diffusion in soil (and thus changes in $\delta^{13}\text{C}$ of PC) is, however, related to soil properties such as soil water content, temperature and clay content as well as the diffusion distance within the soil profile. The above-mentioned 4.4‰ ^{13}C enrichment in soil CO_2 by diffusion should therefore be analyzed for various soils with contrasting physical and chemical properties.

(3) Natural and anthropogenic effects on PC and consequences for the concentration of atmospheric CO_2

- The contribution of CaCO_3 to CO_2 fluxes from soil to the atmosphere because of fertilization and management is completely unknown. Soil acidification due to urea or ammonium fertilization as well as legume cultivation strongly affects CaCO_3 dissolution and CO_2 release to the atmosphere. This calls for investigating the effects of various soil cultivation systems such as fertilizer forms and levels, as well as management practices – till, no-till, liming, irrigation frequency and other managements – on CaCO_3 dissolution and CO_2 efflux. These anthropogenic effects on CaCO_3 dissolution should be compared to the rates of natural acidification processes related to litter decomposition and rhizosphere fluxes of H^+ ions and organic acids.

- Development of a mechanism-based model predicting the upper and maximal depths of PC accumulation in soil profiles is important for understanding soil genesis as well as fertilization and irrigation management. This requires incorporating the relations between the depth of PC accumulation and various environmental parameters – not only mean annual precipitation as in Fig. 9 but also soil water balance, its seasonal dynamics, the initial carbonate content in parent material and soil physical properties.

Concluding, despite the importance of SIC and PC for terrestrial C stocks and the global C cycle, the number of studies on SIC is very limited, especially compared to those dealing with SOC. Most of these studies were descriptive, focused on the presentation of properties, contents, forms and depths of PC. Only few studies attempted to develop the concepts and models of PC formation mechanisms and relate them to environmental factors. Such a mechanism-based understanding and models will strongly contribute to predicting terrestrial C stocks and changes in the global C cycle. This will help closely link long-term geological with short-term biological C cycles.

1.8. Acknowledgements

We would like to acknowledge the German Research Foundation (DFG) for their support (KU 1184/34-1). Special thanks to Dr. Otto Ehrmann (<http://www.bildarchiv-boden.de>) for providing us photos of earthworm biospherolith (fig. 2, right) and calcite hypocoating (fig. 4, right). Special thanks to Miss. Yue Sun for drawing graphics in Figures 3, 4, 6 and 8. We would like to thank the Soil Science Department, University of Tehran (Karaj, Iran), for their help in preparing soil thin sections and the University of Tarbiat Modares (Tehran, Iran) for SEM images of calcified root cells (Fig. 3).

1.9. References

- Adams, J.M., Post, W.M., 1999. A preliminary estimate of changing calcrete carbon storage on land since the Last Glacial Maximum. *Glob. Planet. Change* 20, 243–256. doi:10.1016/S0921-8181(99)00015-6
- Adamson, K., Candy, I., Whitfield, L., 2015. Coupled micromorphological and stable isotope analysis of Quaternary calcrete development. *Quat. Res.* xxx, xxx–xxx. doi:10.1016/j.yqres.2015.05.002
- Alonso-Zarza, A.M., 2003. Palaeoenvironmental significance of palustrine carbonates and calcretes in the geological record. *Earth-Sci. Rev.* 60, 261–298. doi:10.1016/S0012-8252(02)00106-X
- Alonso-Zarza, A.M., 1999. Initial stages of laminar calcrete formation by roots: examples from the Neogene of central Spain. *Sediment. Geol.* 126, 177–191. doi:10.1016/S0037-0738(99)00039-1
- Amit, R., Simhai, O., Ayalon, A., Enzel, Y., Matmon, A., Crouvi, O., Porat, N., McDonald, E., 2011. Transition from arid to hyper-arid environment in the southern Levant deserts as recorded by early Pleistocene cumbulic Aridisols. *Quat. Sci. Rev.* 30, 312–323. doi:10.1016/j.quascirev.2010.11.007
- Amoroso, L., 2006. Age calibration of carbonate rind thickness in late Pleistocene soils for surficial deposit age estimation, Southwest USA. *Quat. Res.* 65, 172–178. doi:10.1016/j.yqres.2005.06.003

Amundson, R.G., Doner, H.E., Chadwick, O.A., Sowers, J.M., 1989. The Stable Isotope Chemistry of Pedogenic Carbonates at Kyle Canyon, Nevada. *Soil Sci. Soc. Am. J.* 53, 201. doi:10.2136/sssaj1989.03615995005300010037x

Amundson, R., Graham, R.C., Franco-Vizcaíno, E., 1997. Orientation of Carbonate Laminations in Gravelly Soils Along A Winter/Summer Precipitation Gradient in Baja California, Mexico. *Soil Sci.* 162, 940–952. doi:10.1097/00010694-199712000-00009

Amundson, R., Wang, Y., Chadwick, O., Trumbore, S., McFadden, L., McDonald, E., Wells, S., DeNiro, M., 1994. Factors and processes governing the ^{14}C content of carbonate in desert soils. *Earth Planet. Sci. Lett.* 125, 385–405. doi:10.1016/0012-821X(94)90228-3

Andrews, J.A., Schlesinger, W.H., 2001. Soil CO₂ dynamics, acidification, and chemical weathering in a temperate forest with experimental CO₂ enrichment. *Glob. Biogeochem. Cycles* 15, 149–162. doi:10.1029/2000GB001278

Aylward, G.H., 2007. SI chemical data, Auflage: 6. Auflage. ed. John Wiley & Sons, Milton, Qld.

Badía, D., Martí, C., Palacio, E., Sancho, C., Poch, R.M., 2009. Soil evolution over the Quaternary period in a semiarid climate (Segre river terraces, northeast Spain). *CATENA* 77, 165–174. doi:10.1016/j.catena.2008.12.012

Barker, S.L. I., Cox, S.F., 2011. Oscillatory zoning and trace element incorporation in hydrothermal minerals: insights from calcite growth experiments. *Geofluids* 11, 48–56. doi:10.1111/j.1468-8123.2010.00305.x

Barta, G., 2011. Secondary carbonates in loess-paleosoil sequences: a general review. *Cent. Eur. J. Geosci.* 3, 129–146. doi:10.2478/s13533-011-0013-7

Batjes, N. h., 1996. Total carbon and nitrogen in the soils of the world. *Eur. J. Soil Sci.* 47, 151–163. doi:10.1111/j.1365-2389.1996.tb01386.x

Baumhardt, R.L., Lascano, R.J., 1993. physical and hydraulic properties of a calcic horizon. *Soil Sci.* 155, 368–375. doi:10.1097/00010694-199306000-00002

Becze-Deák, J., Langohr, R., Verrecchia, E.P., 1997. Small scale secondary CaCO₃ accumulations in selected sections of the European loess belt. Morphological forms and potential for paleoenvironmental reconstruction. *Geoderma* 76, 221–252. doi:10.1016/S0016-7061(96)00106-1

Berna, F., Matthews, A., Weiner, S., 2004. Solubilities of bone mineral from archaeological sites: the recrystallization window. *J. Archaeol. Sci.* 31, 867–882. doi:10.1016/j.jas.2003.12.003

Berthelin, J., 1988. Microbial Weathering Processes in Natural Environments, in: Lerman, A., Meybeck, M. (Eds.), *Physical and Chemical Weathering in Geochemical Cycles*, NATO ASI Series. Springer Netherlands, pp. 33–59.

Birkeland, 1999. *Soils and Geomorphology*. Oxford University Press.

Blisniuk, K., Osokin, M., Fletcher, K., Rockwell, T., Sharp, W., 2012. Assessing the reliability of U-series and 10Be dating techniques on alluvial fans in the Anza Borrego Desert, California. *Quat. Geochronol.* 13, 26–41. doi:10.1016/j.quageo.2012.08.004

Bockheim, J.G., Douglass, D.C., 2006. Origin and significance of calcium carbonate in soils of southwestern Patagonia. *Geoderma* 136, 751–762. doi:10.1016/j.geoderma.2006.05.013

Boettinger, J.L., Southard, R.J., 1991. Silica and Carbonate Sources for Aridisols on a Granitic Pediment, Western Mojave Desert. *Soil Sci. Soc. Am. J.* 55, 1057. doi:10.2136/sssaj1991.03615995005500040028x

Borchardt, G., Lienkaemper, J.J., 1999. Pedogenic calcite as evidence for an early Holocene dry period in the San Francisco Bay area, California. *Geol. Soc. Am. Bull.* 111, 906–918.

Braissant, O., Cailleau, G., Dupraz, C., Verrecchia, E.P., 2003. Bacterially induced mineralization of calcium carbonate in terrestrial environments: the role of exopolysaccharides and amino acids. *J. Sediment. Res.* 73, 485–490. doi: 10.1306/111302730485

Brock, A.L., Buck, B.J., 2009. Polygenetic development of the Mormon Mesa, NV petrocalcic horizons: Geomorphic and paleoenvironmental interpretations. *CATENA* 77, 65–75. doi:10.1016/j.catena.2008.12.008

Brock, A.L., Buck, B.J., 2005. A new formation process for calcic pendants from Pahranagat Valley, Nevada, USA, and implication for dating Quaternary landforms. *Quat. Res.* 63, 359–367. doi:10.1016/j.yqres.2005.01.007

Bughio, M.A., Wang, P., Meng, F., Qing, C., Kuzyakov, Y., Wang, X., Junejo, S.A., 2016. Neoformation of pedogenic carbonates by irrigation and fertilization and their contribution to carbon sequestration in soil. *Geoderma* 262, 12–19. doi:10.1016/j.geoderma.2015.08.003

Callot, G., Chamayou, H., Maertens, C., Salsac, L., 1982. Mieux comprendre les interactions sol-racine. Incidence sur la nutrition minerale. INRA.

Candy, I., Black, S., 2009. The timing of Quaternary calcrete development in semi-arid southeast Spain: Investigating the role of climate on calcrete genesis. *Sediment. Geol.* 218, 6–15. doi:10.1016/j.sedgeo.2009.03.005

Candy, I., Black, S., Sellwood, B.W., 2005. U-series isochron dating of immature and mature calcretes as a basis for constructing Quaternary landform chronologies for the Sorbas basin, southeast Spain. *Quat. Res.* 64, 100–111. doi:10.1016/j.yqres.2005.05.002

Capo, R.C., Chadwick, O.A., 1999. Sources of strontium and calcium in desert soil and calcrete. *Earth Planet. Sci. Lett.* 170, 61–72.

Catoni, M., Falsone, G., Bonifacio, E., 2012. Assessing the origin of carbonates in a complex soil with a suite of analytical methods. *Geoderma* 175–176, 47–57. doi:10.1016/j.geoderma.2012.01.022

Cerling, T.E., 1991. Carbon Dioxide in the atmosphere: evidence from Cenozoic and Mesozoic paleosols. *Am. J. Sci.* 291, 377–400. doi:10.2475/ajs.291.4.377

Cerling, T.E., 1984. The stable isotopic composition of modern soil carbonate and its relationship to climate. *Earth Planet. Sci. Lett.* 71, 229–240. doi:10.1016/0012-821X(84)90089-X

Cerling, T.E., Quade, J., 1993. Stable Carbon and Oxygen Isotopes in Soil Carbonates, in: Swart, P.K., Lohmann, K.C., Mckenzie, J., Savin, S. (Eds.), *Climate Change in Continental Isotopic Records*. American Geophysical Union, pp. 217–231.

Cerling, T.E., Quade, J., Wnag, Y., Bowman, J.R., 1989. Carbon isotopes in soils and palaeosols as ecology and palaeoecology indicators. *Nature* 341, 139–139. doi:10.1038/341138a0

Chadwick, O.A., Sowers, J.M., Amundson, R.G., 1989. Morphology of calcite crystals in clast coatings from four soils in the Mojave desert region. *Soil Sci. Soc. Am. J.* 53, 211–219.

Chen, Y., Polach, H., 1986. Validity of ^{14}C ages of carbonate in sediments. *Radiocarbon* 28, 464–472. doi:10.2458/azu_js_rc.28.957

Chiquet, A., Michard, A., Nahon, D., Hamelin, B., 1999. Atmospheric input vs in situ weathering in the genesis of calcretes: An Sr isotope study at Galvez (Central Spain). *Geochim. Cosmochim. Acta* 63, 311–323.

Clark-Balzan, L.A., Candy, I., Schwenninger, J-L., Bouzouggar, A., Blockley, S., Nathan, R., Barton, N.E., 2012. Coupled U-series and OSL dating of a Late Pleistocene cave sediment sequence, Morocco, North Africa: Significance for constructing Palaeolithic chronologies. *Quaternary Geochronology*, 12. 53-64.

- Courty, M.-A., Marlin, C., Dever, L., Tremblay, P., Vachier, P., 1994. The properties, genesis and environmental significance of calcitic pendants from the High Arctic (Spitsbergen). *Geoderma* 61, 71–102. doi:10.1016/0016-7061(94)90012-4
- Dettman, D.L., Reische, A.K., Lohmann, K.C., 1999. Controls on the stable isotope composition of seasonal growth bands in aragonitic fresh-water bivalves (unionidae). *Geochim. Cosmochim. Acta* 63, 1049–1057. doi:10.1016/S0016-7037(99)00020-4
- Díaz-Hernández, J.L., Fernández, E.B., González, J.L., 2003. Organic and inorganic carbon in soils of semiarid regions: a case study from the Guadix–Baza basin (Southeast Spain). *Geoderma* 114, 65–80. doi:10.1016/S0016-7061(02)00342-7
- Drees, L.R., Wilding, L.P., Nordt, L.C., 2001. Reconstruction of soil inorganic and organic carbon sequestration across broad geoclimatic regions, in: Soil Carbon Sequestration and the Greenhouse Effect, SSSA Special Publication Number 57. Soil Science Society of America, Inc., Madison, WI, USA.
- Durand, N., Monger, H.C., Canti, M.G., 2010. Calcium Carbonate Features, in: Interpretation of Micromorphological Features of Soils and Regoliths. Elsevier, pp. 149–194.
- Egli, M., Fitze, P., 2001. Quantitative aspects of carbonate leaching of soils with differing ages and climates. *CATENA* 46, 35–62. doi:10.1016/S0341-8162(01)00154-0
- Eiler, J.M., 2007. “Clumped-isotope” geochemistry—The study of naturally-occurring, multiply-substituted isotopologues. *Earth Planet. Sci. Lett.* 309–327. doi:10.1016/j.epsl.2007.08.020
- Eisenlohr, L., Meteva, K., Gabrovšek, F., Dreybrodt, W., 1999. The inhibiting action of intrinsic impurities in natural calcium carbonate minerals to their dissolution kinetics in aqueous H₂O–CO₂ solutions. *Geochim. Cosmochim. Acta* 63, 989–1001. doi:10.1016/S0016-7037(98)00301-9
- Ekart, D.D., Cerling, T.E., Montanez, I.P., Tabor, N.J., 1999. A 400 million year carbon isotope record of pedogenic carbonate: implications for paleoatmospheric carbon dioxide. *Am. J. Sci.* 299, 805–827.
- Elis, F., 2002. Contribution of termites to the formation of hardpans in soils of arid and semiarid region of south africa. Presented at the 17th WCSS, Thiland.
- Emmerich, W.E., 2003. Carbon dioxide fluxes in a semiarid environment with high carbonate soils. *Agric. For. Meteorol.* 116, 91–102.
- Eswaran, H., Reich, P.F., Kimble, J.M., Beinroth, F.H., Padmanabhan, E., Moncharoen, P., 2000. Global carbon stocks, in: Lal, R., Kimble, J.M., Eswaran, H., Stewart, B.A. (Eds.), *Global Climate Change and Pedogenic Carbonates*. CRC Press, Boca Raton, Fla, pp. 15–25.
- FAO, 1996. Global climate change and agricultural production. Direct and indirect effects of changing hydrological, pedological and plant physiological processes. John Wiley & Sons Ltd., West Sussex, England.
- Feakins, S.J., Levin, N.E., Liddy, H.M., Sieracki, A., Eglinton, T.I., Bonnefille, R., 2013. Northeast African vegetation change over 12 m.y. *Geology* 41, 295–298. doi:10.1130/G33845.1
- Finneran, D.W., Morse, J.W., 2009. Calcite dissolution kinetics in saline waters. *Chem. Geol.* 268, 137–146. doi:10.1016/j.chemgeo.2009.08.006
- Gabitov, R.I., Gaetani, G.A., Watson, E.B., Cohen, A.L., Ehrlich, H.L., 2008. Experimental determination of growth rate effect on U⁶⁺ and Mg²⁺ partitioning between aragonite and fluid at elevated U⁶⁺ concentration. *Geochim. Cosmochim. Acta* 72, 4058–4068. doi:10.1016/j.gca.2008.05.047

- Georgen, P.G., Davis-Carter, J., Taylor, H.M., 1991. Root Growth and Water Extraction Patterns from a Calcic Horizon. *Soil Sci. Soc. Am. J.* 55, 210. doi:10.2136/sssaj1991.03615995005500010036x
- Ghosh, P., Adkins, J., Affek, H., Balta, B., Guo, W., Schable, E.A., Schrag, D., Eiler, J.M., 2006a. ^{13}C - ^{18}O bonds in carbonate minerals: A new kind of paleothermometer. *Geochim. Cosmochim. Acta* 70, 1439–1456. doi:10.1016/j.gca.2005.11.014
- Ghosh, P., Garzione, C.N., Eiler, J.M., 2006b. Rapid Uplift of the Altiplano Revealed Through ^{13}C - ^{18}O Bonds in Paleosol Carbonates. *Science* 311, 511–515. doi:10.1126/science.1119365
- Gile, L.H., 1999. Eolian and Associated Pedogenic Features of the Jornada Basin Floor, Southern New Mexico. *Soil Sci. Soc. Am. J.* 63, 151. doi:10.2136/sssaj1999.03615995006300010022x
- Gile, L.H., 1993. Carbonate stages in sandy soils of the Leasburg Surface, southern New Mexico. *Soil Sci.* 156, 101–110. doi:10.1097/00010694-199308000-00006
- Gile, L.H., 1961. A Classification of ca Horizons in Soils of a Desert Region, Dona Ana County, New Mexico1. *Soil Sci. Soc. Am. J.* 25, 52. doi:10.2136/sssaj1961.03615995002500010024x
- Gile, L.H., Peterson, F.F., Grossman, R.B., 1966. Morphological and genetic sequences of carbonate accumulation in desert soils. *Soil Sci.* 101. doi:10.1097/00010694-196605000-00001
- Gocke, M., Kuzyakov, Y., 2011. Effect of temperature and rhizosphere processes on pedogenic carbonate recrystallization: Relevance for paleoenvironmental applications. *Geoderma* 166, 57–65. doi:10.1016/j.geoderma.2011.07.011
- Gocke, M., Pustovoytov, K., Kühn, P., Wiesenberg, G.L.B., Löscher, M., Kuzyakov, Y., 2011a. Carbonate rhizoliths in loess and their implications for paleoenvironmental reconstruction revealed by isotopic composition: $\delta^{13}\text{C}$, ^{14}C . *Chem. Geol.* 283, 251–260. doi:10.1016/j.chemgeo.2011.01.022
- Gocke, M., Pustovoytov, K., Kuzyakov, Y., 2012. Pedogenic carbonate formation: Recrystallization versus migration—Process rates and periods assessed by ^{14}C labeling. *Glob. Biogeochem. Cycles* 26, GB1018. doi:10.1029/2010GB003871
- Gocke, M., Pustovoytov, K., Kuzyakov, Y., 2011b. Carbonate recrystallization in root-free soil and rhizosphere of *Triticum aestivum* and *Lolium perenne* estimated by ^{14}C labeling. *Biogeochemistry* 103, 209–222. doi:10.1007/s10533-010-9456-z
- Gocke, M., Pustovoytov, K., Kuzyakov, Y., 2010. Effect of CO₂ concentration on the initial recrystallization rate of pedogenic carbonate — Revealed by ^{14}C and ^{13}C labeling. *Geoderma* 155, 351–358. doi:10.1016/j.geoderma.2009.12.018
- Goudie, A., 1972. The Chemistry of World Calcrete Deposits. *J. Geol.* 80, 449–463.
- Hamada, Y., Tanaka, T., 2001. Dynamics of carbon dioxide in soil profiles based on long-term field observation. *Hydrol. Process.* 15, 1829–1845. doi:10.1002/hyp.242
- Hedges, R.M., Lee-Thorp, J.A., Tuorss, N.C., 1995. Is Tooth Enamel Carbonate a Suitable Material for Radiocarbon Dating? *Radiocarbon* 37, 285–290. doi:10.2458/azu_js_rc.37.1675
- Heidari, A., Mahmoodi, S., Stoops, G., Mees, F., 2004. Micromorphological Characteristics of Vertisols of Iran, Including Nonsmectitic Soils. *Arid Land Res. Manag.* 19, 29–46. doi:10.1080/15324980590887164
- Hinsinger, P., 1998. How Do Plant Roots Acquire Mineral Nutrients? Chemical Processes Involved in the rhizosphere. *Adv. Agron. - ADVAN AGRON* 64, 225–265. doi:10.1016/S0065-2113(08)60506-4

- Hoppe, K.A., Stover, S.M., Pascoe, J.R., Amundson, R., 2004. Tooth enamel biomineralization in extant horses: implications for isotopic microsampling. *Palaeogeogr. Palaeoclimatol. Palaeoecol.* 206, 355–365. doi:10.1016/j.palaeo.2004.01.012
- Hough, B.G., Fan, M., Passey, B.H., 2014. Calibration of the clumped isotope geothermometer in soil carbonate in Wyoming and Nebraska, USA: Implications for paleoelevation and paleoclimate reconstruction. *Earth Planet. Sci. Lett.* 391, 110–120. doi:10.1016/j.epsl.2014.01.008
- Hsieh, J.C.C., Chadwick, O.A., Kelly, E.F., Savin, S.M., 1998a. Oxygen isotopic composition of soil water: Quantifying evaporation and transpiration. *Geoderma* 82, 269–293. doi:10.1016/S0016-7061(97)00105-5
- Hsieh, J.C.C., Savin, .Samuel M., Kelly, E.F., Chadwick, O.A., 1998b. Measurement of soil-water $\delta^{18}\text{O}$ values by direct equilibration with CO₂. *Geoderma* 82, 255–268. doi:10.1016/S0016-7061(97)00104-3
- Hsieh, Y.-P., 1993. Radiocarbon Signatures of Turnover Rates in Active Soil Organic Carbon Pools. *Soil Sci. Soc. Am. J.* 57, 1020. doi:10.2136/sssaj1993.03615995005700040023x
- Huang, C.M., Retallack, G.J., Wang, C.S., 2012. Early Cretaceous atmospheric pCO₂ levels recorded from pedogenic carbonates in China. *Cretac. Res.* 33, 42–49. doi:10.1016/j.cretres.2011.08.001
- IPCC, 2007. Climate Change 2007: Synthesis Report.
- Jacks, G., Sharma, V.P., 1995. Geochemistry of calcic horizons in relation to hillslope processes, southern India. *Geoderma* 67, 203–214. doi:10.1016/0016-7061(95)00002-6
- Jaillard, B., 1987. Les structures rhizomorphes calcaires: modèle de reorganisation des minéraux du sol par les racines. Montpellier.
- Janz, L., Elston, R.G., Burr, G.S., 2009. Dating North Asian surface assemblages with ostrich eggshell: implications for palaeoecology and extirpation. *J. Archaeol. Sci.* 36, 1982–1989. doi:10.1016/j.jas.2009.05.012
- Kandel, A.W., Conard, N.J., 2005. Production sequences of ostrich eggshell beads and settlement dynamics in the Geelbek Dunes of the Western Cape, South Africa. *J. Archaeol. Sci.* 32, 1711–1721. doi:10.1016/j.jas.2005.05.010
- Karberg, N.J., Pregitzer, K.S., King, J.S., Friend, A.L., Wood, J.R., 2005. Soil carbon dioxide partial pressure and dissolved inorganic carbonate chemistry under elevated carbon dioxide and ozone. *Oecologia* 142, 296–306. doi:10.1007/s00442-004-1665-5
- Kelly, E.F., Amundson, R.G., Marino, B.D., DeNiro, M.J., 1991. Stable Carbon Isotopic Composition of Carbonate in Holocene Grassland Soils. *Soil Sci. Soc. Am. J.* 55, 1651. doi:10.2136/sssaj1991.03615995005500060025x
- Khadkikar, A.S., Merh, S.S., Malik, J.N., Chamyal, L.S., 1998. Calcretes in semi-arid alluvial systems: formative pathways and sinks. *Sediment. Geol.* 116, 251–260. doi:10.1016/S0037-0738(97)00103-6
- Khormali, F., Abtahi, A., Mahmoodi, S., Stoops, G., 2003. Argillic horizon development in calcareous soils of arid and semiarid regions of southern Iran. *CATENA* 53, 273–301. doi:10.1016/S0341-8162(03)00040-7
- Khormali, F., Abtahi, A., Stoops, G., 2006. Micromorphology of calcitic features in highly calcareous soils of Fars Province, Southern Iran. *Geoderma* 132, 31–46. doi:10.1016/j.geoderma.2005.04.024

- Khormali, F., Ghergherechi, S., Kehl, M., Ayoubi, S., 2012. Soil formation in loess-derived soils along a subhumid to humid climate gradient, Northeastern Iran. *Geoderma* 179–180, 113–122. doi:10.1016/j.geoderma.2012.02.002
- Khresat, S.A., 2001. Calcic horizon distribution and soil classification in selected soils of north-western Jordan. *J. Arid Environ.* 47, 145–152. doi:10.1006/jare.2000.0712
- Klappa, C.F., 1980. Rhizoliths in terrestrial carbonates: classification, recognition, genesis and significance. *Sedimentology* 27, 613–629.
- Klein, C., 2002. *Manual of Mineral Science*. John Wiley & Sons Australia, Limited.
- Knuteson, J.A., Richardson, J.L., Patterson, D.D., Prunty, L., 1989. Pedogenic Carbonates in a Calciaquoll Associated with a Recharge Wetland. *Soil Sci. Soc. Am. J.* 53, 495. doi:10.2136/sssaj1989.03615995005300020032x
- Kovda, I., Morgun, E., Gongalsky, K., 2014. Stable isotopic composition of carbonate pedofeatures in soils along a transect in the southern part of European Russia. *CATENA, Landscapes and Soils through Time* 112, 56–64. doi:10.1016/j.catena.2013.01.005
- Kovda, I.V., Wilding, L.P., Drees, L.R., 2003. Micromorphology, submicroscopy and microprobe study of carbonate pedofeatures in a Vertisol gilgai soil complex, South Russia. *CATENA, Achievements in Micromorphology* 54, 457–476. doi:10.1016/S0341-8162(03)00121-8
- Kraimer, R.A., Monger, H.C., 2009. Carbon isotopic subsets of soil carbonate—A particle size comparison of limestone and igneous parent materials. *Geoderma* 150, 1–9. doi:10.1016/j.geoderma.2008.11.042
- Krauskopf, K.B., Bird, D.K., 1994. *Introduction To Geochemistry*, 3rd edition. ed. McGraw-Hill Science/Engineering/Math, New York.
- Krueger, H.W., 1991. Exchange of carbon with biological apatite. *J. Archaeol. Sci.* 18, 355–361. doi:10.1016/0305-4403(91)90071-V
- Ku, T.-L., Bull, W.B., Freeman, S.T., Knauss, K.G., 1979. Th230-U234 dating of pedogenic carbonates in gravelly desert soils of Vidal Valley, southeastern California. *Geol. Soc. Am. Bull.* 90, 1063. doi:10.1130/0016-7606(1979)90<1063:TDOPCI>2.0.CO;2
- Kuznetsova, A.M., Khokhlova, O.S., 2012. Submicromorphology of pedogenic carbonate accumulations as a proxy of modern and paleoenvironmental conditions. *Bol. Soc. Geológica Mex.* 64, 199–205.
- Kuzyakov, Y., 2006a. Sources of CO₂ efflux from soil and review of partitioning methods. *Soil Biol. Biochem.* 38, 425–448. doi:10.1016/j.soilbio.2005.08.020
- Kuzyakov, Y., 2006b. *Bodengeographische und Agrarökologische Exkursion: Moskau – Volgograd*. Selbstverlag. 56 p.
- Kuzyakov, Y., Domanski, G., 2002. Model for rhizodeposition and CO₂ efflux from planted soil and its validation by ¹⁴C pulse labelling of ryegrass. *Plant Soil* 239, 87–102. doi:10.1023/A:1014939120651
- Kuzyakov, Y., Shevtsova, E., Pustovoytov, K., 2006. Carbonate re-crystallization in soil revealed by ¹⁴C labeling: Experiment, model and significance for paleo-environmental reconstructions. *Geoderma* 131, 45–58. doi:10.1016/j.geoderma.2005.03.002
- Lal, R., 2012. *World Soils and the Carbon Cycle in Relation to Climate Change and Food Security*. Carbon Management and Sequestration Center, the Ohio State University, Columbus, USA.

- Lal, R., Kimble, J.M., 2000. Pedogenic carbonates and the global carbon cycle, in: Lal, R., Kimble, J.M., Eswaran, H., Stewart, B.A. (Eds.), *Global Climate Change and Pedogenic Carbonates*. CRC Press, Boca Raton, Fla, pp. 1–14.
- Lambers, H., Mougel, C., Jaillard, B., Hinsinger, P., 2009. Plant-microbe-soil interactions in the rhizosphere: an evolutionary perspective. *Plant Soil* 321, 83–115. doi:10.1007/s11104-009-0042-x
- Lambkin, D.C., Gwilliam, K.H., Layton, C., Canti, M.G., Pearce, T.G., Hodson, M.E., 2011. Production and dissolution rates of earthworm-secreted calcium carbonate. *Pedobiologia*, 9th International Symposium on Earthworm EcologyXalapa, Veracruz, Mexico, 5th – 10th September 2010 54, Supplement, S119–S129. doi:10.1016/j.pedobi.2011.09.003
- Landi, A., Mermut, A.R., Anderson, D.W., 2003. Origin and rate of pedogenic carbonate accumulation in Saskatchewan soils, Canada. *Geoderma* 117, 143–156. doi:10.1016/S0016-7061(03)00161-7
- Levin, N.E., Brown, F.H., Behrensmeyer, A.K., Bobe, R., Cerling, T.E., 2011. Paleosol carbonates from the Omo Group: Isotopic records of local and regional environmental change in East Africa. *Palaeogeogr. Palaeoclimatol. Palaeoecol.* 307, 75–89. doi:10.1016/j.palaeo.2011.04.026
- Liu, B., Phillips, F.M., Campbell, A.R., 1996. Stable carbon and oxygen isotopes of pedogenic carbonates, Ajo Mountains, southern Arizona: implications for paleoenvironmental change. *Palaeogeogr. Palaeoclimatol. Palaeoecol.* 124, 233–246. doi:10.1016/0031-0182(95)00093-3
- Liu, Z., Dreybrodt, W., Wang, H., 2010. A new direction in effective accounting for the atmospheric CO₂ budget: Considering the combined action of carbonate dissolution, the global water cycle and photosynthetic uptake of DIC by aquatic organisms. *Earth-Sci. Rev.* 99, 162–172. doi:10.1016/j.earscirev.2010.03.001
- Long, A., Hendershott, R., Martin, P.S., 1983. Radiocarbon dating of fossil eggshell. *Radiocarbon* 25, 533–539. doi:10.2458/azu_js_rc.25.811
- Machette, M.N., 1985. Calcic soils of the southwestern United States. *Geol. Soc. Am. Spec. Pap.* 203, 1–22. doi:10.1130/SPE203-p1
- Ma, Y.F., Gao, Y.H., Feng, Q.L., 2010. Effects of pH and temperature on CaCO₃ crystallization in aqueous solution with water soluble matrix of pearls. *J. Cryst. Growth* 312, 3165–3170. doi:10.1016/j.jcrysGro.2010.07.053
- Magee, J.W., Miller, G.H., Spooner, N.A., Questiaux, D.G., McCulloch, M.T., Clark, P.A., 2009. Evaluating Quaternary dating methods: Radiocarbon, U-series, luminescence, and amino acid racemization dates of a late Pleistocene emu egg. *Quaternary Geochronology*, 4. 84–92.
- Magnani, G., Bartolomei, P., Cavulli, F., Esposito, M., Marino, E.C., Neri, M., Rizzo, A., Scaruffi, S., Tosi, M., 2007. U-series and radiocarbon dates on mollusc shells from the uppermost layer of the archaeological site of KHB-1, Ra's al Khabbah, Oman. *Journal of Archaeological Science* 34. 749–755.
- McLaren, S.J., Rowe, P.J., 1996. The reliability of uranium-series mollusc dates from the western Mediterranean basin. *Quaternary Science Reviews* 15, 709–717.
- Miller, J.J., Acton, D.F., St. Arnaud, R.J., 1985. The effect of groundwater on soil formation in a morainal landscape in saskatchewan. *Can. J. Soil Sci.* 65, 293–307. doi:10.4141/cjss85-033
- Miller, J.J., Dudas, M.J., Longstaffe, F.J., 1987. Identification of pedogenic carbonate minerals using stable carbon and oxygen isotopes, x-ray diffraction and sem analyses. *Can. J. Soil Sci.* 67, 953–958. doi:10.4141/cjss87-090

- Monger, C., 2002. pedogenic carbonate links between biotic and abiotic caco3. Presented at the 17th WCSS, Thailand.
- Monger, H.C., Adams, H.P., 1996. Micromorphology of Calcite-Silica Deposits, Yucca Mountain, Nevada. *Soil Sci. Soc. Am. J.* 60, 519. doi:10.2136/sssaj1996.03615995006000020026x
- Monger, H.C., Cole, D.R., Buck, B.J., Gallegos, R.A., 2009. Scale and the isotopic record of C4 plants in pedogenic carbonate: from the biome to the rhizosphere. *Ecology* 90, 1498–1511.
- Monger, H.C., Daugherty, L.A., Lindemann, W.C., Liddell, C.M., 1991. Microbial precipitation of pedogenic calcite. *Geology* 19, 997–1000. doi:10.1130/0091-7613(1991)019<0997:MPOPC>2.3.CO;2
- Monger, H.C., Gallegos, R.A., 2000. Biotic and abiotic processes and rates of pedogenic carbonate accumulation in the southwestern United States: Relationship to atmospheric CO₂ sequestration, in: Lal, R., Kimble, J.M., Eswaran, H., Stewart, B.A. (Eds.), *Global Climate Change and Pedogenic Carbonates*. CRC Press, Boca Raton, Fla.
- Monger, H.C., Kraimer, R.A., Khresat, S., Cole, D.R., Wang, X., Wang, J., 2015. Sequestration of inorganic carbon in soil and groundwater. *Geology* 43, 375–378. doi:10.1130/G36449.1
- Naiman, Z., Quade, J., Patchett, P.J., 2000. Isotopic evidence for eolian recycling of pedogenic carbonate and variations in carbonate dust sources throughout the southwest United States. *Geochim. Cosmochim. Acta* 64, 3099–3109. doi:10.1016/S0016-7037(00)00410-5
- Nieder, R., Benbi, D.K., 2008. *Carbon and Nitrogen in the Terrestrial Environment*. Springer.
- Nordt, L.C., Hallmark, C.T., Wilding, L.P., Boutton, T.W., 1998. Quantifying pedogenic carbonate accumulations using stable carbon isotopes. *Geoderma* 82, 115–136. doi:10.1016/S0016-7061(97)00099-2
- Nordt, L., Wilding, L., Hallmark, C., Jacob, J., 1996. Stable carbon isotope composition of pedogenic carbonates and their use in studying pedogenesis, in: Boutton, T.W., Yamasaki, S. (Eds.), *Mass Spectrometry of Soils*. Marcel Dekker, New York, pp. 133–154.
- Pendall, E.G., Harden, J.W., Trumbore, S.E., Chadwick, O.A., 1994. Isotopic Approach to Soil Carbonate Dynamics and Implications for Paleoclimatic Interpretations. *Quat. Res.* 42, 60–71. doi:10.1006/qres.1994.1054
- Perito, B., Marvasti, M., Barabesi, C., Mastromei, G., Bracci, S., Vendrell, M., Tiano, P., 2014. A *Bacillus subtilis* cell fraction (BCF) inducing calcium carbonate precipitation: Biotechnological perspectives for monumental stone reinforcement. *J. Cult. Herit.* 15, 345–351. doi:10.1016/j.culher.2013.10.001
- Peters, N.A., Huntington, K.W., Hoke, G.D., 2013. Hot or not? Impact of seasonally variable soil carbonate formation on paleotemperature and O-isotope records from clumped isotope thermometry. *Earth Planet. Sci. Lett.* 361, 208–218. doi:10.1016/j.epsl.2012.10.024
- Prendergast, A.L., Stevens, R.E., Hill, E.A., Barker, G.W., Hunt, C., O'Connell, T.C., 2015. Carbon isotope signatures from land snail shells: Implications for palaeovegetation reconstruction in the eastern Mediterranean. *Quat. Int.* doi:10.1016/j.quaint.2014.12.053
- Pustovoytov, K., 2003. Growth rates of pedogenic carbonate coatings on coarse clasts. *Quat. Int., Paleopedology: V International Symposium and Field workshop, Suzdal, Russia* 106–107, 131–140. doi:10.1016/S1040-6182(02)00168-4
- Pustovoytov, K., 2002. 14C Dating of Pedogenic Carbonate Coatings on Wall Stones at Göbekli Tepe (Southeastern Turkey). *Neo-Lithics* 2, 3–4.

- Pustovoytov, K., 1998. Pedogenic carbonate cutans as a record of the Holocene history of relic tundra–steppes of the Upper Kolyma Valley (North-Eastern Asia). *CATENA* 34, 185–195. doi:10.1016/S0341-8162(98)00088-5
- Pustovoytov, K.E., Riehl, S., Mittmann, S., 2004. Radiocarbon age of carbonate in fruits of *Lithospermum* from the early Bronze Age settlement of Hirbet ez-Zeraqōn (Jordan). *Veg. Hist. Archaeobotany* 13, 207–212. doi:10.1007/s00334-004-0044-9
- Pustovoytov, K., Leisten, T., 2002. Diagenetic alteration of artificial lime mortar in a Mediterranean soil: ^{14}C and stable carbon isotopic data. Presented at the 17th WCSS, Thiland.
- Pustovoytov, K., Riehl, S., Hilger, H.H., Schumacher, E., 2010. Oxygen isotopic composition of fruit carbonate in *Lithospermeae* and its potential for paleoclimate research in the Mediterranean. *Glob. Planet. Change, Oxygen isotopes as tracers of Mediterranean variability: linking past, present and future* 71, 258–268. doi:10.1016/j.gloplacha.2009.11.015
- Pustovoytov, K., Schmidt, K., Parzinger, H., 2007a. Radiocarbon dating of thin pedogenic carbonate laminae from Holocene archaeological sites. *The Holocene* 17, 835–843. doi:10.1177/0959683607080524
- Pustovoytov, K., Schmidt, K., Taubald, H., 2007b. Evidence for Holocene environmental changes in the northern Fertile Crescent provided by pedogenic carbonate coatings. *Quat. Res., Reconstructing past environments from remnants of human occupation and sedimentary archives in western Eurasia* 67, 315–327. doi:10.1016/j.yqres.2007.01.002
- Pustovoytov, K., Terhorst, B., 2004. An isotopic study of a late Quaternary loess-paleosol sequence in SW Germany. *Rev. Mex. Cienc. Geológicas* 21, 88–93.
- Qualls, R.G., Bridgman, S.D., 2005. Mineralization rate of ^{14}C -labelled dissolved organic matter from leaf litter in soils of a weathering chronosequence. *Soil Biol. Biochem.* 37, 905–916. doi:10.1016/j.soilbio.2004.08.029
- Quast, A., Hoefs, J., Paul, J., 2006. Pedogenic carbonates as a proxy for palaeo-CO₂ in the Palaeozoic atmosphere. *Palaeogeogr. Palaeoclimatol. Palaeoecol.* 242, 110–125. doi:10.1016/j.palaeo.2006.05.017
- Rabenhorst, M.C., Wilding, L.P., 1986. Pedogenesis on the Edwards Plateau, Texas: III. New Model for the Formation of Petrocalcic Horizons1. *Soil Sci. Soc. Am. J.* 50, 693. doi:10.2136/sssaj1986.03615995005000030029x
- Rawlins, B.G., Henrys, P., Bewerd, N., Robinson, D.A., Keith, A.M., Garcia-Bajo, M., 2011. The importance of inorganic carbon in soil carbon databases and stock estimates: a case study from England. *Soil Use Manag.* 27, 312–320. doi:10.1111/j.1475-2743.2011.00348.x
- Reddy, M.M., 2012. Calcite growth-rate inhibition by fulvic acid and magnesium ion—Possible influence on biogenic calcite formation. *J. Cryst. Growth* 352, 151–154. doi:10.1016/j.jcrysgr.2011.12.069
- Reeves, J.C.C., 1970. Origin, Classification, and Geologic History of Caliche on the Southern High Plains, Texas and Eastern New Mexico. *J. Geol.* 78, 352–362.
- Regev, L., Eckmeier, E., Mintz, E., Weiner, S., Boaretto, E., 2011. Radiocarbon Concentrations of Wood Ash Calcite: Potential for Dating. *Radiocarbon* 53, 117–127. doi:10.2458/azu_js_rc.53.3446
- Retallack, G.J., 2009. Refining a pedogenic-carbonate CO₂ paleobarometer to quantify a middle Miocene greenhouse spike. *Palaeogeogr. Palaeoclimatol. Palaeoecol.* 281, 57–65. doi:10.1016/j.palaeo.2009.07.011

- Retallack, G.J., 2005. Pedogenic carbonate proxies for amount and seasonality of precipitation in paleosols. *Geology* 33, 333–336. doi:10.1130/G21263.1
- Riera, V., Anadón, P., Oms, O., Estrada, R., Maestro, E., 2013. Dinosaur eggshell isotope geochemistry as tools of palaeoenvironmental reconstruction for the upper Cretaceous from the Tremp Formation (Southern Pyrenees). *Sediment. Geol.* 294, 356–370. doi:10.1016/j.sedgeo.2013.06.001
- Robbins, C.W., 1985. The CaCO₃-CO₂-H₂O system in soils. *J. Agron. Educ.* 14.
- Royer, D.L., 1999. Depth to pedogenic carbonate horizon as a paleoprecipitation indicator? *Geology* 27, 1123–1126. doi:10.1130/0091-7613(1999)027<1123:DTPCHA>2.3.CO;2
- Royer, D.L., Berner, R.A., Beerling, D.J., 2001. Phanerozoic atmospheric CO₂ change: evaluating geochemical and paleobiological approaches. *Earth-Sci. Rev.* 54, 349–392. doi:10.1016/S0012-8252(00)00042-8
- Salomons, W., Mook, W.G., 1976. Isotope Geochemistry of Carbonate Dissolution and Reprecipitation in Soils. *Soil Sci.* 122. doi:10.1097/00010694-197607000-00003
- Sauer, D., Stein, C., Glatzel, S., Kühn, J., Zarei, M., Stahr, K., 2015. Duricrusts in soils of the Alentejo (southern Portugal)—types, distribution, genesis and time of their formation. *J. Soils Sediments* 15, 1437–1453. doi:10.1007/s11368-015-1066-x
- Schlesinger, W.H., 1985. The formation of caliche in soils of the Mojave Desert, California. *Geochim. Cosmochim. Acta* 49, 57–66. doi:10.1016/0016-7037(85)90191-7
- Schlesinger, W.H., Marion, G.M., Fonteyn, P.J., 1989. Stable Isotope Ratios and the Dynamics of Caliche in Desert Soils, in: Rundel, P.W., Ehleringer, J.R., Nagy, K.A. (Eds.), *Stable Isotopes in Ecological Research, Ecological Studies*. Springer New York, pp. 309–317.
- Seth, B., Thirlwall, M.F., Houghton, S.L., Craig, C-A., 2003. Accurate measurements of Th–U isotope ratios for carbonate geochronology using MC-ICP-MS. *Journal of Analytical Atomic Spectrometry* 18, 1323–1330.
- Sharp, W.D., Ludwig, K.R., Chadwick, O.A., Amundson, R., Glaser, L.L., 2003. Dating fluvial terraces by ²³⁰Th/U on pedogenic carbonate, Wind River Basin, Wyoming. *Quat. Res.* 59, 139–150. doi:10.1016/S0033-5894(03)00003-6
- Shi, Y., Baumann, F., Ma, Y., Song, C., Kühn, P., Scholten, T., He, J.-S., 2012. Organic and inorganic carbon in the topsoil of the Mongolian and Tibetan grasslands: pattern, control and implications. *Biogeosciences* 9, 2287–2299. doi:10.5194/bg-9-2287-2012
- Soil Survey Staff, 2010. *Keys to Soil Taxonomy*, 2010, 11 edition. ed. Natural Resources Conservation Service, Washington.
- Spooner, P.T., Chen, T., Robinson, L.F., Coath, C.D., 2016. Rapid uranium-series age screening of carbonates by laser ablation mass spectrometry. *Quaternary Geochronology* 31, 28–39.
- Stern, L.A., Johnson, G.D., Chamberlain, C.P., 1994. Carbon isotope signature of environmental change found in fossil ratite eggshells from a South Asian Neogene sequence. *Geology* 22, 419–422. doi:10.1130/0091-7613(1994)022<0419:CISOEC>2.3.CO;2
- Stumm, W., Morgan, J.J., 1996. *Aquatic Chemistry: Chemical Equilibria and Rates in Natural Waters*, 3rd edition. ed. Wiley-Interscience, New York.
- Suchý, V., 2002. The “white beds” - a fossil caliche of the Barrandian area: its origin and paleoenvironmental significance. *J. Czech Geol. Soc.* 47, 45–54.
- Thomas, D.S.G., 2011. *Arid Zone Geomorphology: Process, Form and Change in Drylands*. John Wiley & Sons.

Treadwell-Steitz, C., McFadden, L.D., 2000. Influence of parent material and grain size on carbonate coatings in gravelly soils, Palo Duro Wash, New Mexico. *Geoderma* 94, 1–22. doi:10.1016/S0016-7061(99)00075-0

Ueda, S., Go, C.-S.U., Ishizuka, S., Tsuruta, H., Iswandi, A., Murdiyarso, D., 2005. Isotopic assessment of CO₂ production through soil organic matter decomposition in the tropics 71, 109–116. doi:10.1007/s10705-004-1197-8

USDA-NRCS, 2000. Soil Inorganic Carbon Map.

Verrecchia, E.P., 2011. Pedogenic Carbonates, in: Encyclopedia of Earth Sciences Series. Springer Science+Business Media B.V.

Verrecchia, E.P., Dumont, J.-L., Verrecchia, K.E., 1993. Role of calcium oxalate biomineralization by fungi in the formation of calcretes; a case study from Nazareth, Israel. *J. Sediment. Res.* 63, 1000–1006. doi:10.1306/D4267C6C-2B26-11D7-8648000102C1865D

Verrecchia, E.P., Freytet, P., Verrecchia, K.E., Dumont, J.-L., 1995. Spherulites in Calcrete Laminar Crusts: Biogenic CaCO₃ Precipitation as a Major Contributor to Crust Formation. *J. Sediment. Res.* 65.

Verrecchia, E.P., Verrecchia, K.E., 1994. Needle-fiber Calcite: A Critical Review and a Proposed Classification. *J. Sediment. Res.* 64.

Versteegh, E.A.A., Black, S., Canti, M.G., Hodson, M.E., 2013. Earthworm-produced calcite granules: A new terrestrial palaeothermometer? *Geochim. Cosmochim. Acta* 123, 351–357. doi:10.1016/j.gca.2013.06.020

Villagran, X.S., Poch, R.M., 2014. A new form of needle-fiber calcite produced by physical weathering of shells. *Geoderma* 213, 173–177. doi:10.1016/j.geoderma.2013.08.015

Violette, A., Riotte, J., Braun, J.-J., Oliva, P., Marechal, J.-C., Sekhar, M., Jeandel, C., Subramanian, S., Prunier, J., Barbiero, L., Dupre, B., 2010. Formation and preservation of pedogenic carbonates in South India, links with paleo-monsoon and pedological conditions: Clues from Sr isotopes, U–Th series and REEs. *Geochim. Cosmochim. Acta* 74, 7059–7085. doi:10.1016/j.gca.2010.09.006

Vogel, J.C., Visser, E., Fuls, A., 2001. Suitability of Ostrich eggshell for radiocarbon dating.

Wang, X., Wang, J., Xu, M., Zhang, W., Fan, T., Zhang, J., 2015. Carbon accumulation in arid croplands of northwest China: pedogenic carbonate exceeding organic carbon. *Sci. Rep.* 5. doi:10.1038/srep11439

Wang, Y., Li, Y., Ye, X., Chu, Y., Wang, X., 2010. Profile storage of organic/inorganic carbon in soil: From forest to desert. *Sci. Total Environ.* 408, 1925–1931. doi:10.1016/j.scitotenv.2010.01.015

Wang, Y., McDonald, E., Amundson, R., McFadden, L., Chadwick, O., 1996. An isotopic study of soils in chronological sequences of alluvial deposits, Providence Mountains, California. *Geol. Soc. Am. Bull.* 108, 379–391. doi:10.1130/0016-7606(1996)108<0379:AISOSI>2.3.CO;2

Werth, M., Kuzyakov, Y., 2010. ¹³C fractionation at the root–microorganisms–soil interface: A review and outlook for partitioning studies. *Soil Biol. Biochem.* 42, 1372–1384. doi:10.1016/j.soilbio.2010.04.009

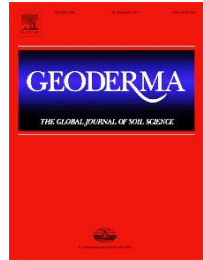
West, L.T., Wilding, L.P., Hallmark, C.T., 1988. Calciustolls in Central Texas: II. Genesis of Calcic and Petrocalcic Horizons. *Soil Sci. Soc. Am. J.* 52, 1731. doi:10.2136/sssaj1988.03615995005200060040x

Whipkey, C.E., Capo, R.C., Chadwick, O.A., Stewart, B.W., 2000. The importance of sea spray to the cation budget of a coastal Hawaiian soil: a strontium isotope approach. *Chem. Geol.* 168, 37–48.

- Wieder, M., Yaalon, D.H., 1982. Micromorphological fabrics and developmental stages of carbonate nodular forms related to soil characteristics. *Geoderma* 28, 203–220. doi:10.1016/0016-7061(82)90003-9
- Williams, G.E., Polach, H.A., 1969. The evaluation of ¹⁴C ages for soil carbonate from the arid zone. *Earth Planet. Sci. Lett.* 7, 240–242. doi:10.1016/0012-821X(69)90059-4
- World reference base for soil resources, 2014. FAO.
- Wright, V.P., Beck, V.H., Sanz-Montero, M.E., Verrecchia, E.P., Freytet, P., Verrecchia, K.E., Dumont, J.-L., 1996. Spherulites in calcrete laminar crusts; biogenic CaCO₃ precipitation as a major contributor to crust formation; discussion and reply. *J. Sediment. Res.* 66, 1040–1044. doi:10.2110/jsr.66.1040
- Xie, J., Li, Y., Zhai, C., Li, C., Lan, Z., 2008. CO₂ absorption by alkaline soils and its implication to the global carbon cycle. *Environ. Geol.* 56, 953–961. doi:10.1007/s00254-008-1197-0
- Xu, B., Gu, Z., Han, J., Liu, Z., Pei, Y., Lu, Y., Wu, N., Chen, Y., 2010. Radiocarbon and Stable Carbon Isotope Analyses of Land Snails from the Chinese Loess Plateau: Environmental and Chronological Implications. *Radiocarbon* 52, 149–156. doi:10.2458/azu_js_rc.52.3243
- Yanes, Y., Gómez-Puche, M., Esquembre-Bebia, M.A., Fernández-López-De-Pablo, J., 2013. Younger Dryas – early Holocene transition in the south-eastern Iberian Peninsula: insights from land snail shell middens. *J. Quat. Sci.* 28, 777–788. doi:10.1002/jqs.2673
- Yang, S., Ding, Z., Gu, Z., 2014. Acetic acid-leachable elements in pedogenic carbonate nodules and links to the East-Asian summer monsoon. *CATENA*, Loess and dust dynamics, environments, landforms, and pedogenesis: a tribute to Edward Derbyshire 117, 73–80. doi:10.1016/j.catena.2013.06.030
- Zamanian, K., 2005. Study of Fashand-Hashtgerd soils and investigation of the mechanisms of petrocalcic horizon formation in these soils (master thesis). Tehran, Iran.
- Zazzo, A., Saliège, J.-F., 2011. Radiocarbon dating of biologicalapatites: A review. *Palaeogeogr. Palaeoclimatol. Palaeoecol.* 310, 52–61. doi:10.1016/j.palaeo.2010.12.004
- Zazzo, A., Saliège, J.-F., Person, A., Boucher, H., 2009. Radiocarbon Dating of Calcined Bones: Where Does the Carbon Come from? *Radiocarbon* 51, 601–611. doi:10.2458/azu_js_rc.51.3519
- Zhou, J., Chafetz, H.S., 2010. Pedogenic Carbonates in Texas: Stable-Isotope Distributions and Their Implications for Reconstructing Region-Wide Paleoenvironments. *J. Sediment. Res. - J SEDIMENT RES* 80, 137–150. doi:10.2110/jsr.2010.018

2. Recrystallization of shell carbonate in soil: ^{14}C labeling, modeling and relevance for dating and paleo-reconstructions

Published: Geoderma 282 (2016): 87-95



Kazem Zamanian¹, Konstantin Pustovoytov², Yakov Kuzyakov^{1,3}

¹. Department of Soil Science of Temperate Ecosystems, University of Göttingen, Büsgenweg 2, 37077 Göttingen, Germany

². Institute of Soil Science and Land Evaluation (310), University of Hohenheim, Schloss Hohenheim 1, 70599 Stuttgart,

³. Department of Agricultural Soil Science, University of Goettingen, Buesgenweg 2, 37077, Goettingen, Germany

2.1. Abstract

Mollusk shells are commonly present in a broad array of geological and archaeological contexts. The shell carbonate can serve for numerical age determination ($\Delta^{14}\text{C}$) and as a paleoenvironmental indicator ($\delta^{18}\text{O}$, $\delta^{13}\text{C}$). Shell carbonate recrystallization in soils, however, may re-equilibrate the C isotopic signature with soil CO_2 . The equilibration dynamics remain poorly understood because of the absence of suitable experimental approaches. Here we used the artificial ^{14}C -labelling technique to study the process of shell carbonate recrystallization as a function of time.

Organic-free and organic-containing shell particles of *Protothaca staminea* were mixed with loess or a carbonate-free loamy soil. The mixtures were placed in air-tight bottles, where the bottle air containing $^{14}\text{CO}_2$ ($p\text{CO}_2 = 2\%$). The ^{14}C activity of shells was measured over time and related to the recrystallization of shell carbonate.

Recrystallization of shell carbonate already began after one day. The recrystallization rates were $10^{-3} \text{ \% day}^{-1}$ in organic-containing shell embedded in soil and $1.6 \cdot 10^{-2} \text{ \% day}^{-1}$ in organic-free shells in loess. Removal of organic compounds increased shell porosity, and so, increased the contact surface for exchange with soil solution. Organic-free shells recrystallized much faster in loess (0.56% in 56 days) than in other treatments. Recrystallization was 2 to 7 times higher in loess (in the presence and absence of organic compounds, respectively) than in carbonate-free soil. Loess carbonate itself can recrystallize and accumulate on shells, leading to overestimation of shell

carbonate recrystallization. A model for shell carbonate recrystallization as a function of time was developed. The model considers the presence or absence of organic compounds in shell structure and geogenic carbonates in the embedding matrix. The model enabled all results to be fitted with $R^2 = 0.98$.

The modeled time necessary for nearly full recrystallization (95% of shell carbonate) was 88 years for organic-free shells in loess and up to 770 years for organic-containing shells in carbonate-free soil. After this period, the original isotopic signature will vanish completely and will be replaced by a new $\delta^{13}\text{C}$ and $\Delta^{14}\text{C}$ signature in the shell structure. Thus, shell carbonate recrystallization may proceed relatively rapidly in terms of geologic time. This is necessary to consider in the interpretation of dating results and paleoenvironmental reconstructions.

Keywords: biogenic carbonates, geogenic carbonates, recrystallization, porosity, shell, ^{14}C labeling

2.2. Introduction

Mollusk shells are among the most common findings at archaeological sites (Thomas, 2015, and references therein). Their carbonate fraction represents a useful paleoenvironmental and chronological proxy (Pigati et al., 2004; Pigati et al., 2010; Xu et al., 2010; Pigati, 2013; Yanes et al., 2013). The CaCO_3 fraction of shells can be especially useful for such investigations if the preservation of organic compounds is poor, such as in arid environments or coastal regions (Russo et al., 2010; Zazzo and Saliège, 2011). Under such circumstances, shell carbonate can be the only alternative to paleoenvironmental and chronological studies (Chappell and Pollach, 1972; Újvári et al., 2014).

Mollusk shells are usually well preserved in sediment after burial (Pigati et al., 2004; Pigati et al., 2010), but their elemental and/or isotopic composition can be influenced by recrystallization processes (Webb et al., 2007; Collins, 2012). Recrystallization occurs following soil dryness, increased Ca^{2+} concentration and/or a drop in soil CO_2 partial pressure (Chappell and Pollach, 1972; Russo et al., 2010). Since the amount of soil CO_2 and its isotopic composition is in equilibrium with CO_2 respired by roots and rhizosphere organisms, the isotopic signature ($\delta^{13}\text{C}$, $\Delta^{14}\text{C}$) of recrystallized carbonate will equilibrate with soil CO_2 (Cerling et al., 1989). In this case, the $\delta^{13}\text{C}$ in recrystallized carbonate in soil will save fingerprints of dominant vegetation during the recrystallization phase and the $\Delta^{14}\text{C}$ will reflect the age of the recrystallization event. The presence of even a few percent of modern C can significantly affect the results of paleoenvironmental and

chronological studies based on shell carbonate (Webb et al., 2007). For instance, the presence of 10-15% of modern C as carbonate in 30 ka-old shells leads to an 11 ka error in age (Webb et al., 2007).

Considering the significant effect of modern C on radiocarbon dating, various techniques have been proposed to assure the fidelity of geochemical signals. Evidence of recrystallization can be detected using optical and electron microscopes (Cochran et al., 2010), X-ray analysis (Chappell and Pollach, 1972; Piepenbrink, 1989; Cochran et al., 2010), trace element measurements (Shemesh, 1990; Oliver et al., 1996; Cochran et al., 2010) and density analysis (Russo et al., 2010). It is also advisable to verify the consistency of measured ages with other datable materials or stratigraphic positions (Bonadonna et al., 1999; Webb et al., 2007; Janz et al., 2009). The selected samples should also be subjected to physical and chemical pre-treatments such as soaking in acid or mechanical abrasion, to reduce the influence of suspected recrystallization (Krueger, 1991; Bezerra et al., 2008).

Despite the progress in laboratory methods, the dynamics of shell carbonate recrystallization in sedimentary environments and its affecting factors remain poorly understood. Furthermore, in some cases the proposed techniques for sample selection may have drawbacks. In certain environments the recrystallized carbonate could be aragonitic (Webb et al., 2007). Analysis with a scanning electron microscope is restricted to a small portion of the samples, which risks overlooking recrystallized carbonates when these are few (Douka et al., 2010), especially when the recrystallized carbonate is patchily distributed (Webb et al., 2007).

In soils, shell carbonate may be found very well preserved (i.e. without recrystallization) up to nearly completely recrystallized (Chappell and Pollach, 1972). Various biological and environmental parameters seem to control the rate of dissolution and subsequently recrystallization of shell carbonates (Yates et al., 2002). These include porosity (Nielsen-Marsh and Hedges, 1999; Collins, 2012) and organic compounds present in the shell structure (Hall and Kennedy, 1967; Nielsen-Marsh and Hedges, 2000), microbial attack (Nielsen-Marsh and Hedges, 1999; Janz et al., 2009), soil pH (Piepenbrink, 1989; Berna et al., 2004), presence of geogenic carbonates (GeoC) for example limestone (Yates et al., 2002; Berna et al., 2004), water availability (Douka et al., 2010; Cochran et al., 2010) and water circulation (Forman and Polyak, 1997), temperature (Douka et al., 2010) and age (Chappell and Pollach, 1972).

The dissolution of shell carbonate can begin immediately after burial (Fairbridge, 1967) and be associated with changes in elemental composition (Walls et al., 1977; Ragland et al., 1979) and

exfoliation (Yates, 1986). Dissolution is related to surface area (Nielsen-Marsh and Hedges, 1999; Collins, 2012), which increases with pore space of the skeletal structure (Henrich and Wefer, 1986; Nielsen-Marsh and Hedges, 2000). Therefore, recrystallization may occur both at the surface and/or inner parts of a shell fragment (Yates, 1986). Exfoliation and oxidation of organic compounds causes gaps and pore spaces in the shell structure, making it more susceptible to recrystallization (Yates, 1986; Webb et al., 2007). In isotopic studies, heating of samples is usually used to eliminate organic compounds (Dauphin et al., 2006). Heating also causes some crystallographic changes in shell structure (Collins, 2012). The occluded water will be removed (Lécuyer and O’Neil, 1994) and trace elements become mobile (Lécuyer, 1996; Dauphin et al., 2006). Therefore, heating increases shell porosity (Collins, 2012) and thus promotes recrystallization. Recrystallization on the shell surface may not merely reflect shell carbonate dissolution. If other source(s) of carbonate (e.g. GeoC) are present in the embedding matrix or if soluble Ca is available, then carbonate may precipitate on the shell surface from external sources as well (Yates et al., 2002; Prendergast and Stevens, 2014). As a consequence, shells embedded in calcareous soils may be contaminated by secondary carbonate, which can exhibit a higher susceptibility to recrystallization (Forman and Polyak, 1997).

The low solubility of calcium carbonate ($K_{sp}=10^{-9}$ at 25 °C) (Robbins, 1985) and its low recrystallization rate complicate experimental research on shell carbonate recrystallization under controlled laboratory conditions. Recently, the sensitive technique of ^{14}C labeling (Kuzyakov et al., 2006; Gocke et al., 2010; Gocke et al., 2011) has been shown to help understand the processes and dynamics of recrystallization and its effects on the C isotopic composition of shell carbonate. This technique is based on $^{14}\text{CO}_2$ labeling of the soil atmosphere and subsequent tracing of ^{14}C activity in a carbonate sample in the soil. The method enables the amount of recrystallized carbonate and rate of recrystallization to be calculated. In this study we 1) determine the recrystallization of shell carbonate as a function of time, 2) investigate the effect of geogenic carbonates in soil on shell carbonate recrystallization rates, and 3) evaluate the effect of organic compounds on recrystallization. Based on the experimentally measured recrystallization, we discuss the consequences for dating and paleoenvironmental reconstructions based on the C isotopic composition of shell carbonate.

2.3. Material and methods

2.3.1. Matrix materials and shells

Loess deposits and a loamy soil were chosen as matrix materials. Loess and soil were collected from a single profile in an open mine in Nussloch, SW Germany (49.19°N , 8.43°E , 217 m asl. (Kuzyakov et al., 2006)). The soil was collected from the A horizon at a depth of 0.1 m (Table 3) and the loess from 10 m depth. The loess comprised 29.8% CaCO_3 equivalent and 0.19% organic carbon content with silt loam as particle size distribution (for further information about loess see (Antoine et al., 2009). Loess and soil samples before beginning the experiment were air dried and sieved through a 2 mm pore size screen.

Table 3: Chemical and physical properties of the soil

Texture	$\text{pH}_{1:1}$	CaCO_3 content %	Organic matter	Cation exchange capacity	Exchangeable cations			
					Ca^{2+} $\text{cmol}^+ \text{kg}^{-1}$	Mg^{2+}	K^+	Na^+
silty clay loam	6.8	-	1.1	16.3	13.2	2.05	0.42	0.02

Pacific little-neck clams (*Protothaca staminea*) were selected as shell materials. The shells were collected from the North Sea coast in north-west Germany (53.68°N 6.99°E). The shells were washed carefully with distilled water ultrasonically to exclude the contaminants and dried at 60°C overnight. The dried shells were broken to small particles with a hammer and sieved to a particle size ranging from 2 to 2.5 mm. To examine the effects of organic compounds on shell carbonate recrystallization rate, half of the shells were heated to 550°C in a furnace for 3 h to eliminate the organic compounds (Table 4).

Table 4: Elemental composition of shell carbonates before and after organic compounds elimination by heating at 550 °C.

Elemental composition	Al	Ca	Fe	K	Mg	Mn	Na	P	S
mg g ⁻¹									
Organic-containing shells	0.02	365	0.54	0.25	0.35	0.02	4.81	0.31	0.71
Organic-free shells	0.03	370	0.60	0.29	0.39	0.02	4.94	0.33	0.75

2.3.2. Experiment setup

300 mg (16-20 particles) of organic-containing and organic-free shells were mixed with 7.8 g of loess or soil and packed into 25 mL glass bottles with an inner surface area of 7.07 cm². The bulk density of loess and soil in bottles were 1.1 g cm⁻³. The depth of loess and soil in bottles was 1 cm hence led to equal CO₂ diffusion in the whole sample. Thereafter, 1.97 mL distilled water was added to each bottle. The water content corresponded to 60% of the saturated water content of loess and soil. Two plastic vials (0.5 mL) were also placed into each bottle (Fig. 11): one for the labeling and the second for removal of remaining CO₂ (see 2.4.), and the bottles were sealed air tight. The experiment therefore included four treatments:

- a) Organic-containing shells in Loess (Org+loess)
- b) Organic-free shells in Loess (NoOrg+loess)
- c) Organic-containing shells in soil (Org+soil)
- d) Organic-free shells in soil (NoOrg+soil)

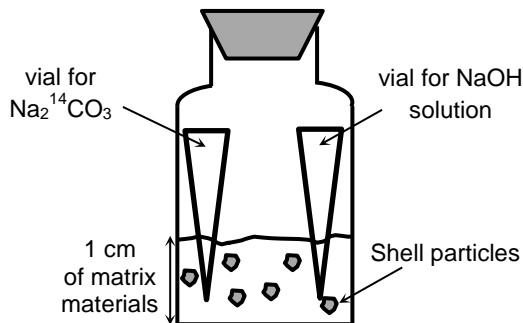


Figure 11: The experiment layout and the labelling technique. $^{14}\text{CO}_2$ was released by injecting H_3PO_4 into the vial containing $\text{Na}_2^{14}\text{CO}_3$. The $^{14}\text{CO}_2$ remaining at the end of the recrystallization period (not participated in recrystallized carbonate) was trapped before each sampling by adding NaOH into the second vial. The H_3PO_4 was injected by syringe through the septa at the beginning of labelling, and NaOH injected at the end of labelling.

2.3.3. Labeling technique and sampling

^{14}C labeled Na_2CO_3 (0.2 mL, 0.9 kBq) was injected by syringe into one of the vials in each bottle (Fig. 1). Injecting H_3PO_4 (0.07 M) into the vial containing $\text{Na}_2^{14}\text{CO}_3$ released the $^{14}\text{CO}_2$. The concentration of ^{14}C in shells was negligible comparing to the added ^{14}C . Therefore, the initial ^{14}C of shells has no effect on the measured and calculated results. The partial pressure of CO_2 ($p\text{CO}_2$) in bottles was 2% which is the common CO_2 concentration at presence of roots and microbial respiration in soils (Pausch and Kuzyakov, 2012). The necessary amount of $\text{Na}_2^{14}\text{CO}_3$ to reach the mentioned $p\text{CO}_2$ was calculated considering the ideal gas law (1 mol = 22.4 L). The air volume was determined by subtracting the volume of matrix particles and the added water from the total volume of bottle. The labeled samples were incubated for time periods of 1, 3, 10, 21 and 56 days at room temperature. At the end of each period, 0.4 mL of 1 M NaOH solution was injected into the second vial to absorb CO_2 in the bottle's air. After one day of CO_2 absorption, the bottles were opened. Loess and soil along with shell particles were washed with 10 ml of slightly alkalized distilled water to remove dissolved organic (DOC) and inorganic (DIC) carbon. Then the samples were let dry at 60 °C overnight. Afterward the shell particles were separated from the matrixes using tweezers. To ensure that no loess or soil materials remained on the shell surface, the shell particles were washed again ultrasonically and dried at 60 °C. Dried shell particles were then ground to fine homogenized powder.

2.3.4. ^{14}C analyses

The ^{14}C activity was quantified in five carbon pools: shells, loess and soil, soluble phase (DIC and DOC), remaining CO_2 in the bottle's air, and the remaining labeling solution. This measurement enabled us to calculate the budget and distribution of added ^{14}C in the samples.

The carbonate in shell particles, loess and soil was released as CO_2 by adding H_3PO_4 to an aliquot of shell particles (0.1 g), loess (0.5 g) and soil (2.0 g). The released CO_2 was trapped in 1.5 mL of 1 M NaOH solution overnight. Adding phenolphthalein to an aliquot of this NaOH solution clarified if the NaOH solution was not completely neutralized by absorption.

An aliquot of the above-mentioned alkali solutions as well as solutions containing dissolved C and labeling remaining were mixed with scintillation cocktail (Rotiszint EcoPlus, Carl Roth, Germany). After the chemiluminescence decayed, the ^{14}C activity of solutions was measured using a multi radio isotope counter (Beckman LS6500, USA). The ^{14}C counting efficiency was at least 70% and the measurement error was 5% at the maximum.

2.3.5. Calculations and statistical analyses

Considering the total amount of C and total ^{14}C activity added to the bottles, the measured ^{14}C activity in NaOH solutions related to the shells, loess and soil will reveal the amount of C recrystallized as carbonate on shells, loess and soil, respectively. The ^{14}C activity was recalculated as a percentage of the measured ^{14}C activity in relation to the total ^{14}C added to the bottles and also as the amount of recrystallized carbonate (mg) on shell particles, loess and soil. The experiment was done with 4 replications for each sampling period. The mean values, standard errors and regression lines were calculated and drawn using SigmaPlot 12.0 (Systat Software Inc., California, USA). The significance of differences between recrystallization amount of various treatments was calculated by post-hoc Fisher LSD test at $\alpha = 0.05$ error probability level (STATISTICA 10, StatSoft Inc., Tulsa, USA).

2.4. Results

As expected, the highest ^{14}C activity was measured in air bottle CO_2 for all treatments except NoOrg+Loess (Fig. 12). The highest ^{14}C activity for NoOrg+Loess was instead in the loess. ^{14}C

activity was generally higher in the loess than the shell particles (Fig. 12). ^{14}C activity in the shells, however, increased continuously with time.

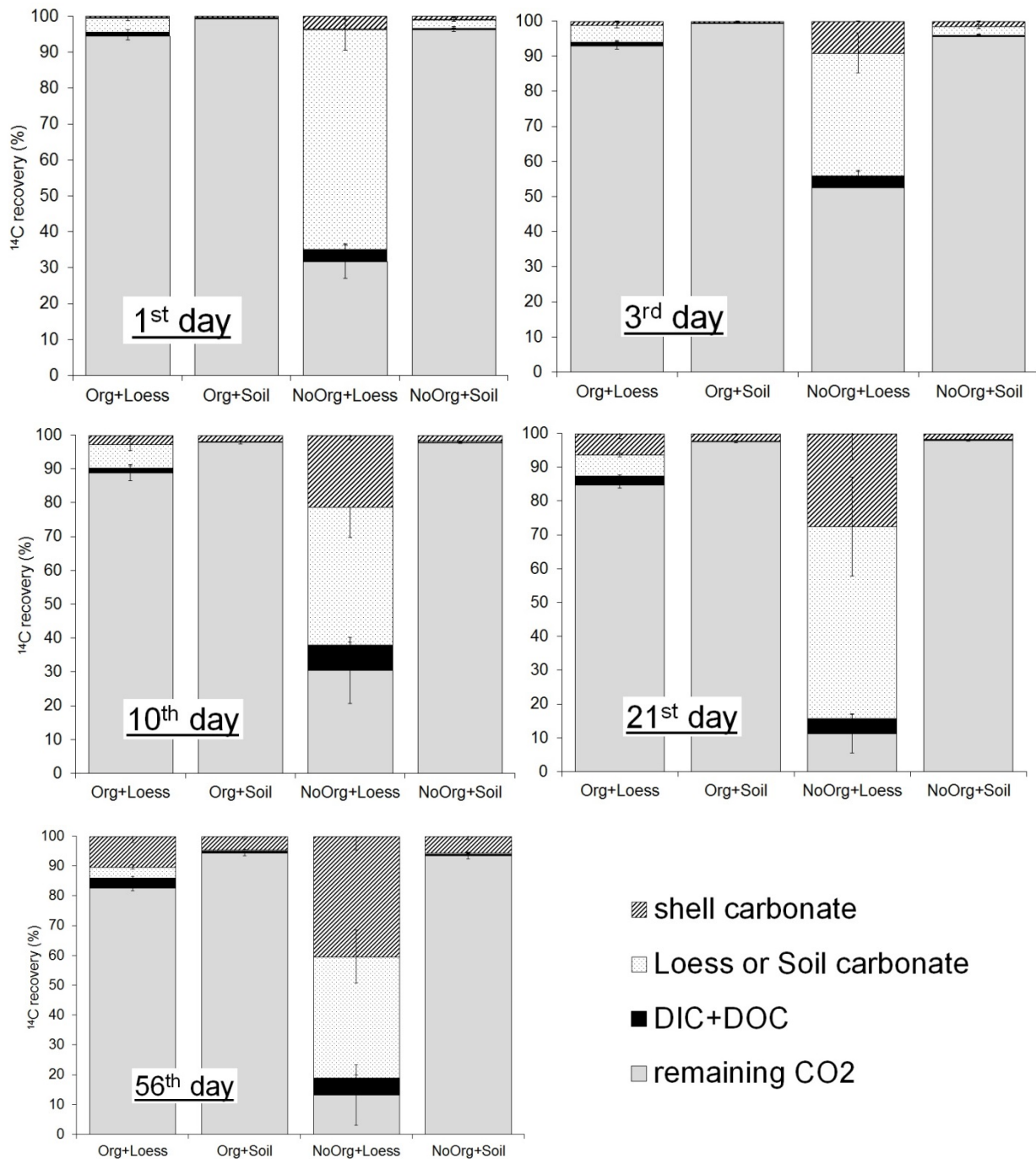


Figure 12: The distribution of measured ^{14}C activity between phases depending on time after labeling. Bar lines show standard errors.

The amount of recrystallized matrix carbonate was 0.51 mg in NoOrg+loess after two months, while the value for Org+loess was 0.05 mg (Fig. 13). Recrystallization in soil was calculated as 0.0038 to 0.0041 mg.

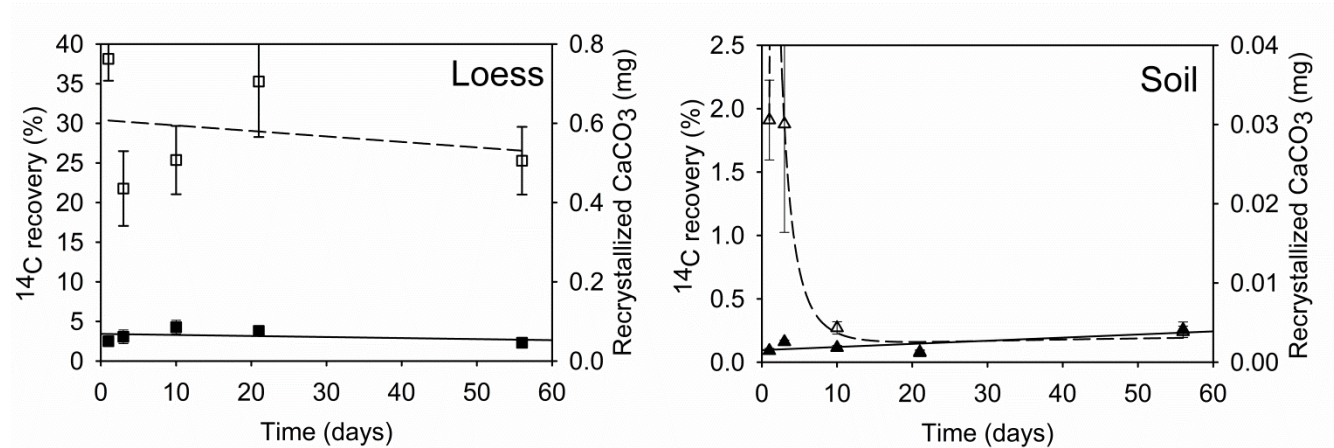


Figure 13: ^{14}C activity and recrystallized amounts of CaCO_3 in loess and soil depending on recrystallization time. The filled and open symbols refer to the shells containing and free of organic compounds, respectively. Bar lines show standard errors. Note the different scales of Y axes.

The recrystallization of shell carbonate already took place on the first day and increased exponentially with time (Fig. 14). The values in the loess were 2 to 7 times higher (for Org+loess and NoOrg+loess, respectively) than for shells in the carbonate-free soil. Removing organic compounds from the shell material increased recrystallization of shell carbonate. Therefore, the difference between the amounts of recrystallization in organic-containing and organic-free shells increased as a function of time. The highest measured recrystallization rate for 300 mg shell carbonate was $1.6 \cdot 10^{-4} \text{ day}^{-1}$ in NoOrg+loess, while the lowest was $1.0 \cdot 10^{-5} \text{ day}^{-1}$ in Org+soil. The presence of organic compounds in the shell decreased the recrystallization rates by a factor of 4 in loess and 2.6 in soil. Shell carbonate recrystallization after two months in loess was 0.56% in organic-free shells and 0.14% in organic-containing shells. In soil, recrystallization was 1.2 times higher for the organic-free shells (ca. 0.08%) than for organic-containing shells (0.06%).

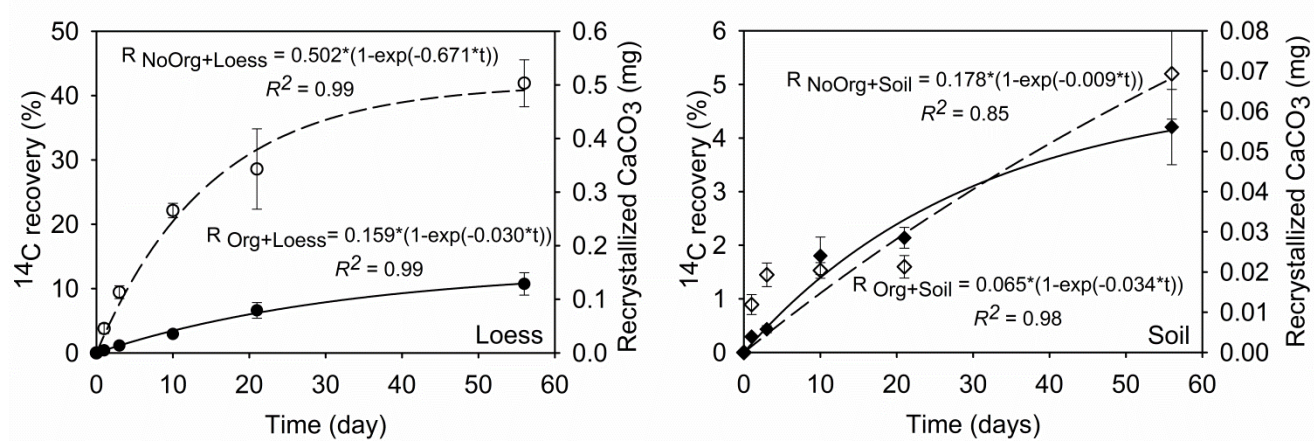


Figure 14: ^{14}C activity and recrystallized amounts of CaCO_3 on shells in loess and soil as a function of time (R_i). The filled and open symbols refer to the shells containing and free of organic compounds, respectively. Bar lines show standard errors. Note the different scales on Y-axes.

Theoretically, the entire shell fragment can undergo dissolution and recrystallization. The higher the recrystallization rate, the less non-recrystallized or original shell carbonate will remain. Therefore, after two months, NoOrg+Loess showed the lowest (99.44%) and Org+Soil the highest (99.94%) amounts of remaining, non-recrystallized shell carbonate (Fig. 15). Carbonate recrystallization is exponential with time (Kuzyakov et al., 2006) and, according to the equation, never reaches 100%. We therefore calculated the time necessary for recrystallization of 95% of the shell carbonate, and considered this as the time for full recrystallization. It is important to stress that for this assessment, the recrystallization is considered as an uninterrupted and uniform process. The exponential equations calculated from our experimental results leveled off at values far from complete recrystallization at least in NoOrg+Loess. However, to have an estimation of full recrystallization, fitted exponential equations were extrapolated to 5% remaining shell carbonate. This showed the time necessary for full recrystallization of shell carbonate in NoOrg+loess was around 90 years (Fig. 15, b). The corresponding values for shell carbonate in Org+Loess, NoOrg+soil and Org+soil were respectively around 320, 700 and 770 years (Fig. 15, c and d).

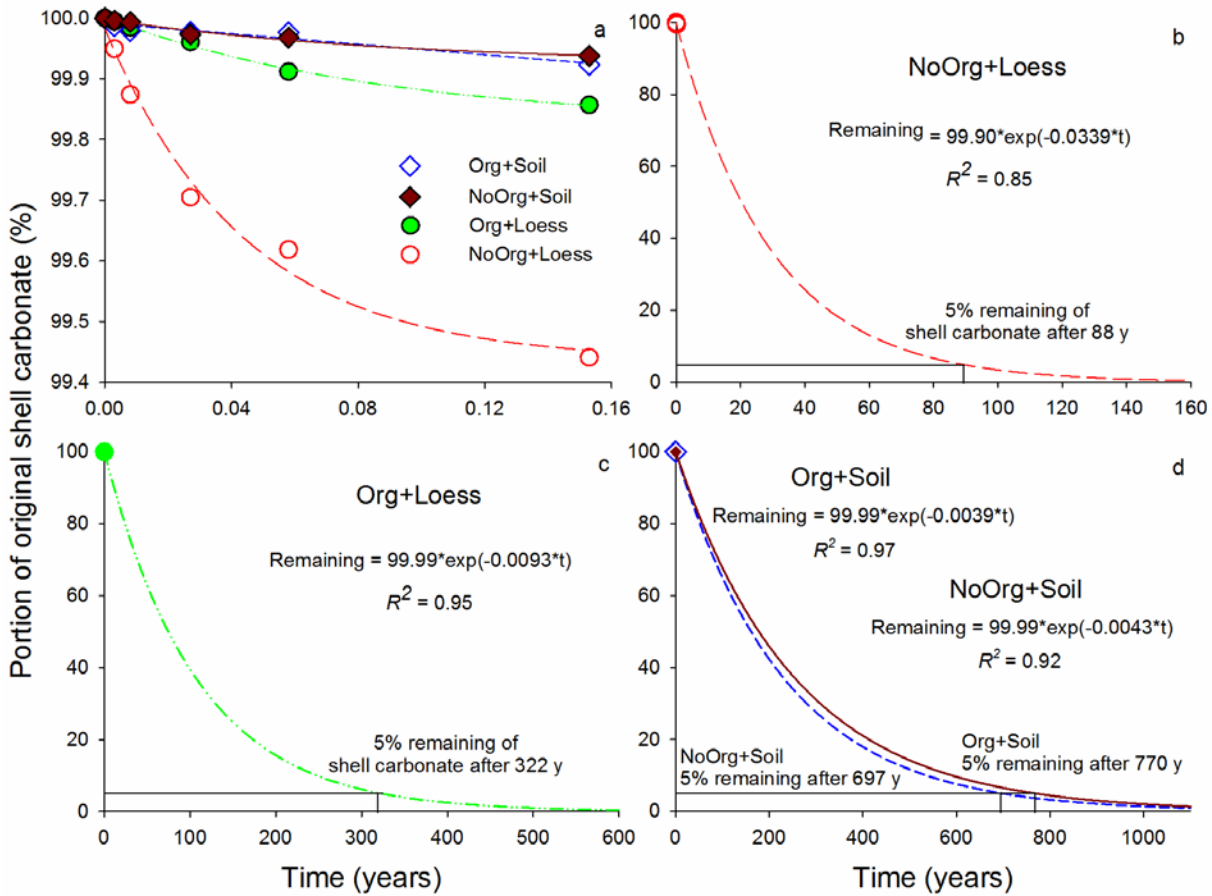


Figure 15: (a) Percentage of shell carbonate remaining not-recrystallized after 56 days, (b, c and d) the calculated time for full recrystallization of shell carbonate containing or free of organic compounds in loess or soil (95% recrystallization assumed as full recrystallization). Circles and diamonds refer to shells in loess and loamy soil, respectively. Filled and open symbols show shells containing and free of organic compounds, respectively. The model line for each treatment is shown in different line styles.

2.5. Discussion

2.5.1. Matrix carbonate recrystallization in loess and carbonate-free soil

Recrystallization of matrix carbonate was higher in the loess than in the carbonate-free soil. Recrystallization in loess was expected because it contained ca. 30% CaCO_3 (i.e. GeoC). The dissolution of GeoC and isotopic re-equilibration with labeled $^{14}\text{CO}_2$ during recrystallization

introduced ^{14}C into the loess carbonate (Gocke et al., 2010). Unexpectedly, we also measured ^{14}C in the matrix of carbonate-free soil following shell carbonate dissolution and recrystallization.

Recrystallization in NoOrg+soil was higher in the first 10 days (Fig. 13, Soil). This confirms the results of Lécuyer (1996), who showed that heating (>400 °C) increases the release of Ca^{2+} from shell structure into to the leachate (i.e. deionized water). The released Ca^{2+} into the soil solution and consequently recrystallization inside the soil, however, rapidly decreased with time (Fig. 13, Soil). This can be explained by the following. (1) The recrystallized carbonate had been dissolved in the solution and later recrystallized on shells instead of the soil. A higher rate of dissolution for recrystallized carbonate than shell carbonate is expected because of the very fine particle size, and hence large surface area, of recrystallized carbonate (Nordt et al., 1998). (2) The Ca^{2+} ions of recrystallized carbonate had been exchanged with other ions (e.g. K^+ or Na^+) on exchange sites of clay minerals or SOM. Therefore, other forms of carbonate such as Na_2CO_3 or K_2CO_3 were generated and leached out by soil washing. A similar exchange occurs in aquifers because of calcite dissolution in geologic time spans. The higher affinity of Ca^{2+} to clay minerals can displace Na^+ , K^+ and even Mg^{2+} (Appelo, 1994).

2.5.2. Recrystallization of shell carbonate

The measured shell carbonate recrystallization after one day confirms that carbonate dissolution and recrystallization can start immediately after the exposure of carbonate to CO_2 (Fairbridge, 1967). Furthermore, recrystallization increases with elimination of organic compounds from the shell structure and in the presence of GeoC in the embedding matrix when compared to the organic-containing shells in a carbonate-free matrix (Fig. 14). To discuss about the effect of organic compounds elimination and presence of GeoC on shell carbonate recrystallization, the recrystallization amounts in NoOrg+soil, Org+loess and NoOrg+loess were compared to Org+soil.

2.5.2.1. Effects of organic compound elimination on shell carbonate recrystallization

According to Fig. 4 (Loess), shell carbonate recrystallization in Org+soil ($R_{\text{Org+soil}}$) as a function of time (t) can be modelled with Eq. 2.

Eq. 2

$$R_{\text{Org+soil}} \text{ (mg)} = 0.065 \times (1 - \exp(-0.034 \times t))$$

Heating up to 550 °C eliminated nearly all shell organic compounds (Dauphin et al., 2006) and their protective effect (Hall and Kennedy, 1967; Nielsen-Marsh and Hedges, 2000). Organic compound elimination also increases shell porosity, increasing the contact surface between shell carbonate and solution and thus promoting carbonate dissolution (Collins, 2012) and recrystallization. Therefore, the recrystallization difference between NoOrg+soil and Org+soil (i.e. organic-free and organic-containing shells in soil, respectively) shows the effect of organic compounds on shell carbonate recrystallization. We suggest introducing a term characterizing the effect of organic compounds elimination on shell carbonate, K_{org} (Eq. 3).

$$Eq. 3: \quad K_{org} \text{ (mg)} = R_{NoOrg+soil} - R_{Org+soil}$$

where $R_{NoOrg+soil}$ and $R_{Org+soil}$ are the amounts of recrystallized carbonate on organic-free and organic-containing shells in soil, respectively.

The difference in recrystallization between $R_{NoOrg+soil}$ and $R_{Org+soil}$ for all measured dates was similar. Therefore, the average of all dates ($0.0048 \pm 0.008 \text{ mg CaCO}_3$) was used as the constant amount (K_{org}) to show the effect of organic compounds elimination. Accordingly, adding 0.0048 mg to Eq. 2 yields the amount of recrystallization for NoOrg+soil (R^2 between observed and predicted data: 0.75).

2.5.2.2. The effect of geogenic carbonate on shell recrystallization

The higher recrystallization rates of shell carbonate in loess versus soil (Fig. 14) demonstrated the effect of GeoC on shell carbonate recrystallization (Forman and Polyak, 1997). Therefore, higher recrystallization of organic-containing shells in loess (Org+loess) versus Org+soil shows the effect of GeoC (K_{GeoC}) on recrystallization (Eq. 4).

$$Eq. 4: \quad K_{GeoC} \text{ (mg)} = R_{Org+loess} - R_{Org+soil}$$

where $R_{Org+loess}$ and $R_{Org+soil}$ are the amounts of recrystallized carbonate for organic-containing shells in loess and soil, respectively, for each measuring date.

The amount of carbonate recrystallization due to the presence of GeoC increased exponentially with time. Therefore, instead of merely calculating the mean (as a constant amount), Eq. 5 was used to show this trend.

$$\text{Eq. 5: } K_{\text{GeoC}} \text{ (mg)} = 0.0667 \times (1 - \exp(-0.107 \times t))$$

To test the accuracy of Eq. 5, the calculated amounts of recrystallized CaCO_3 using this equation were added to the results of Eq. 2 to estimate the extent of recrystallization in Org+loess. The R^2 between measured amounts of recrystallization and the predicted data for Org+loess was 0.88. We assumed, however, that the dissolution rates of GeoC (i.e. loess carbonate) and shell carbonate were similar. Considering the disseminated structure of loess carbonate and fine particle size distribution compared to the shell carbonate, higher dissolution and recrystallization of loess carbonate is expected.

2.5.2.3. The combined effect of organic compounds and geogenic carbonate on shell carbonate recrystallization

Differences between the measured amounts of recrystallization in NoOrg+loess and NoOrg+soil should also show the effect of GeoC on shell carbonate recrystallization. However, these differences did not agree with the results of Eq. 4. Furthermore, adding K_{org} (calculated as 0.0048 mg) to K_{GeoC} (Eq. 6) did not yield the measured recrystallization of shells in NoOrg+loess. Eliminating the protective effect of shell organic compounds (Hall and Kennedy, 1967; Nielsen-Marsh and Hedges, 2000) as well as increasing the shell porosity (Collins, 2012) made shell carbonate more vulnerable to dissolution. Accordingly, recrystallization took place not only on the shell surface but also in the interior of the shell structure (Yates, 1986). Organic compound elimination therefore intensified the effect of GeoC (K_{GeoC} in the equations below) on shell carbonate recrystallization. To show this intensification we used the difference between measured amounts of recrystallization in NoOrg+loess and Org+soil (Eq. 7). Adding the term intensification (int.) to Eq. 6 equating it to Eq. 7 allows the amount of intensification to be calculated (Eq. 8).

$$\text{Eq. 6: } K_{(\text{GeoC} + \text{NoOrg})} = (R_{\text{Org+loess}} - R_{\text{Org+soil}}) + (R_{\text{NoOrg+soil}} - R_{\text{Org+soil}}) =$$

$$R_{\text{Org+loess}} + R_{\text{NoOrg+soil}} - 2R_{\text{Org+soil}}$$

$$\text{Eq. 7: } K_{(\text{GeoC} + \text{NoOrg})} = R_{\text{NoOrg+loess}} - R_{\text{Org+soil}}$$

$$\text{Eq. 8: } K_{(\text{GeoC} + \text{NoOrg} + \text{int.})} = E_{(\text{GeoC} + \text{NoOrg})} =$$

$$R_{\text{Org+loess}} + R_{\text{NoOrg+soil}} - 2R_{\text{Org+soil}} + \text{int.} = R_{\text{NoOrg+loess}} - R_{\text{Org+soil}} \rightarrow$$

$$\text{int.} = (R_{\text{NoOrg+loess}} - R_{\text{Org+soil}}) - (R_{\text{Org+loess}} + R_{\text{NoOrg+soil}} - 2R_{\text{Org+soil}}) =$$

$$(R_{\text{NoOrg+loess}} + R_{\text{Org+soil}}) - (R_{\text{Org+loess}} + R_{\text{NoOrg+soil}})$$

We used Eq. 9 to determine the ratio between the calculated recrystallization due to intensification (Eq. 8) and the effect of GeoC and organic compound elimination (Eq. 6). Since Eq. 9 predicts similar values for all dates, the mean of all dates was used as the constant rate, showing intensification of $K_{\text{int.}} = 4.80 \pm 1.1$. Using this calculated constant rate ($K_{\text{int.}}$), we estimated the amount of recrystallized shell carbonate in NoOrg+loess as a function of time (Eq. 10). The formulated equation (Eq. 10) was then used to predict shell carbonate recrystallization ($R_{\text{shell carbonate}}$) of all treatments on all dates. The R^2 of the linear regression between measured and predicted data of all treatments and dates using Eq. 10 was 0.98 (Fig. 16).

$$\text{Eq. 9: } K_{\text{int.}} = \text{int.} / K_{(\text{GeoC} + \text{NoOrg})} = 4.8029$$

$$\text{Eq. 10: } R_{\text{shell carbonate}} = R_{\text{Org+soil}} + K_{\text{GeoC}} + K_{\text{NoOrg}} + \text{int.} = (R_{\text{Org+soil}} + K_{\text{GeoC}} + K_{\text{org}}) \times K_{\text{int.}}$$

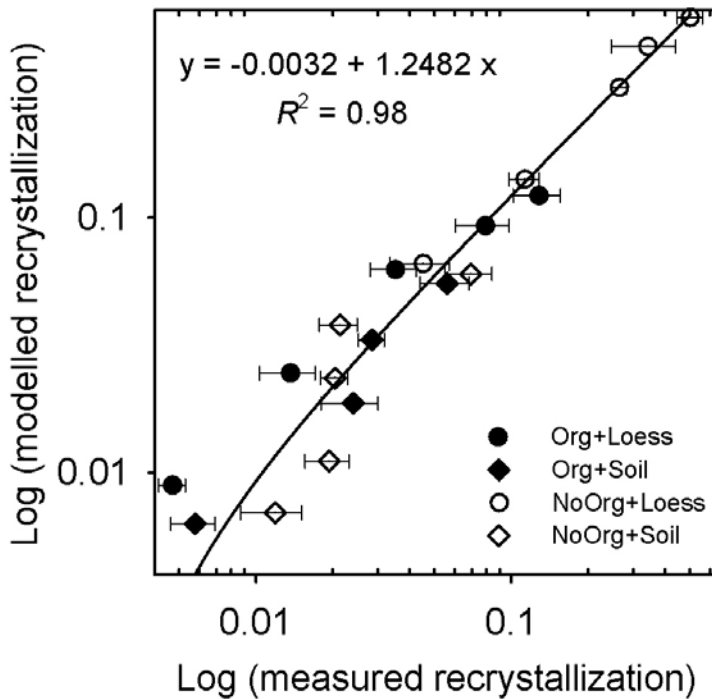


Figure 16: The relation between modelled amounts of shell-carbonate recrystallization using Eq. (9) for all treatments and times with measured recrystallization. Bar lines show standard errors of measured recrystallization of each of four treatments at various dates.

2.5.3. Time required for full recrystallization of shell carbonate

Full recrystallization time calculated in this study was at least 10 times shorter than earlier estimations of 90% recrystallization after 7000 y (Chappell and Pollach, 1972). Different properties of the deposition areas (Yates et al., 2002) are one reason for the various estimates. In the littoral zone (Chappell and Pollach, 1972) water circulation (Forman and Polyak, 1997) washed out the dissolved Ca^{2+} ions, prolonging the time necessary for full recrystallization of shell carbonate. Moreover, solubility of CaCO_3 in seawater with alkaline pH (Jacobson, 2005) is lower than in soil solution ($p\text{CO}_2 = 2\%$) (Pausch and Kuzyakov, 2012). Also noteworthy is that our time estimation is based on the assumption that shell carbonate recrystallization is a continuous process.

The recrystallization process is exponential in time (Kuzyakov et al., 2006). Since the recrystallized carbonate is thought to first fill all the gaps in the outer shell layers and cover the shell surface (Webb et al., 2007), it protects the rest of the shell carbonate from further dissolution. Therefore, pre-treatments (e.g. washing with acids) before ^{14}C dating of shell carbonate provide

more reliable dates (Yates, 1986). In calcareous soils or sediments (e.g. loess), where the recrystallization involves not only shell carbonate but also GeoC (Yates et al., 2002; Prendergast and Stevens, 2014), the time necessary for full recrystallization will be longer than estimated. In turn, recrystallized carbonate on the shell surface will undergo repeated recrystallization. This can buffer CO₂ reactions and protect the shell carbonate from further recrystallization. Analysis of this time delay requires a specific experimental layout.

After full recrystallization of shell carbonate, however, the isotopic composition of C is no longer related to the environmental conditions during the life time of the mollusk or its diet regime. The C isotopes will contain information about the properties of the environment in which it is embedded and the recrystallization conditions (Prendergast and Stevens, 2014).

2.5.4. Significance of the results for archaeology and paleoenvironmental research

The findings of this study have implications in archaeology and related disciplines. Since shell carbonate can serve both as a dating material and a paleoenvironmental proxy, a profound understanding of its geochemical behavior in cultural layers, soils and sediments over long periods of time is essential. Moreover, it frequently represents the only proxy record available, especially in arid regions. It should be also noted that some archaeological sites, such as shell middens, consist almost entirely of shell carbonate (Álvarez et al., 2011). The findings are, further, equally relevant to research on other finds of carbonate materials in cultural layers, for example egg shells (Magee et al., 2009).

Notwithstanding the existence of analytical tools for testing the integrity of mollusk shell carbonate for dating purposes or paleoenvironmental reconstructions, surprisingly little is known about the dynamics of diagenetic shell recrystallization in different sedimentological environments. The relatively low rate of carbonate dissolution limits the feasibility of reproducing the process with conventional methods. Currently, the outcome of shell carbonate exposure to CO₂ in different sedimentological settings appears difficult to predict without experiment or modelling. To sum up, three issues of our study deserve particular attention.

(1) The ¹⁴C-labelling approach enables detecting of very low concentrations of newly-formed CaCO₃. Our data showed that the ¹⁴C label is present in both shell and matrix carbonate very soon after the exposure to ¹⁴CO₂. The method thus offers a new experimental perspective for research on the recrystallization of biogenic carbonates under fine-tuned, controlled, laboratory conditions.

The proposed model also suggests an approach to estimate and predict the extent of recrystallization in a given sample when investigating paleoenvironment reconstructions, or for dating purposes.

(2) Most chronological and paleoecological studies neglect both the character of original organic matter in a mollusk shell and the carbonate content of its ambient matrix. Our experiments demonstrate that these parameters are essential when assessing the probability of carbonate recrystallization and interpreting radiometric and isotopic shell characteristics (Fig. 17). This is especially important if archaeological contexts involve burned material with mollusk shells (Rodrigues et al., 2009).

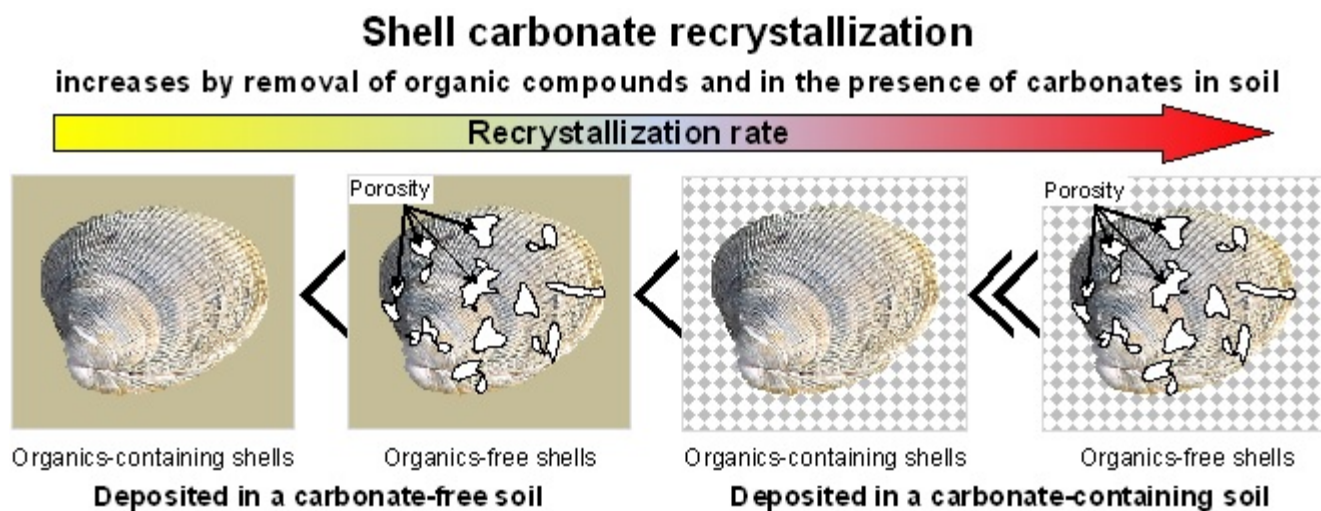


Figure 17: Shell carbonate recrystallization depending on presence of organic compounds in shell structure and geogenic carbonates in soil. Organic compounds elimination increases shell porosity and make it vulnerable to recrystallization. Geogenic carbonates may also undergo dissolution and may recrystallize on shell surface or fill shell's structural porosities.

(3) When extrapolating the results of this study to real archaeological settings, it must be borne in mind that the conditions of our experiment comply with a relatively limited spectrum of geochemical systems. Experimental conditions corresponded to the CO₂ concentrations occurring commonly in the uppermost horizons of exposed (non-buried) soils with developed root systems of vegetation and a certain degree of microbial activity. In terrestrial environments, such conditions are rare at depths greater than ca. 1 m below the land surface and in extremely cool, hot or dry

climates. Also, except in wet tropical environments, the annual soil CO₂ production is usually not uninterrupted, but restricted in time to the vegetative period. Its duration and combination with other climate parameters should be taken into account when the recrystallization period is the focus of interest.

A key goal for future research will be to increase the practical value of ¹⁴C-labeling research on mollusk shells by conducting experiments that approximate natural carbonate recrystallization processes. The experiments should be appropriately modified by adding living root systems and varying factors such as depth, temperature and moisture regimes. Furthermore, future investigations should focus on comparisons between experimentally deduced recrystallization values and native samples of shell carbonate of known age that have been exposed to CO₂ under known or predictable conditions.

2.6. Conclusions

Shell carbonate recrystallization begins very soon after embedding in soils and increases exponentially with time. Within two months, 0.06 to 0.56 mg per 100 mg shell carbonate was recrystallized, depending on the presence of organic compounds in the shell structure and geogenic carbonates in the soil.

Shell and environmental properties affect the rates of shell carbonate recrystallization. Removing structural organic compounds and thus enhancing shell porosity increased the rate by 0.0048 mg (2-2.5 mm shell size). In the presence of geogenic carbonate, shell recrystallization increased because part of the recrystallized carbonate originated from re-precipitation of dissolved geogenic carbonate. The effect of geogenic carbonates was time-dependent and was intensified after elimination of structural organic compounds with associated increases in shell porosity. This intensification increased the measured recrystallized carbonate up to 4.8 times compared with pristine shells in carbonate-free soil. Recrystallization should be considered when interpreting of dating results and paleoenvironmental reconstructions.

The ¹⁴C labeling approach was sensitive in assessing recrystallization rates of biogenic carbonate such as shell carbonate, within reasonably short times. ¹⁴C labeling provides a useful tool to examine the effects of individual factors on shell carbonate recrystallization.

2.7. Acknowledgement

We acknowledge Heidelberg Cement AG for sampling permission in their queries specially Dr. Manfred Löscher for discussion in the field. We would like to thank Anita Kriegel and Shibin Liu for their help during sampling and analyses. Special thanks to Ingrid Ostermeyer and Martina Gebauer for measuring soil properties and the elemental composition of shells. We gratefully acknowledge Mohsen Zarebanadkouki for his comments on the manuscript and Kyle Mason-Jones for English editing of the text. The study was supported by German Research Foundation (DFG) (KU 1184/34-1).

2.8. References

- Álvarez M., Briz Godino I., Balbo A. and Madella M. (2011) Shell middens as archives of past environments, human dispersal and specialized resource management. *Quat. Int.* **239**, 1–7.
- Antoine P., Rousseau D.-D., Moine O., Kunesch S., Hatté C., Lang A., Tissoux H. and Zöller L. (2009) Rapid and cyclic aeolian deposition during the Last Glacial in European loess: a high-resolution record from Nussloch, Germany. *Quat. Sci. Rev.* **28**, 2955–2973.
- Appelo C. a. J. (1994) Cation and proton exchange, pH variations, and carbonate reactions in a freshening aquifer. *Water Resour. Res.* **30**, 2793–2805.
- Berna F., Matthews A. and Weiner S. (2004) Solubilities of bone mineral from archaeological sites: the recrystallization window. *J. Archaeol. Sci.* **31**, 867–882.
- Bezerra F. H. R., Vita-Finzi C. and Lima Filho F. P. (2008) The use of marine shells for radiocarbon dating of coastal deposits. *Braz. J. Geol.* **30**, 211–213.
- Bonadonna F. P., Leone G. and Zanchetta G. (1999) Stable isotope analyses on the last 30 ka molluscan fauna from Pampa grassland, Bonaerense region, Argentina. *Palaeogeogr. Palaeoclimatol. Palaeoecol.* **153**, 289–308.
- Cerling T. E., Quade J., Wnag Y. and Bowman J. R. (1989) Carbon isotopes in soils and palaeosols as ecology and palaeoecology indicators. *Nature* **341**, 139–139.
- Chappell J. and Pollach H. A. (1972) Some Effects of Partial Recrystallisation on 14C Dating Late Pleistocene Corals and Molluscs. *Quaternary Research* **2**, 244–252.
- Cochran J. K., Kallenberg K., Landman N. H., Harries P. J., Weinreb D., Turekian K. K., Beck A. J. and Cobban W. A. (2010) Effect of diagenesis on the Sr, O, and C isotope composition of late Cretaceous mollusks from the Western Interior Seaway of North America. *Am. J. Sci.* **310**, 69–88.
- Collins J. D. (2012) Assessing mussel shell diagenesis in the modern vadose zone at Lyon's Bluff (22OK520), Northeast Mississippi. *J. Archaeol. Sci.* **39**, 3694–3705.
- Dauphin Y., Cuif J.-P. and Massard P. (2006) Persistent organic components in heated coral aragonitic skeletons—Implications for palaeoenvironmental reconstructions. *Chem. Geol.* **231**, 26–37.
- Douka K., Higham T. F. G. and Hedges R. E. M. (2010) Radiocarbon dating of shell carbonates: old problems and new solutions. *Munibe Suplemento* **31**, 18–27.
- Fairbridge R. W. (1967) Chapter 2 Phases of Diagenesis and Authigenesis. In *Developments in Sedimentology* (ed. G. L. and G. V. Chilingar). Diagenesis in Sediments. Elsevier. pp. 19–89.

Available at: <http://www.sciencedirect.com/science/article/pii/S0070457108708410> [Accessed January 10, 2015].

- Forman S. L. and Polyak L. (1997) Radiocarbon content of pre-bomb marine mollusks and variations in the ^{14}C Reservoir age for coastal areas of the Barents and Kara Seas, Russia. *Geophys. Res. Lett.* **24**, 885–888.
- Gocke M., Pustovoytov K. and Kuzyakov Y. (2011) Carbonate recrystallization in root-free soil and rhizosphere of *Triticum aestivum* and *Lolium perenne* estimated by ^{14}C labeling. *Biogeochemistry* **103**, 209–222.
- Gocke M., Pustovoytov K. and Kuzyakov Y. (2010) Effect of CO_2 concentration on the initial recrystallization rate of pedogenic carbonate — Revealed by ^{14}C and ^{13}C labeling. *Geoderma* **155**, 351–358.
- Hall A. and Kennedy W. J. (1967) Aragonite in Fossils. *Proc. R. Soc. Lond. B Biol. Sci.* **168**, 377–412.
- Henrich R. and Wefer G. (1986) Dissolution of biogenic carbonates: Effects of skeletal structure. *Mar. Geol.* **71**, 341–362.
- Jacobson M. Z. (2005) Studying ocean acidification with conservative, stable numerical schemes for nonequilibrium air-ocean exchange and ocean equilibrium chemistry. *J. Geophys. Res. Atmospheres* **110**, D07302.
- Janz L., Elston R. G. and Burr G. S. (2009) Dating North Asian surface assemblages with ostrich eggshell: implications for palaeoecology and extirpation. *J. Archaeol. Sci.* **36**, 1982–1989.
- Krueger H. W. (1991) Exchange of carbon with biological apatite. *J. Archaeol. Sci.* **18**, 355–361.
- Kuzyakov Y., Shevtsova E. and Pustovoytov K. (2006) Carbonate re-crystallization in soil revealed by ^{14}C labeling: Experiment, model and significance for paleo-environmental reconstructions. *Geoderma* **131**, 45–58.
- Lécuyer C. (1996) Effects of heating on the geochemistry of biogenic carbonates. *Chem. Geol.* **129**, 173–183.
- Lécuyer C. and O'Neil J. . (1994) Stable isotope compositions of fluid inclusions in biogenic carbonates. *Geochim. Cosmochim. Acta* **58**, 353–363.
- Magee J. W., Miller G. H., Spooner N. A., Questiaux D. G., McCulloch M. T. and Clark P. A. (2009) Evaluating Quaternary dating methods: Radiocarbon, U-series, luminescence, and amino acid racemization dates of a late Pleistocene emu egg. *Quat. Geochronol.* **4**, 84–92.
- Nielsen-Marsh C. M. and Hedges R. E. M. (1999) Bone Porosity and the Use of Mercury Intrusion Porosimetry in Bone Diagenesis Studies*. *Archaeometry* **41**, 165–174.
- Nielsen-Marsh C. M. and Hedges R. E. M. (2000) Patterns of Diagenesis in Bone I: The Effects of Site Environments. *J. Archaeol. Sci.* **27**, 1139–1150.
- Nordt L. C., Hallmark C. T., Wilding L. P. and Boutton T. W. (1998) Quantifying pedogenic carbonate accumulations using stable carbon isotopes. *Geoderma* **82**, 115–136.
- Oliver A., Solís C., Rodríguez-Fernandez L. and Andrade E. (1996) Chemical diagenesis in fossil shells from Baja California, México studied using PIXE and mass spectrometry. *Nucl. Instrum. Methods Phys. Res. Sect. B Beam Interact. Mater. At.* **118**, 414–417.
- Pausch J. and Kuzyakov Y. (2012) Soil organic carbon decomposition from recently added and older sources estimated by $\delta^{13}\text{C}$ values of CO_2 and organic matter. *Soil Biol. Biochem.* **55**, 40–47.
- Piepenbrink H. (1989) Examples of chemical changes during fossilisation. *Appl. Geochem.* **4**, 273–280.

Pigati D. J. S. (2013) Radiocarbon Dating of Terrestrial Carbonates. In *Encyclopedia of Scientific Dating Methods* (eds. W. J. Rink and J. Thompson). Springer Netherlands. pp. 1–9. Available at: http://link.springer.com/referenceworkentry/10.1007/978-94-007-6326-5_152-1 [Accessed March 4, 2016].

Pigati J. S., Quade J., Shahanan T. M. and Haynes Jr. C. V. (2004) Radiocarbon dating of minute gastropods and new constraints on the timing of late Quaternary spring-discharge deposits in southern Arizona, USA. *Palaeogeogr. Palaeoclimatol. Palaeoecol.* **204**, 33–45.

Pigati J. S., Rech J. A. and Nekola J. C. (2010) Radiocarbon dating of small terrestrial gastropod shells in North America. *Quat. Geochronol.* **5**, 519–532.

Prendergast A. L. and Stevens R. E. (2014) Molluscs (isotopes) – Analyses in environmental archaeology. In *The Encyclopedia of Global Archaeology*. Springer.

Ragland P. C., Pilkey O. H. and Blackwelder B. W. (1979) Diagenetic changes in the elemental composition of unrecrystallized mollusk shells. *Chem. Geol.* **25**, 123–134.

Robbins C. W. (1985) The CaCO₃-CO₂-H₂O system in soils. *J. Agron. Educ.* **14**. Available at: <https://dl.sciencesocieties.org/files/publications/jnrlse/pdfs/jnr014/014-01-0003.pdf> [Accessed January 10, 2015].

Rodrigues S. I., Porsani J. L., Santos V. R. N., DeBlasis P. A. D. and Giannini P. C. F. (2009) GPR and inductive electromagnetic surveys applied in three coastal sambaqui (shell mounds) archaeological sites in Santa Catarina state, South Brazil. *J. Archaeol. Sci.* **36**, 2081–2088.

Russo C. M., Tripp J. A., Douka K. and Higham T. F. (2010) A New Radiocarbon Pretreatment Method for Molluscan Shell Using Density Fractionation of Carbonates in Bromoform. *Radiocarbon* **52**, 1301–1311.

Shemesh A. (1990) Crystallinity and diagenesis of sedimentary apatites. *Geochim. Cosmochim. Acta* **54**, 2433–2438.

Thomas K. D. (2015) Molluscs emergent, Part I: themes and trends in the scientific investigation of mollusc shells as resources for archaeological research. *J. Archaeol. Sci.* **56**, 133–140.

Újvári G., Molnár M., Novothny Á., Páll-Gergely B., Kovács J. and Várhegyi A. (2014) AMS 14C and OSL/IRSL dating of the Dunaszekcső loess sequence (Hungary): chronology for 20 to 150 ka and implications for establishing reliable age–depth models for the last 40 ka. *Quat. Sci. Rev.* **106**, 140–154.

Walls R. A., Ragland P. C. and Crisp E. L. (1977) Experimental and natural early diagenetic mobility of Sr and Mg in biogenic carbonates. *Geochim. Cosmochim. Acta* **41**, 1731–1737.

Webb G. E., Price G. J., Nothdurft L. D., Deer L. and Rintoul L. (2007) Cryptic meteoric diagenesis in freshwater bivalves: Implications for radiocarbon dating. *Geology* **35**, 803–806.

Xu B., Gu Z., Han J., Liu Z., Pei Y., Lu Y., Wu N. and Chen Y. (2010) Radiocarbon and Stable Carbon Isotope Analyses of Land Snails from the Chinese Loess Plateau: Environmental and Chronological Implications. *Radiocarbon* **52**, 149–156.

Yanes Y., Gómez-Puche M., Esquembre-Bebia M. A. and Fernández-López-De-Pablo J. (2013) Younger Dryas – early Holocene transition in the south-eastern Iberian Peninsula: insights from land snail shell middens. *J. Quat. Sci.* **28**, 777–788.

Yates T. (1986) Studies of non-marine mollusks for the selection of shell samples for radiocarbon dating. *Radiocarbon* **28**, 457–463.

Yates T. J. S., Spiro B. F. and Vita-Finzi C. (2002) Stable isotope variability and the selection of terrestrial mollusc shell samples for 14C dating. *Quat. Int. - QUATERN INT* **87**, 87–100.

Zazzo A. and Saliège J.-F. (2011) Radiocarbon dating of biologicalapatites: A review. *Palaeogeogr. Palaeoclimatol. Palaeoecol.* **310**, 52–61.

3. Cation exchange retards shell carbonate recrystallization: Consequences for dating and paleoenvironmental reconstructions

Published: **Catena** 142 (2016): 134-138



Kazem Zamanian¹, Konstantin Pustovoytov², Yakov Kuzyakov^{1,3}

¹. Department of Soil Science of Temperate Ecosystems, Department of Agricultural Soil Science, University of Göttingen, Büsgenweg 2, 37077 Göttingen, Germany

². Institute of Soil Science and Land Evaluation (310), University of Hohenheim, Schloss Hohenheim 1, 70599 Stuttgart, Germany

³. Institute of Environmental Sciences, Kazan Federal University, Kazan, Russia

3.1. Abstract

The radiocarbon method has been frequently used to date mollusk shell carbonate. The accuracy of estimated ages, however, depends on the degree and completeness of shell carbonate recrystallization. Although the effect of contamination of the shell CaCO_3 with environmental carbon (C) is well known, the role of Ca^{2+} in diagenetic processes remains unclear. Addition of young C to shells during diagenesis occurs in soil solution, where the Ca^{2+} concentration is in equilibrium with exchangeable Ca^{2+} and/or weathering of Ca-bearing minerals. While the exchange process takes place within seconds, the dissolution equilibrium requires longer timescales (on the order of months). It has therefore been hypothesized that the dissolution and recrystallization of shell carbonate in soils with higher cation exchange capacity (CEC) should proceed slower compared to those with low CEC. The objective was to determine the effects of soil CEC and exchangeable cations on shell carbonate recrystallization using the ^{14}C labeling approach. Shell particles of the bivalve *Protothaca staminea* were mixed with carbonate-free sand ($\text{CEC} = 0.37 \text{ cmol}^+ \text{ kg}^{-1}$) (Sand), a loamy soil ($\text{CEC} = 16 \text{ cmol}^+ \text{ kg}^{-1}$) (Loam) or the same loamy soil saturated with KCl, where exchangeable cations were replaced with K^+ (Exchanged). The high-sensitivity ^{14}C labeling/tracing approach was used to determine carbonate recrystallization rates. Shell carbonate recrystallization after 120 days in Loam and Exchanged (0.016 and 0.024 mg CaCO_3 , respectively) showed one order of magnitude lower recrystallization than in Sand (0.13 mg CaCO_3). A high level of soil

exchangeable Ca^{2+} decreased the solubility of shell carbonate and consequently its recrystallization because the exchange is faster than dissolution. Therefore, soil CEC and cation composition are determinant factors of shell carbonate recrystallization. Shells in soils with low CEC may undergo more intensive recrystallization; hence they may need further pretreatments before the dating procedure.

Keywords: cation exchange capacity, biogenic carbonates, recrystallization, ^{14}C labeling

3.2. Introduction

The radiocarbon ($\Delta^{14}\text{C}$) age of shell carbonate has a long history of application for dating purposes (Arrhenius et al., 1951; Kulp et al., 1951; Scholl, 1964; Douka et al., 2010; Pigati et al., 2010). To achieve reliable dating, however, shell carbonate should behave as a closed system in respect to C after deposition in soils (Pigati et al., 2010). An addition of merely 10-15% modern C from the embedding soil matrix, for example, may lead to an 11 ka age difference in ca. 30 ka year-old shells (Webb et al., 2007). Modern C addition to shell carbonate occurs by precipitation of secondary carbonate minerals on shells, when the solubility constants are achieved in soil solution. Therefore, the ions' concentration in soil solution will be the key determinant of secondary carbonate formation rates (Pate et al., 1989). The $\Delta^{14}\text{C}$ of these newly formed secondary carbonates, however, will differ from the $\Delta^{14}\text{C}$ of shell carbonate and reflect the time of precipitation rather than shell carbonate age. Thus, a complete understanding of the processes by which secondary carbonate can become incorporated into shell material is critical for evaluating the veracity of shell ^{14}C ages.

Several approaches have been proposed to solve the problem of ^{14}C contamination in radiometric dating of biogenic carbonates in soils and sediments. The non-modified carbonate can be mechanically separated from the newly-formed fraction and be dated thereafter (Douka et al., 2010). Usually, however, the risk of encountering diagenetically altered carbonate is assessed by comparing the measured ^{14}C ages of carbonate with the known ages of other, independent sources (Pigati et al., 2004, 2013; Pustovoytov & Riehl, 2006; Magee et al., 2009). Furthermore, the rate of carbonate recrystallization in soil can be estimated experimentally by ^{14}C -labeling of CO_2 under controlled conditions (Kuzyakov et al., 2006; Gocke et al., 2012). The latter method offers a possibility of studying the effects of recrystallization on ^{14}C contamination of carbonates within a relatively short time (weeks to months). At the same time, precise knowledge of the effects of

specific soil properties on carbonate recrystallization is needed to extrapolate experimental results to natural soils and sediments.

Here, we address the effect of the cation exchange capacity (CEC), one of the main inherent soil characteristics, on the diagenetic alteration of shell carbonate using the ^{14}C labeling technique. The concentration of cations, i.e. Ca^{2+} , in soil solution is in equilibrium with the exchangeable Ca^{2+} on surfaces of clay minerals and organic matter and with the dissolution of Ca-bearing minerals such as calcite in shell structure. The concentration of exchangeable Ca^{2+} in soils depends on total clay content and total soil organic matter as well as the mineralogy of dominant clay minerals. CaCO_3 solubility in soil solution is controlled by CO_2 partial pressure in soil atmosphere (Karberg et al., 2005) which is usually between 0.15 and 2.5% and may reach even to 12% (in Stolwijk & Thimann, 1957). Therefore, in slightly acidified soil solution i.e. following CO_2 dissolution, the solubility of CaCO_3 increases (Aylward, 2007). However, the exchange process is completed within a few seconds to a few days and is faster than dissolution equilibria – months to years (Sears & Langmuir, 1982). Therefore, the exchange process is the main source of cations buffering changes in soil solution chemistry, for example following acidification (Sears & Langmuir, 1982; Norrström, 1995).

Considering that the exchange rate is faster than dissolution, we hypothesized that shell recrystallization will be the slowest in soils with high CEC. This is because cations released from exchange sites will buffer changes in soil solution chemistry before shell carbonate dissolution can reach the equilibrium. Accordingly, shell carbonate undergoes less dissolution and consequently less recrystallization. Here we examine the role of soil matrix CEC on shell carbonate recrystallization using ^{14}C labeling. The objectives were to: (1) determine how soil CEC affects the rate of carbonate recrystallization in shells, (2) clarify whether the elemental composition of cations modifies the recrystallization rates, and (3) underline the consequences for radiocarbon dating and paleoenvironmental reconstructions.

3.3. Materials and methods

3.3.1. Matrix materials

Carbonate-free sand particles and a carbonate-free loamy soil were used to examine the effect of CEC on shell carbonate recrystallization (Table 5). Sand particle diameters ranged from 0.5-1.5 mm. The particle size distribution of loamy soil (Loam) was 25.1% clay, 68.4% silt and 6.5% sand.

To examine the effect of cation types at the soil exchange sites and the concentration of exchangeable Ca^{2+} on shell carbonate recrystallization, a subsample of the Loam saturated with 1 N KCl to substitute exchangeable Ca^{2+} with potassium (K). 33 mL of KCl solution was added to 5 g of soil. The suspension was shaken for 5 min followed by 5 min centrifugation in 2500 rpm. After decanting the supernatant, the procedure of KCl addition and centrifugation was repeated two more times. Subsequently, the exchanged soil was washed out 3-4 times with distilled water to remove the remaining chlorine ions (Cl^-) from the soil solution. The presence of Cl^- in the supernatant was tested by adding a few drops of 1 M AgNO_3 . The absence of white precipitate showed the complete removal of Cl^- . The treated soil (Exchanged) was dried afterward at 105 °C overnight.

Table 5: Exchangeable cations in sand and soil and cation contents in shells

	Ca^{2+}	K^+	Mg^{2+}	Na^+	CEC
$\text{mmol}^+ \text{kg}^{-1}$					
Sand	0.79	0.06	0.17	0.07	3.71
Loam	132	4.21	20.5	0.22	163
Exchanged	19.4	119	4.33	0.26	156
mg g^{-1}					
Shell	370	0.29	0.35	4.80	

3.3.2. Experimental setup and analyses

300 mg of heated (550 °C) shell particles of Pacific little-neck clams (*Protothaca staminea*) (Table 5) in the size range of 2 - 2.5 mm were mixed with 7 g of Sand, Loam and Exchanged in 250 mL glass bottles. 1.68 mL of distilled water was added to the Sand as well as 2.37 mL to the Loam and Exchanged to bring the soil moisture to 80% of water holding capacity. Two 1.5 mL plastic vials were placed in the bottles for labeling (see below). The bottles were then sealed air-tight and kept at room temperature for 5, 20, 60 and 120 days.

Following sealing, 0.2 mL of $\text{Na}_2^{14}\text{CO}_3$ was added to one of the plastic vials. The concentration of $\text{Na}_2^{14}\text{CO}_3$, considering the air volume in bottles after subtraction of soil and water, was 2% CO_2 partial pressure after neutralizing the $\text{Na}_2^{14}\text{CO}_3$ by acid. 2% $p\text{CO}_2$ is the common soil $p\text{CO}_2$ in the presence of living roots (Pausch & Kuzyakov, 2012). Afterwards by injecting 0.2 mL of 1 M H_3PO_4

solution into the vial containing $\text{Na}_2^{14}\text{CO}_3$ solution, the ^{14}C -labeled CO_2 was released into the bottle's air as the first labeling ($t = 0$). The second labeling was done in the same way at day 55 ($t = 55$). The ^{14}C activity at both labeling times was 9.35 kBq in Sand and 6.92 kBq in Loam and Exchanged.

One day before opening the bottles at each sampling date (i.e. 5, 20, 60 and 120 days), 0.4 mL of 1 N NaOH was injected into the second plastic vial to trap the remaining CO_2 , i.e. not incorporated in carbonate recrystallization. The amount of recrystallized carbonates on shells and in matrices was calculated, considering the known C amounts added to the bottles, the total added ^{14}C and the measured ^{14}C activity in shells and matrices (Kuzyakov et al., 2006).

After opening of bottles, the matrices were washed with 10 mL of distilled water. The shell particles were removed from the matrices with tweezers and washed ultrasonically to remove any adhering matrix particles. Shell particles as well as the matrix materials were ground into a fine powder. 0.1 g of shell powder and 2 g of matrix materials were acidified to release carbonates as CO_2 , which was trapped in 1 M NaOH solution. Then, scintillation cocktail (Rotiszint EcoPlus, Carl Roth, Germany) was added to an aliquot of alkali solutions (i.e. NaOH in plastic vials and NaOH used to trap released CO_2 by acidification of shells and matrices) and washing water. After few hours waiting for chemiluminescence decay, ^{14}C activity was measured by a multi radio-isotope counter (Beckman LS6500, USA). The ^{14}C counting efficiency was at least 70% and the measurement error was 5% at maximum.

Besides the treatments containing shell particles, solely matrix materials with the same water content and labeling procedures were prepared to determine whether carbonate precipitation takes place because of Ca^{2+} release from exchange sites. Recrystallization in these samples, however, was measured just at the end of experiment i.e. after 120 days.

CEC of the matrix materials and the composition of exchangeable cations were measured at each sampling period. CEC and exchangeable cations were determined by percolating soil samples with 100 ml of 1 M NH_4Cl adjusted to pH = 8.1 for 4 h (König & Fortmann, 1996) and measuring cations in percolates using an inductively coupled plasma-atomic emission spectrometer (iCAP 6300 Duo VIEW ICP Spectrometer, Thermo Fischer Scientific GmbH, Dreieich, Germany).

The concentration of cations in shell particles (Table 5) as well as the concentration of dissolved ions in matrix solutions at the beginning of the experiment and in the matrix solutions at each sampling date were also determined using an ICP spectrometer.

3.3.3. Statistics

The statistical analyses were done using STATISTICA 10 (StatSoft Inc., Tulsa, USA). The mean values and standard errors were calculated for 4 replications of each treatment at each sampling period. The significance of differences between the amounts of recrystallized carbonates between treatments at various dates was analyzed using the post-hoc Fisher LSD test at $\alpha = 0.05$ probability level.

3.3.4. Results

The highest shell carbonate recrystallization (Fig. 18, top) during the first labeling was in Sand with an average of 0.043 mg for days 5 and 20, followed by Loam and Exchanged, with 0.010 and 0.003 mg, respectively. During the second labeling, shell carbonate recrystallization in Sand and Exchanged increased, while shell carbonate recrystallization was fairly constant in Loam. The average shell carbonate recrystallization between dates 60 and 120 was 0.131, 0.016 and 0.024 mg in Sand, Loam and Exchanged, respectively.

The amounts of precipitated carbonates during first labeling in the presence of shell particles were similar in Sand, Loam and Exchanged (Fig. 18, middle). After the second labeling the precipitated carbonate increased by up to two orders of magnitude in Sand and Exchanged and one order of magnitude in Loam, compared to the first labeling.

Carbonate precipitation was also detected in matrices without the presence of any shell particles (Fig. 18, bottom). The precipitated carbonates in these matrices after 120 days and with one labeling pulse were 0.0004, 0.0079 and 0.0110 mg in Sand, Loam and Exchanged, respectively. After second labeling, the amounts of formerly precipitated carbonates decreased to 0.0001 mg in Sand and 0.0083 mg in Exchanged, whereas in Loam the value increased to 0.0143 mg (Fig. 18, bottom).

The significant increase in soil exchangeable Ca^{2+} was evident in Sand (Fig. 19, top). The values in Loam showed a decreasing trend, while in Exchanged it remained constant (Fig. 19, top). Unlike the exchangeable Ca^{2+} , the exchangeable sodium (Na^+) showed an exponential increase over time in all matrices (Fig. 19, bottom). Considering the negligible amounts of exchangeable Na^+ in the matrices, the source of Na^+ should be solely shells (Table 5). Therefore, soil exchangeable Na^+ was a good indicator showing shell dissolution as well as exchange process.

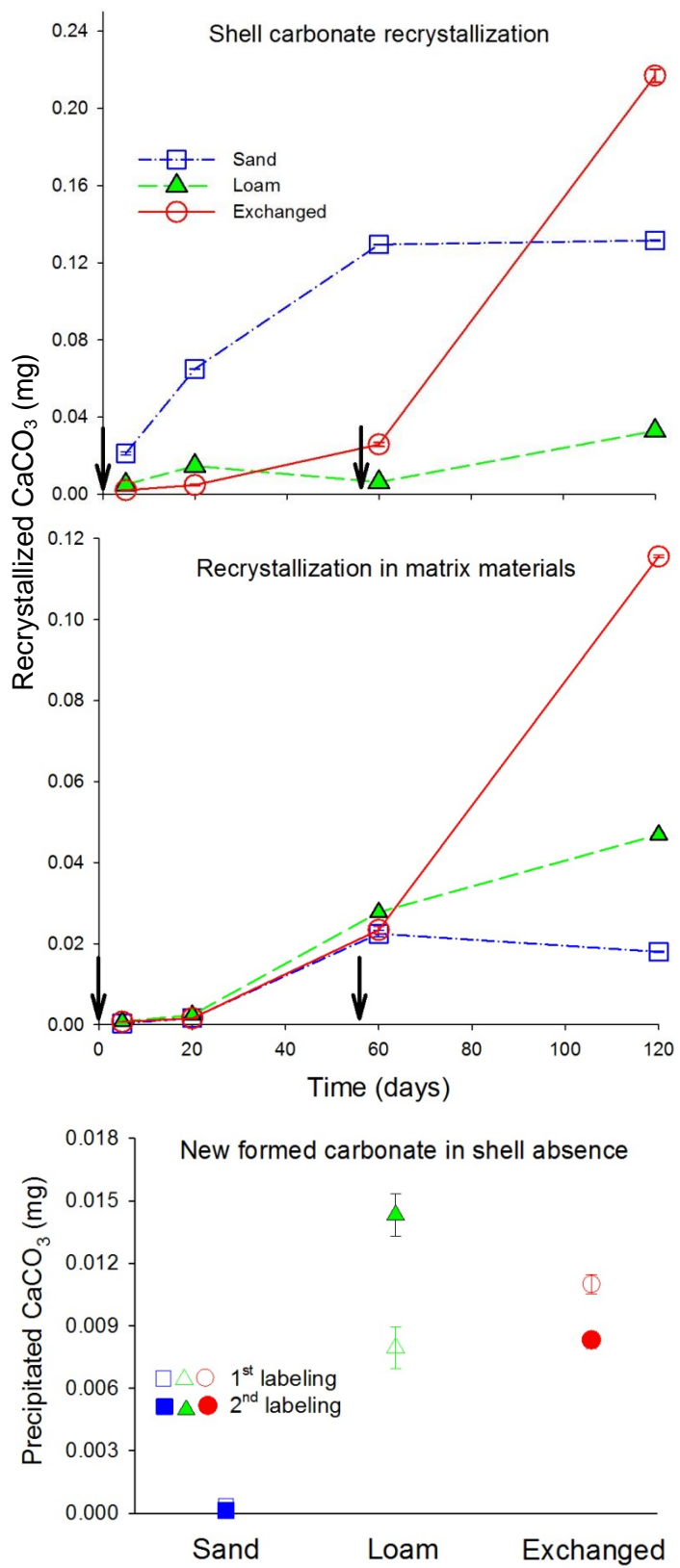


Figure 18: (top) Carbonate recrystallization of shells in various matrixes. (middle) Carbonate recrystallization inside the matrix materials in the presence of shell particles. (bottom) Carbonate recrystallization inside the matrix materials in the absence of shell particles after 120 days. Black arrows show the time of labeling at the beginning of the experiment and at day 55.

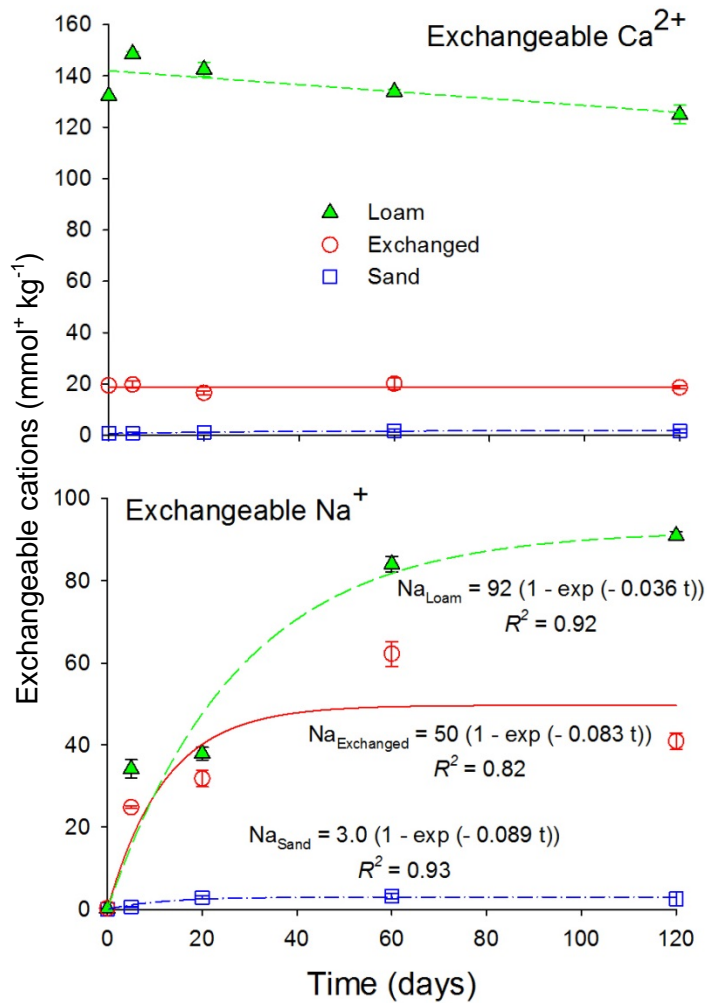


Figure 19: Changes in concentrations of exchangeable Ca^{2+} (top) and exchangeable Na^+ (bottom) during the 120-day experiment period. Trend lines are shown in different styles.

The concentration of dissolved Ca^{2+} in matrix solutions increased over 120 days in Sand but decreased in Loam and Exchanged (Fig. 20 top). Nonetheless, only the concentrations of dissolved Ca^{2+} in Sand during first labeling were significantly different with Loam and Exchanged. The Na^+ concentration increased exponentially in all solutions, without a difference between matrices at each sampling time (except day 120 for Sand).

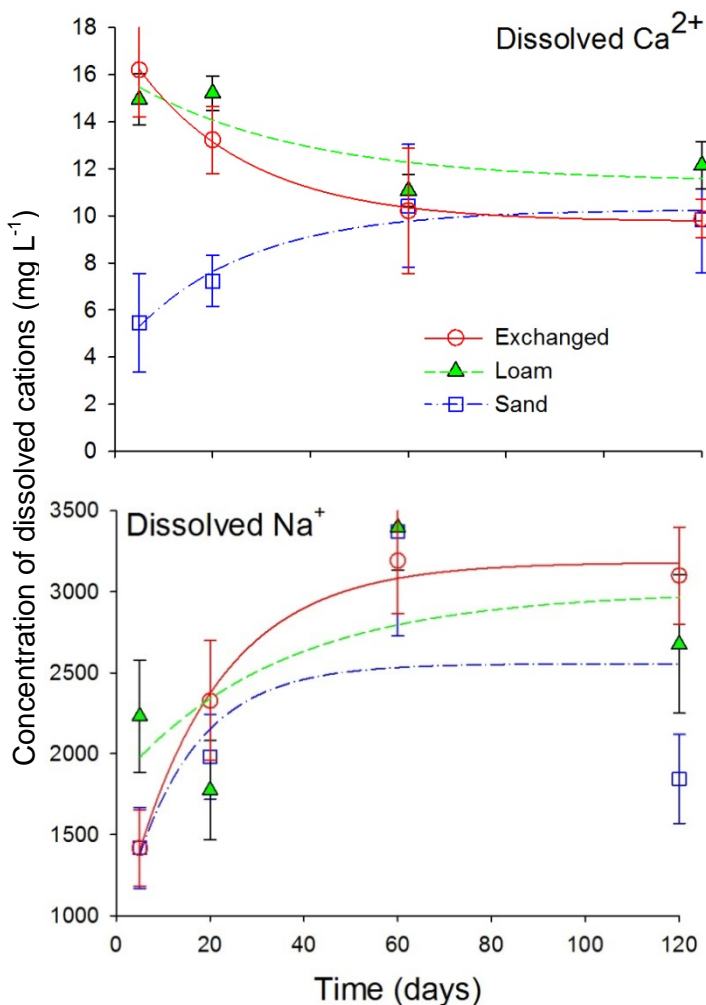


Figure 20: Changes in concentrations of dissolved Ca^{2+} (top) and dissolved Na^{+} (bottom) during the 120-day experiment period.

3.4. Discussion

Shell carbonate dissolution and release of Ca^{2+} from exchange sites occurred concurrently with changes in soil solution chemistry (Levy, 1980) – in the present case CO_2 release into solution due to an increase in $p\text{CO}_2$ by labeling (Pate et al., 1989). Soil exchangeable Ca^{2+} was released to buffer excess H^+ ions (Norrström, 1995) following CO_2 dissolution. The released exchangeable Ca^{2+} was bound to bicarbonate ions, leading to precipitation of new-formed CaCO_3 . Hence, more carbonate was precipitated in Loam and Exchanged with higher exchangeable Ca^{2+} compared to Sand (Fig. 18, bottom). Consequently, more carbonate precipitation is expected following further

CO_2 dissolution i.e. after the second labeling. Carbonate precipitation, however, increased only in Loam (Fig. 18, bottom). The decline in the content of formerly precipitated carbonates in Exchanged and Sand should solely reflect partial dissolution of these carbonates. Due to lower exchangeable Ca^{2+} in Exchanged and Sand, carbonate dissolution took part in buffering excess H^+ (Levy, 1980; Kelly et al., 1998; Chadwick et al., 2003). As long as Ca^{2+} ions remain in soil solution, more CO_2 in the form of HCO_3^- will be neutralized, i.e. $\text{Ca}(\text{HCO}_3^-)_2$ in solution vs. solid CaCO_3 . The effective contribution of carbonates to H^+ buffering is also recognizable by comparing the carbonate amounts precipitated in matrices with and without shells. Precipitation in Exchanged and Sand matrices containing shells was higher than in matrices without shells (Fig. 18, middle and bottom).

Shell carbonate dissolution is confirmed by tracing changes in soil exchangeable Na^+ concentration (Fig. 19, bottom). The exchangeable Na^+ increased in all matrices over 120 days, despite negligible initial concentrations both as exchangeable or dissolved Na^+ (Fig. 19 and 20 bottom, at $t = 0$). Accordingly, the exponential increase of exchangeable Na^+ should be due solely to shell carbonate dissolution and release of dissolved Na^+ into soil solutions. Na is present in mollusk shell structure (Table 5), and concentrations exceeding 2000 ppm are generally indicative of shells from marine environments (Hahn et al., 2012; Findlater et al., 2014; O'Neil & Gillikin, 2014). An increasing Na^+ concentration (Fig. 20, bottom) therefore had to exchange Na^+ with other cations on soil exchange sites (Ferrell & Brooks, 1971; Levy, 1980). Although the concentrations of other elements on soil exchange sites, especially of exchangeable Ca^{2+} , remained nearly constant (Fig. 19, top), Loam and Exchanged with higher CEC showed more exchangeable Na^+ than Sand (Fig. 19, bottom). The lower value in Exchanged vs. Loam, however, reflects the inability to exchange K^+ ions that were fixed in soil clay minerals.

Shell carbonate dissolution and recrystallization were the highest in Sand because it has the lowest CEC. Therefore, more shell carbonate dissolved to buffer excess H^+ (Porder et al., 2015). An increase in soil CEC and exchangeable Ca^{2+} decreases the solubility of shell carbonate and consequently the recrystallization. This is because exchange processes have faster rates than dissolution (Fig. 21). Following changes in soil solution chemistry, e.g. increasing soil $p\text{CO}_2$, shell carbonate recrystallization increases comparatively slowly in soils with high CEC (Fig. 21). This calls for examining the properties of the environment embedding the shells, especially the total clay content and mineralogy as well as the composition of exchangeable and dissolved cations during sampling for radiocarbon dating. Furthermore, more precise models describing shell carbonate diagenesis require including soil CEC and exchangeable cation parameters.

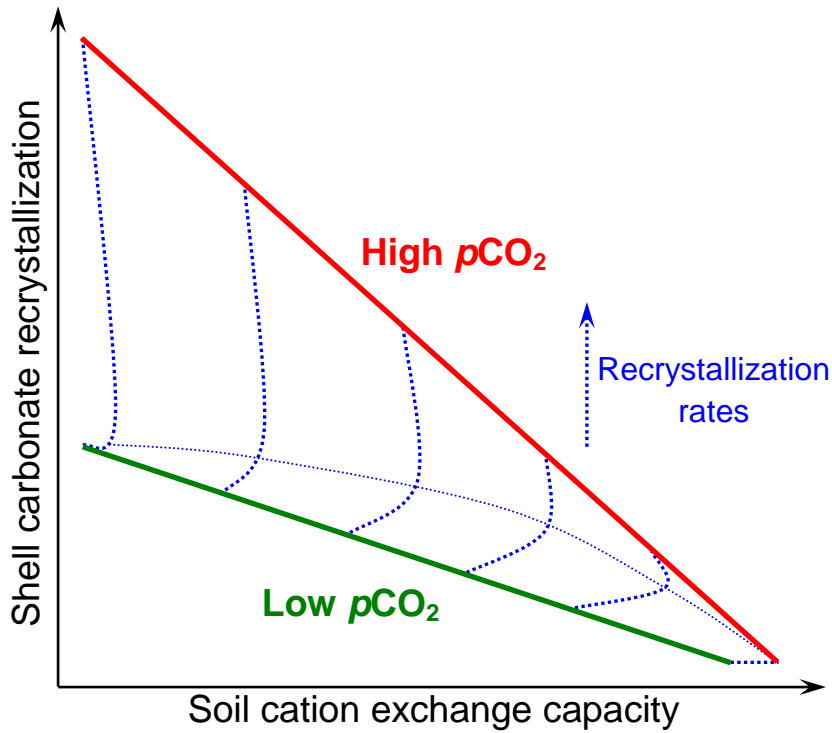


Figure 21: Shell carbonate recrystallization depending on soil cation exchange capacity and Ca^{2+} concentration: Shell carbonate recrystallization decreases as soil CEC increases (green and red lines). Shell carbonate recrystallization rates in similar time spans increase faster in soils with less CEC with increasing soil $p\text{CO}_2$ (Blue dotted lines).

Carbonate dissolution rates depend on the CaCO_3 saturation state in solution. Any changes in the chemical composition of soil solution are initially buffered by releasing the exchangeable cations (Levy, 1980). Accordingly, soil CEC is the key determinant of carbonate recrystallization rates. The effect of CEC on shell carbonate recrystallization is important for any studies related to paleoenvironment reconstructions based on carbonate $\delta^{13}\text{C}$ signatures and radiocarbon dating. This is especially the case in areas where the shell carbonate fraction is the only available proxy, for example in arid regions due to decomposition of organic materials (Zazzo & Saliège, 2011). Furthermore, various types of biogenic carbonates such as bones (Zazzo et al., 2009), eggshells (Janz et al., 2009), teeth (Feakins et al., 2013) and calcified seeds (Pustovoytov et al., 2004) are also frequently used for paleoenvironment reconstructions and dating. These biogenic carbonates may undergo diagenesis as well. Biogenic carbonate diagenesis, however, proceeds at relatively slow rates, making it difficult to study diagenesis rates in short periods (Kuzyakov et al., 2006). ^{14}C labeling showed a high potential to trace very small changes in shell CaCO_3 -C isotopic composition following dissolution and recrystallization. Therefore, ^{14}C labeling may overcome the above

limitation, which makes it suited to study the diagenesis dynamics of biogenic carbonates under various environmental conditions. Moreover, ^{14}C labeling can be recommended in investigations related to weathering of Ca-bearing minerals. Tracing ^{14}C activity added as a label to systems similar to the ones in this study, but containing individual minerals instead of shells, may help reveal the weathering rates of such minerals.

3.5. Conclusion

Shell carbonate dissolution and recrystallization decrease with increasing soil CEC. This is because the equilibrium between exchangeable and dissolved cations will be reached much faster than mineral dissolution, e.g. of CaCO_3 in shells. Therefore, the isotopic composition of shells may show less variation than the initial amounts in soils with relatively high CEC. This effect of CEC calls for including parameters such as total CEC and the equilibria between exchangeable and dissolved cations in models predicting shell diagenesis. ^{14}C labeling showed a high potential to trace minor changes in the isotopic composition of shells following diagenesis and thus to better understand diagenesis dynamics. The ^{14}C labeling approach can also be used to determine the weathering rates of other Ca-bearing minerals.

3.6. Acknowledgement

We would like to acknowledge the German Research Foundation (DFG) for their support (KU 1184/34-1). Special thanks to Ronia Zarebanadkouki for collecting shells, and Martina Gebauer and Karin Schmidt for measuring soil CEC and the elemental composition of shells.

3.7. References

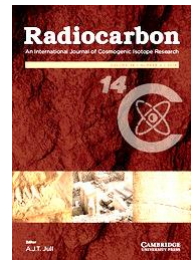
- Arrhenius, G., Kjellberg, G., & Libby, W.F. 1951. Age Determination of Pacific Chalk Ooze by Radiocarbon and Titanium Content. *Tellus* **3**, 222–229.
- Aylward, G.H. 2007. SI chemical data. Auflage: 6. Auflage. John Wiley & Sons, Milton, Qld.
- Chadwick, O.A., Gavenda, R.T., Kelly, E.F., Ziegler, K., Olson, C.G., Elliott, W.C., & Hendricks, D.M. 2003. The impact of climate on the biogeochemical functioning of volcanic soils. *Chemical Geology* **202**, 195–223.
- Douka, K., Higham, T.F.G., & Hedges, R.E.M. 2010. Radiocarbon dating of shell carbonates: old problems and new solutions. *31*, 18–27.
- Feakins, S.J., Levin, N.E., Liddy, H.M., Sieracki, A., Eglinton, T.I., & Bonnefille, R. 2013. Northeast African vegetation change over 12 m.y. *Geology* **41**, 295–298.
- Ferrell, R.E., & Brooks, R.A. 1971. The selective adsorption of sodium by clay minerals in Lakes Pontchartrain and Maurepas, Louisiana. *Clays and Clay Minerals* **19**, 75–81.

- Findlater, G., Shelton, A., Rolin, T., & Andrews, J. 2014. Sodium and strontium in mollusc shells: preservation, palaeosalinity and palaeotemperature of the Middle Pleistocene of eastern England. *Proceedings of the Geologists' Association* **125**, 14–19.
- Gocke, M., Pustovoytov, K., & Kuzyakov, Y. 2012. Pedogenic carbonate formation: Recrystallization versus migration—Process rates and periods assessed by ^{14}C labeling. *Global Biogeochemical Cycles* **26**, GB1018.
- Hahn, S., Rodolfo-Metalpa, R., Griesshaber, E., Schmahl, W.W., Buhl, D., Hall-Spencer, J.M., Baggini, C., Fehr, K.T., & Immenhauser, A. 2012. Marine bivalve shell geochemistry and ultrastructure from modern low pH environments: environmental effect versus experimental bias. *Biogeosciences* **9**, 1897–1914.
- Janz, L., Elston, R.G., & Burr, G.S. 2009. Dating North Asian surface assemblages with ostrich eggshell: implications for palaeoecology and extirpation. *Journal of Archaeological Science* **36**, 1982–1989.
- Karberg, N.J., Pregitzer, K.S., King, J.S., Friend, A.L., & Wood, J.R. 2005. Soil carbon dioxide partial pressure and dissolved inorganic carbonate chemistry under elevated carbon dioxide and ozone. *Oecologia* **142**, 296–306.
- Kelly, E.F., Chadwick, O.A., & Hilinski, T.E. 1998. The Effect of Plants on Mineral Weathering. *Biogeochemistry* **42**, 21–53.
- König, N., & Fortmann, H. 1996. Probenvorbereitungs-, Untersuchungs- und Elementbestimmungsmethoden des Umweltanalytiklabors der Niedersächsischen Forstlichen Versuchsanstalt und des Zentrallabor 2 des Forschungszentrums Waldökosysteme. Berichte des Forschungszentrums Waldökosysteme.
- Kulp, J.L., Feely, H.W., & Tryon, L.E. 1951. Lamont Natural Radiocarbon Measurements, I. *Science (New York, N.Y.)* **114**, 565–568.
- Kuzyakov, Y., Shevtsova, E., & Pustovoytov, K. 2006. Carbonate re-crystallization in soil revealed by ^{14}C labeling: Experiment, model and significance for paleo-environmental reconstructions. *Geoderma* **131**, 45–58.
- Levy, R. 1980. Sources of soluble calcium and magnesium and their effects on sodium adsorption ratios of solutions in two soils of israel. *Geoderma* **23**, 113–123.
- Magee, J.W., Miller, G.H., Spooner, N.A., Questiaux, D.G., McCulloch, M.T., & Clark, P.A. 2009. Evaluating Quaternary dating methods: Radiocarbon, U-series, luminescence, and amino acid racemization dates of a late Pleistocene emu egg. *Quaternary Geochronology* **4**, 84–92.
- Norrström, A.C. 1995. Acid-base status of soils in groundwater discharge zones — relation to surface water acidification. *Journal of Hydrology* **170**, 87–100.
- O'Neil, D.D., & Gillikin, D.P. 2014. Do freshwater mussel shells record road-salt pollution? *Scientific Reports* **4**, 7168.
- Pate, F.D., Hutton, J.T., & Norrish, K. 1989. Ionic exchange between soil solution and bone: toward a predictive model. *Applied Geochemistry* **4**, 303–316.
- Pausch, J., & Kuzyakov, Y. 2012. Soil organic carbon decomposition from recently added and older sources estimated by $\delta^{13}\text{C}$ values of CO₂ and organic matter. *Soil Biology and Biochemistry* **55**, 40–47.
- Pigati, J.S., McGeehin, J.P., Muhs, D.R., & Bettis III, E.A. 2013. Radiocarbon dating late Quaternary loess deposits using small terrestrial gastropod shells. *Quaternary Science Reviews* **76**, 114–128.

- Pigati, J.S., Quade, J., Shahanan, T.M., & Haynes Jr., C.V. 2004. Radiocarbon dating of minute gastropods and new constraints on the timing of late Quaternary spring-discharge deposits in southern Arizona, USA. *Palaeogeography, Palaeoclimatology, Palaeoecology* **204**, 33–45.
- Pigati, J.S., Rech, J.A., & Nekola, J.C. 2010. Radiocarbon dating of small terrestrial gastropod shells in North America. *Quaternary Geochronology* **5**, 519–532.
- Porder, S., Johnson, A.H., Xing, H.X., Brocard, G., Goldsmith, S., & Pett-Ridge, J. 2015. Linking geomorphology, weathering and cation availability in the Luquillo Mountains of Puerto Rico. *Geoderma* **249–250**, 100–110.
- Pustovoytov, K., & Riehl, S. 2006. Suitability of biogenic carbonate of *Lithospermum* fruits for ^{14}C dating. *Quaternary Research* **65**, 508–518.
- Pustovoytov, K.E., Riehl, S., & Mittmann, S. 2004. Radiocarbon age of carbonate in fruits of *Lithospermum* from the early Bronze Age settlement of Hirbet ez-Zeraqōn (Jordan). *Vegetation History and Archaeobotany* **13**, 207–212.
- Scholl, D.W. 1964. Recent sedimentary record in mangrove swamps and rise in sea level over the southwestern coast of Florida: Part 2. *Marine Geology* **2**, 343–364.
- Sears, S.O., & Langmuir, D. 1982. Sorption and mineral equilibria controls on moisture chemistry in a C-horizon soil. *Journal of Hydrology* **56**, 287–308.
- Stolwijk, J.A.J., & Thimann, K.V. 1957. On the Uptake of Carbon Dioxide and Bicarbonate by Roots, and Its Influence on Growth. 1. *Plant Physiology* **32**, 513–520.
- Webb, G.E., Price, G.J., Nothdurft, L.D., Deer, L., & Rintoul, L. 2007. Cryptic meteoric diagenesis in freshwater bivalves: Implications for radiocarbon dating. *Geology* **35**, 803–806.
- Zazzo, A., & Saliège, J.-F. 2011. Radiocarbon dating of biologicalapatites: A review. *Palaeogeography, Palaeoclimatology, Palaeoecology* **310**, 52–61.
- Zazzo, A., Saliege, J.-F., Person, A., & Boucher, H. 2009. Radiocarbon Dating of Calcined Bones: Where Does the Carbon Come from? *Radiocarbon* **51**, 601–611.

4. Carbon sources in fruit carbonate of *Buglossoides arvensis* and consequences for ^{14}C dating

Published: Radiocarbon 59 (2017): 141-150



Kazem Zamanian¹, Konstantin Pustovoytov^{2,3}, Yakov Kuzyakov^{1,4}

¹. Department of Soil Science of Temperate Ecosystems, University of Göttingen, Büsgenweg 2, 37077 Göttingen, Germany

². Institute of Soil Science and Land Evaluation (310), University of Hohenheim, Schloss Hohenheim 1, 70599 Stuttgart, Germany

³. Institute for Archaeological Sciences, University of Tübingen, Rümelinstr. 23, 72070 Tübingen, Germany

⁴. Institute of Environmental Sciences, Kazan Federal University, Kazan, Russia

4.1. Abstract

Fruit carbonate of *Buglossoides arvensis* (syn. *Lithospermum arvense*) is a valuable dating and paleoenvironmental proxy for late Quaternary deposits and cultural layers because CaCO_3 in fruit is assumed to be accumulated from photosynthetic C. However, considering the uptake of HCO_3^- by roots from soil solution, the estimated age could be too old depending on the source of HCO_3^- allocated in fruit carbonate. Until now, no studies have assessed the contributions of photosynthetic and soil C to the fruit carbonate. To evaluate this, the allocation of photo-assimilated carbon (C) and root uptake of HCO_3^- was examined by ^{14}C labeling and tracing. *B. arvensis* was grown in carbonate-free and carbonate-containing soils (Sand and Loess, respectively), where ^{14}C was provided as 1) $^{14}\text{CO}_2$ in the atmosphere (5 times shoot pulse labeling) or 2) $\text{Na}_2^{14}\text{CO}_3$ in soil solution (root-labeling; 5 times by injecting labeled solution into the soil) during one month of fruit development. Distinctly different patterns of ^{14}C distribution in plant organs after root- and shoot labeling showed the ability of *B. arvensis* to take up HCO_3^- from soil solution. The highest ^{14}C activity from root labeling was recovered in roots, followed by shoots, fruit organics and fruit carbonate. In contrast, ^{14}C activity after shoot labeling was the highest in shoots, followed by fruit organics, roots and fruit carbonate. Total photo-assimilated C incorporated via shoot labeling in Loess grown plants was 1.51 mg lower than in Sand reflecting the presence of dissolved carbonate (i.e. CaCO_3) in Loess. Loess carbonate dissolution and root-respired CO_2 in soil solution are both sources of HCO_3^- for root uptake. Considering this dilution effect by carbonates, the total

incorporated HCO_3^- comprised 0.15% of C in fruit carbonate after 10 hours of shoot labeling. However, if the incorporated HCO_3^- during 10 hours of shoot labeling is extrapolated for the whole month of fruit development (i.e. 420 h photoperiod), fruit carbonate in Loess-grown plants incorporated ca. 6.3% more HCO_3^- than in Sand. Therefore, fruit carbonates from plants grown on calcareous soils may yield overestimated radiocarbon ages around 500 years because of a few % uptake of HCO_3^- by roots. However, the age overestimation because of HCO_3^- uptake becomes insignificant in fruits older than ca. 11,000 y due to increasing uncertainties in age determination.

Keywords: *Buglossoides arvensis*, *Lithospermum arvense*, Biogenic carbonate, Reservoir effect, ^{14}C labeling, Radiocarbon dating, Paleoenvironmental proxy

4.2. Introduction

Buglossoides arvensis (L) I.M.Johnst., syn. *Lithospermum arvense* L., (tribe Lithospermeae, family Boraginaceae) is an annual plant with 10-50 cm height and flowering time between April and July. *B. arvensis* is commonly found in Eurasian arable lands, grasslands and forest margins. The fruits, which are often incorrectly considered as fruits of *B. arvensis*, are small (ca. 2 mm in diameter), ovoid, and contain CaCO_3 in their epidermal cells and parts of sclerenchyma (for more information about *B. arvensis* see (Pustovoytov and Riehl, 2006; and references therein) (Fig. 22).

Fossil fruits of *B. arvensis* and other members of Lithospermeae are often found in late Pleistocene and Holocene deposits as well as in cultural layers of archaeological sites (Pustovoytov and Riehl, 2006). This calls for testing the applicability of carbon (C) isotopes in these fruits for dating purposes and paleoenvironmental reconstructions. Previously, it has been demonstrated that fruit carbonate of another taxon, the genus *Celtis*, can be successfully dated with ^{14}C (Wang et al., 1997; Quade et al., 2014) and serve as a paleoclimate proxy (Jahren et al., 2001). Similar results have been obtained for the tribe Lithospermeae (Pustovoytov et al., 2004; Pustovoytov and Riehl, 2006; Pustovoytov et al., 2010). Aside from a few under- or overestimates the achieved ages showed good consistency with independently estimated ages for the archeological layers. The underestimated ages can be explained by post-sedimentary incorporation of fruits into the deposits (i.e. via bioturbation) (Wang et al., 1997; Pustovoytov et al., 2004; Pustovoytov et al., 2010) or slight diagenetic ^{14}C -contamination effects (Quade et al., 2014). A ca. 400-year overestimate for a

herbarium exemplar from the early 19th century has been attributed to occasional depletion in atmospheric ¹⁴C concentration because of fossil fuel combustion (Pustovoytov and Riehl, 2006).

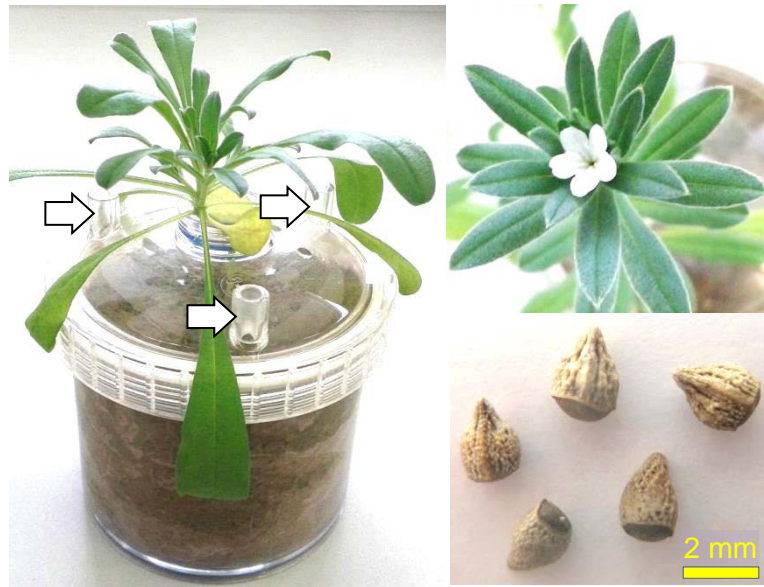


Figure 22: (Left) A ca. one-month-old *B. arvensis* grown in a 250 mL plastic pot; (Right, top) *B. arvensis* flower; (Right, bottom) *B. arvensis* fruits. The arrows show the openings in the pot lid, which were used for irrigation and root labelling (see 2.2. Labelling procedure).

However, since 1940 it has been known that plants can take up HCO₃⁻ from soil solution via their roots (Overstreet et al., 1940; Cramer and Richards, 1999; Cramer et al., 1999; Viktor and Cramer, 2005). It has been shown that the amount of HCO₃⁻ taken up can be 0.8 to 2% of the C assimilated through photosynthesis (Pelkonen et al., 1985; Brix, 1990; Viktor and Cramer, 2003; Ford et al., 2007). However, the HCO₃⁻ uptake depends on its concentration in soil solution (Cramer and Lips, 1995) and the plant species (Stolwijk and Thimann, 1957). Some species, for example oats, are tolerant of high HCO₃⁻ concentrations in the rhizosphere (up to 6.5% CO₂ concentration), but some like tomato may show toxicity symptoms at comparatively low concentrations (ca. 1% CO₂) (Stolwijk and Thimann, 1957). HCO₃⁻ uptake via roots is mostly passive and depends on transpiration rates (Stolwijk and Thimann, 1957; Brix, 1990; Amiro and Ewing, 1992). This may explain why soil-derived HCO₃⁻ is found at highest concentrations in roots, and decreases with distance from the roots (Brix, 1990). However, these concentrations can increase locally in specific

plant organs such as newly formed stems or fine roots, through unknown active mechanisms (Vuorinen et al., 1989; Ford et al., 2007).

The HCO_3^- concentration in soil solution is determined by the dissolution of root- and microbe-respired CO_2 , exchange of CO_2 between the soil and atmosphere and dissolution of carbonate containing minerals such as CaCO_3 . The isotopic composition of C in these HCO_3^- sources differs: while HCO_3^- from carbonate minerals is often totally ^{14}C depleted, the ^{14}C content of respired CO_2 is almost identical with the ^{14}C concentration in modern atmospheric CO_2 . Therefore, even a few percent of old C from carbonate minerals; can modify ^{14}C ages of a sample. We hypothesize that radiocarbon ages based on fruit carbonate could overestimate the true age of a sample if part of the C comes from soil HCO_3^- . Therefore, the main aims of this experiment were: 1) to identify the origin of C in CaCO_3 of fruits, 2) to quantify the contribution of absorbed HCO_3^- from soil, and 3) to calculate the potential effect of root HCO_3^- uptake on radiocarbon dates based on fruit carbonates of *B. arvensis*.

4.3. Material and methods

4.3.1. Experimental layout

250 mL plastic pots with lids (Sartorius AG, Germany) were used for plant growth (Fig. 22, Left). The lids had one main hole in the middle, for the growing plant stem, and three smaller openings, which were used for soil labeling and irrigation. To make a carbonate-containing and a carbonate-free medium for plant growth, a carbonate-free loamy soil (Haplic Luvisol, originated from loess) was mixed with loess and sand particles, respectively, at a 1:1 ratio (200 g of loamy soil to 200 g of loess or sand). The loamy soil, loess and sand particles were air-dried and passed through a 2 mm screen before mixing. Loess samples containing 30% CaCO_3 were taken from an open mine at Nussloch, southwest Germany, from 10 m below the soil surface (see (Kuzyakov et al., 2006) for details). Carbonate-free sand in the size range 0.5-1.5 mm was used. Water content was adjusted to 60% of water holding capacity by adding 96 mL of distilled water to the loamy soil + loess (hereafter called Loess) and 84 mL to the loamy soil + sand (hereafter called Sand). The water content of Loess and Sand was kept at 60% of water holding capacity during the whole experiment by weighing the pots and adding water when needed.

Fruits of *B. arvensis* were pre-germinated in the dark on wet filter paper. When plant height was around 1 cm they were transplanted into the growth pots, the lids closed, and placed into a growing chamber at 25–27 °C, 14-h photoperiod and 180 µmol m⁻² s⁻¹ light intensity.

4.3.2. Labeling procedure

Labeling started one week after the first flowers developed, and was repeated five times over a one-month period thereafter. Labeling was applied to either the roots or the shoots. In both cases, 200 kBq of ¹⁴C in the form of Na₂¹⁴CO₃ solution was used at each labeling occasion. The applied ¹⁴C activity for labeling was several orders of magnitude higher than natural abundance of ¹⁴C in plant organs or soils. Hence, the initial ¹⁴C activity of plant organs or soils had no effect on the results of labeling. Before starting the procedure, the space between the stem and the main opening in the lid was filled with cotton and covered with Vaseline to provide an air-tight seal, which was maintained for the one-month period. The three small openings were only closed for the few hours of each labeling procedure, using tight-fitting plastic pins. Separation of the root and shoot atmospheres during the labeling procedure was necessary to prevent dissolution of ¹⁴CO₂ in the soil solution while labeling the shoots, and to avoid photosynthetic assimilation of labeled ¹⁴CO₂ that might be released from the soil solution during root labeling (Amiro and Ewing, 1992; Cramer and Richards, 1999).

For shoot labeling, the pots were placed in an air-tight labeling chamber made of Plexiglas (0.5 × 0.5 × 0.6 m³), which was fitted with four connections and a fan for circulating ¹⁴CO₂. To produce ¹⁴CO₂, 5 mL of 2.5 M Na₂¹⁴CO₃ was acidified by addition of H₃PO₄. The ¹⁴CO₂ was pumped into the chamber using two inlets. After one hour the chamber was connected via the two outlets to a glass bottle with 20 mL of 1 M NaOH to trap unassimilated ¹⁴CO₂. The trapping period was also one hour. Afterwards, the plants were returned to the normal conditions outside the labeling chamber and the plastic pins were removed.

For root labeling, 3 mL of 0.002 M Na₂¹⁴CO₃ solution was injected deeply into the soil in each pot via the three small openings in the lids (1 mL each) (Fig. 1, left). This fairly low concentration of sodium carbonate had no effect on plant growth or fruit production compared to the shoot-labeled plants.

4.3.3. ^{14}C analyses

One week after the fifth labeling, ^{14}C activity was measured in plant organs (shoots, roots, and fruits), bulk soil and soil solution. After collecting the fruits, the plant stems were cut at the base and soils were washed with distilled water to separate the roots and to collect soil solution. To wash the soils, 1000 mL of distilled water was used for Loess and 880 mL for Sand. The bulk soils, shoots, roots and fruits were dried overnight at 40 °C to determine dry weights. Afterwards, ^{14}C was measured in a subsample of each material.

^{14}C in fruits was measured separately in carbonate and organic components. The fruits were acidified with H_3PO_4 and the released CO_2 was trapped in 1 M NaOH solution. The alkali solution was mixed with scintillation cocktail (Rotiszint EcoPlus, Carl Roth, Germany) and ^{14}C was measured after decay of chemiluminescence with an Automatic TDCR Liquid Scintillation Counter (HIDEX 300 SL, Turku, Finland). The acidified fruits were washed again with distilled water, dried at 40°C and weighed again to determine the weight lost from carbonates. The weight loss after acidification was taken as the fruit carbonate content. The remaining fruit material (i.e. the organic part) was combusted at 900 °C using a Biological Oxidizer (OX 400) to yield CO_2 . The produced CO_2 was trapped in NaOH and ^{14}C activity was measured as described above.

^{14}C measurement in the bulk soil was similar to that for fruits. For soil acidification, 0.1 g of Loess and 2 g of Sand were used. ^{14}C measurements of shoots and roots were performed in the same way as for the organic parts of fruits, but as finely ground powders. ^{14}C in soil solution was measured after addition of scintillation cocktail. To differentiate between dissolved organic carbon (DOC) and dissolved inorganic carbon (DIC), a part of the solution was acidified before addition of scintillation cocktail. This provided a ^{14}C determination in DOC. The difference between ^{14}C activity of total dissolved carbon and that of DOC was the ^{14}C activity in DIC.

4.3.4. Calculation of carbon incorporation into plant organs and age overestimation

The C amounts incorporated into plant organs (mg) were calculated based on the C content of the labeling solution (mg) added to each pot, total ^{14}C activity applied to each pot, and the ^{14}C activity measured in plant organs (i.e. fruit carbonates, fruit organics, roots, shoots) (See Kuzyakov et al., 2006 for more details).

To calculate the age overestimation because of incorporated HCO_3^- carbon, we used the usual ^{14}C decay equation (Bowman, 1995):

$$T = -8267 \cdot \ln (A_{SN} / A_{ON}) \quad (\text{Eq. 1})$$

where A_{SN} is the normalized number of measured ^{14}C atoms in a given sample and A_{ON} is the initial normalized number of ^{14}C atoms at the beginning of decay and T is the time elapsed since the beginning of decay. Assuming a constant atmospheric ^{14}C concentration over time,

$$A_{SN} = A_{ON} \cdot e^{-\lambda T} \quad (\text{Eq. 2})$$

where $\lambda = 1 / 8267$. This law remains true as long as no new fractions of ^{14}C or radiometrically dead C are added to a sample. If a portion P of radiometrically dead carbon is added to a sample, the ^{14}C concentration in such a sample becomes lower by a factor $1/(1+P)$, which modifies Eq. 2 in the following way:

$$A_{SN} = A_{ON} \cdot e^{-\lambda T} \cdot \frac{1}{1+P} \quad (\text{Eq. 3})$$

Combining Eq. 1 and Eq 3., we obtain a formula for the measured age T' of a sample with a portion of radiometrically dead carbon P :

$$T' = -8267 \cdot \ln \left[(A_{ON} \cdot e^{-\lambda T} \cdot \frac{1}{1+P}) / A_{ON} \right] \quad (\text{Eq. 4})$$

It is further apparent that

$$T' = -8267 \cdot \ln \left(\frac{e^{-\lambda T}}{1+P} \right) = T + 8267 \cdot \ln (1 + P) \quad (\text{Eq. 5})$$

Eq. 5 can provide the offset between the measured age of a sample with admixtures of dead carbon and its true age ΔT under stable ^{14}C atmospheric concentration:

$$\Delta T = T' - T = 8267 \cdot \ln (1 + P) \quad (\text{Eq. 6})$$

As it follows from Eq. 6, this offset does not depend on time and is only determined by the quantity of dead carbon admixture.

4.3.5. Statistics

Mean values and standard errors were calculated for 6 replicates of each treatment. The significance of differences between shoot- and root-labeled plants was assessed using the post-hoc Fisher LSD test at $\alpha = 0.05$ significance level. Statistical analyses were done in STATISTICA 10 (StatSoft Inc., Tulsa, USA).

4.4. Results

The ^{14}C distribution via shoot- and root labeling showed obvious and significant differences ($p < 5\%$) between various organs (Table 6). ^{14}C specific activity after shoot labeling was the highest in shoots, followed by fruit organics and roots. In contrast, the highest ^{14}C activity after root labeling was recovered in the roots, followed by DOC and DIC. ^{14}C fraction recovered in shoots was ca. 6 times higher (43-47%) after shoot labeling than root labeling (7-8%). Recovery after shoot labeling was also ca. 9 times higher in fruit organics, but ca. 3 times lower in roots.

Total incorporation of C from shoot labeling by Loess-grown plants was 90.6 mg, lower ($p < 5\%$) than for the Sand-grown plants (92.1 mg). Incorporated C from root labeling was 74.1 and 103 mg for Loess and Sand, respectively (Table 7). Fruit carbonate had greater incorporation from shoot labeling than from root labeling: 1.5 times higher in Sand and 1.9 times in Loess (Table 7).

Table 6: Percentage of ^{14}C label recovered in different plant organs and soils via photosynthesis (Shoot-labeling) or taken up by roots (Root-labeling). Standard errors are shown in parentheses.

Labeled fractions	Shoot-labeling		Root-labeling	
	Sand	Loess	Sand	Loess
Fruit carbonate	0.16 (0.01)	0.15 (0.01)	0.08 (0.01)	0.06 (0.01)
Fruit organics	25.1 (0.98)	30.4 (1.19)	4.38 (0.70)	2.46 (0.23)
Shoots	46.8 (2.64)	43.3 (1.17)	7.88 (0.47)	6.93 (0.39)
Roots	23.6 (2.26)	20.3 (1.66)	69.7 (0.90)	49.8 (3.15)
Dissolved organic carbon	2.86 (0.11)	3.54 (0.05)	13.2 (0.39)	20.4 (1.20)
Dissolved inorganic carbon	1.17 (0.04)	1.14 (0.08)	3.81 (0.34)	9.18 (0.95)
Soil carbonate	0.25 (0.02)	1.17 (0.10)	1.00 (0.05)	11.2 (1.24)

Table 7: Amounts of incorporated labeled carbon (mg) in plant organs after shoot or root labeling of Sand- or Loess-grown plants. Standard errors are shown in parentheses.

Labeled fractions	Shoot-labeling		Root-labeling	
	Sand	Loess	Sand	Loess
Fruit carbonate	0.15 (0.01)	0.14 (0.01)	0.10 (0.01)	0.08 (0.01)
Fruit organics	24.2 (0.94)	29.3 (1.14)	5.47 (0.88)	3.07 (0.29)
Shoots	45.1 (2.54)	41.6 (1.12)	9.85 (0.59)	8.66 (0.49)
Roots	22.7 (2.17)	19.6 (1.60)	87.1 (1.12)	62.3 (3.93)
Total	92.1 (0.13)	90.6 (0.17)	103 (0.90)	74.1 (3.62)

4.5. Discussion

The soil properties (Loess vs. Sand) and the labeling approach (shoot vs. roots) had no effect on total plant growth or individual organs. Therefore, we can directly compare the label incorporation and distribution between the soils and labeling conditions.

The obvious differences in ^{14}C activity of various plant organs after root labeling comparing to shoot labeling reveal that HCO_3^- carbon was taken up by *B. arvensis* roots (Table 6). To determine the amount of HCO_3^- carbon incorporated by *B. arvensis*, the total incorporated C via shoot labeling in Loess and Sand were compared. If we assume no re-uptake via HCO_3^- , there should be no difference between the incorporated C from $^{14}\text{CO}_2$ in Sand- and Loess-grown plants following shoot-labeling. The comparison, however, reveals 1.51 mg less photo-assimilated C in Loess than in Sand (Table 7). CaCO_3 solubility in distilled water is 13.1 mg L^{-1} at 25°C (Aylward, 2007). Therefore, in Loess with ca. 700 mL water³, 9.1 mg CaCO_3 can be dissolved. According to the C mass proportion in CaCO_3 ($12 \text{ mg C } 100 \text{ mg}^{-1} \text{ CaCO}_3$), this amount of dissolved CaCO_3 contains 1.1 mg C (fairly equal to the solubility of CaCO_3). Root-respired CO_2 can dissolve in soil solution and be reabsorbed by roots (Ford et al., 2007). However, root-respired CO_2 is diluted in Loess solution before re-uptake (Fig. 23). Hence, total incorporated C in Loess plants was lower than in Sand plants. In conclusion the so-called reservoir effect, i.e. incorporation of ^{14}C -depleted carbon from soil into biologically formed carbonates which has already been proven for other types of

³ Cumulative amount of water added to the pots to keep the water content of Loess at 60% of water holding capacity during one month labeling.

biogenic carbonates, such as land-snail shells (Pigati et al., 2004; Pigati et al., 2010 and references therein) also takes place in fruit carbonate of *B. arvensis*.

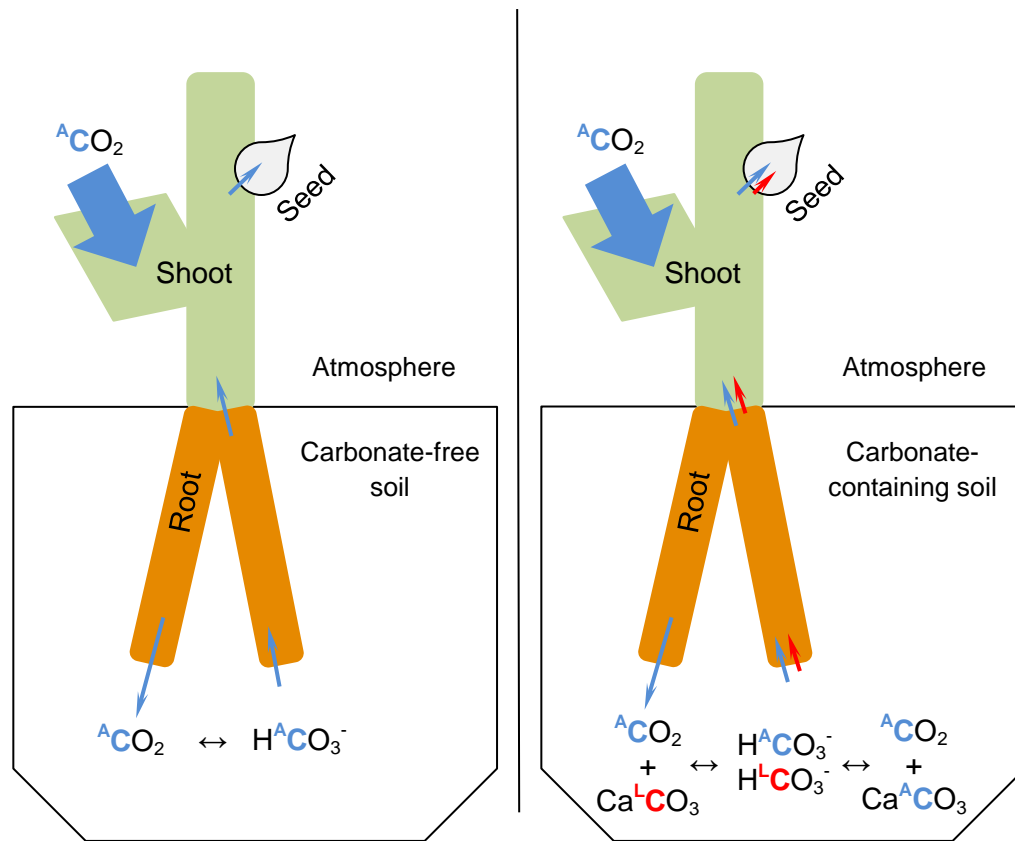


Figure 23: Dilution of ^{14}C content of plant organs by dissolved inorganic C (HCO_3^-) taken from 2 sources: In carbonate-free soils, the only source of HCO_3^- is dissolution of root- and rhizomicrobially-respired CO_2 originally from the atmosphere ($^{\text{A}}\text{CO}_2$). In carbonate-containing soils, the dissolution of lithogenic carbonates ($\text{Ca}^{\text{L}}\text{CO}_3$) is a second source. The HCO_3^- from root-respired CO_2 is diluted by the HCO_3^- from lithogenic carbonates (Kuzyakov et al., 2006; Gocke et al., 2011). For shoot-labeled plants, this process leads to a reduction of the ^{14}C activity in the re-absorbed HCO_3^- .

Since the incorporated C from soil carbonate is radiocarbon dead, this may lead to overestimations of radiocarbon ages based on biogenic carbonates (Goodfriend, 1987). Considering the total weight of C in fruit carbonates (8.08 mg C, based on 20 fruits) and the difference between HCO_3^- incorporation into fruit carbonate in Sand and Loess after shoot labeling

(0.012 mg C) ca. 0.15% of C in fruit carbonate - after 10 h labeling - originated from soil solution. The total HCO_3^- incorporated into the whole plant amounted to 1.6% of dry weight. However, fruit carbonate in Loess after shoot labeling showed 7.6% more HCO_3^- than in Sand (Table 7). Furthermore, extrapolating the 10 h labeling period to the full month of this study (420 h photoperiod) indicates around 6.3% of fruit carbonate in Loess is derived from lithogenic carbonates. A 6.3% share of lithogenic HCO_3^- leads to radiocarbon ages overestimated by 505 ^{14}C years (Eq. 6), based on fruit carbonate of Loess-grown *Buglossoides arvensis*.

In this connection, it is important to note that too old radiocarbon ages on fruit carbonate were reported in literature (Pustovoytov et al., 2004, 2010; Pustovoytov and Riehl, 2006). One of the ways to explain the discrepancy between an age measured on the carbonate fraction of fruits and the true age of the sample could be the uptake of inorganic carbon from the soil by root systems.

Regarding the suitability of fruit carbonate for dating purposes, an age overestimation of order of 500 ^{14}C years, though persistent with increasing sample age, becomes insignificant against the measurement uncertainties in relatively old samples (such as 11,000 y and older, i.e. after two ^{14}C half-lives).

Some of the other findings may also deserve particular attention. As expected, the distribution of C from soil CaCO_3 decreases with the distance of plant organs from the roots (Brix, 1990) (Table 7). The HCO_3^- distribution in plant organs has usually been attributed to passive uptake with transpiration flow (Stolwijk and Thimann, 1957; Amiro and Ewing, 1992). This means that HCO_3^- moves with water from roots towards stomata (Amiro and Ewing, 1992). However, the different ^{14}C activities in various organs following shoot labeling in Sand and Loess, arising from the dilution effect of lithogenic HCO_3^- , suggest the selective incorporation of HCO_3^- carbon in specific organs (Ford et al., 2007). After shoot labeling, there was 3.20 mg more labeled C in roots and shoots and 0.012 mg more labeled C in fruit carbonate of plants grown in Sand than of those in Loess (Table 7). At the same time, Sand-grown plants had 5.11 mg less labeled C in fruit organics. The higher difference indicates a higher dilution effect by soil carbonate and higher incorporation of HCO_3^- . Therefore, the highest HCO_3^- amount was retained in roots and shoots, followed by fruit carbonate, while fruit organics showed the lowest HCO_3^- incorporation. This may suggest some active uptake processes (Vuorinen et al., 1989; Ford et al., 2007) enhancing fruit carbonate compared to the fruit organics, since these components are the same distance from the roots. The apparent lower HCO_3^-

incorporated in Loess- compared to Sand-grown plants after root labeling, on the other hand, is partly due to substitution of added Na_2CO_3 -C with Loess CaCO_3 -C (Fig. 1) (Kuzyakov et al., 2006).

4.6. Conclusions

(1) *Buglossoides arvensis* takes up dissolved inorganic carbon (HCO_3^-) from the soil via roots under laboratory conditions. The source of HCO_3^- can be dissolution of carbonate minerals (radiometrically dead, e.g. loess carbonate) and dissolution of root-respired CO_2 (recent C) in soil solution.

(2) The HCO_3^- uptake is mostly passive; however, HCO_3^- can be preferentially incorporated into organs such as fruit carbonate, which are formed at specific plant development stages.

(3) The incorporated HCO_3^- taken up by roots may contribute more than 6.0% of fruit-carbonate C in plants growing on a carbonate-containing soil. Therefore, an age overestimation of ca. 500 years is possible. Inflated ages based on fruit carbonate can be attributed to HCO_3^- uptake by roots during fruit development. This calls for further investigation of possible effects of calcareous substrates on the outcome of ^{14}C -dating of the fruit carbonate fraction.

(4) The age overestimation because of lithogenic HCO_3^- incorporation in fruit carbonate however, is insignificant in relatively old samples, approximately after two ^{14}C half-lives.

4.7. Acknowledgements

We appreciate the German Research Foundation (DFG) for their support (KU 1184/34-1). We would like to thank Heike Strutz and Susann Enzmann for their help during labeling. Special thanks to Bernd Kopka and the staff in Labor für Radioisotope (LARI), university of Göttingen, to facilitate running the experiment and measuring ^{14}C in plant samples. We thank the seed collection of the botanical garden of University of Göttingen for *Buglossoides arvensis* fruits. Our sincere gratitude goes to Jeff Pigati, who provided many valuable suggestions on the first version of the manuscript. The authors are also thankful the two further anonymous reviewers for their helpful comments.

4.8. References

- Amiro B. D. and Ewing L. L. (1992) Physiological conditions and uptake of inorganic carbon-14 by plant roots. *Environ. Exp. Bot.* **32**, 203–211.
- Aylward G. H. (2007) *SI chemical data*. Auflage: 6. Auflage., John Wiley & Sons, Milton, Qld.
- Brix H. (1990) Uptake and photosynthetic utilization of sediment-derived carbon by *Phragmites australis* (Cav.) Trin. ex Steudel. *Aquat. Bot.* **38**, 377–389.
- Cramer M. D., Gao Z. F. and Lips S. H. (1999) The influence of dissolved inorganic carbon in the rhizosphere on carbon and nitrogen metabolism in salinity-treated tomato plants. *New Phytol.* **142**, 441–450.
- Cramer M. D. and Lips S. H. (1995) Enriched rhizosphere CO₂ concentrations can ameliorate the influence of salinity on hydroponically grown tomato plants. *Physiol. Plant.* **94**, 425–432.
- Cramer M. D. and Richards M. B. (1999) The effect of rhizosphere dissolved inorganic carbon on gas exchange characteristics and growth rates of tomato seedlings. *J. Exp. Bot.* **50**, 79–87.
- Ford C. R., Wurzburger N., Hendrick R. L. and Teskey R. O. (2007) Soil DIC uptake and fixation in *Pinus taeda* seedlings and its C contribution to plant tissues and ectomycorrhizal fungi. *Tree Physiol.* **27**, 375–383.
- Gocke M., Pustovoytov K. and Kuzyakov Y. (2011) Carbonate recrystallization in root-free soil and rhizosphere of *Triticum aestivum* and *Lolium perenne* estimated by ¹⁴C labeling. *Biogeochemistry* **103**, 209–222.
- Goodfriend G. A. (1987) Radiocarbon age anomalies in shell carbonate of land snails from semi-arid areas. *Radiocarbon* **29**, 159–167.
- Jahren A. H., Amundson R., Kendall C. and Wigand P. (2001) Paleoclimatic Reconstruction Using the Correlation in $\delta^{18}\text{O}$ of Hackberry Carbonate and Environmental Water, North America. *Quat. Res.* **56**, 252–263.
- Kuzyakov Y., Shevtsova E. and Pustovoytov K. (2006) Carbonate re-crystallization in soil revealed by ¹⁴C labeling: Experiment, model and significance for paleo-environmental reconstructions. *Geoderma* **131**, 45–58.
- Overstreet R., Ruben S. and Broyer T. C. (1940) The Absorption of Bicarbonate Ion by Barley Plants as Indicated by Studies with Radioactive Carbon. *Proc. Natl. Acad. Sci. U. S. A.* **26**, 688–695.
- Pelkonen P., Vapaavuori E. M. and Vuorinen H. (1985) HCO₃⁻ uptake through the roots in willow and sunflower and effect of HCO₃⁻ uptake on the productivity of willow cuttings. In *Energy from Biomass* (eds. W. Palz, J. Coombs, and D. O. Hall). 3rd E.C. Conference. Elsevier, London. pp. 417–421.
- Pigati J. S., Quade J., Shahanan T. M. and Haynes Jr. C. V. (2004) Radiocarbon dating of minute gastropods and new constraints on the timing of late Quaternary spring-discharge deposits in southern Arizona, USA. *Palaeogeogr. Palaeoclimatol. Palaeoecol.* **204**, 33–45.
- Pigati J. S., Rech J. A. and Nekola J. C. (2010) Radiocarbon dating of small terrestrial gastropod shells in North America. *Quat. Geochronol.* **5**, 519–532.
- Pustovoytov K. E., Riehl S. and Mittmann S. (2004) Radiocarbon age of carbonate in fruits of *Lithospermum* from the early Bronze Age settlement of Hirbet ez-Zeraqōn (Jordan). *Veg. Hist. Archaeobotany* **13**, 207–212.
- Pustovoytov K. and Riehl S. (2006) Suitability of biogenic carbonate of *Lithospermum* fruits for ¹⁴C dating. *Quat. Res.* **65**, 508–518.

Pustovoytov K., Riehl S., Hilger H. H. and Schumacher E. (2010) Oxygen isotopic composition of fruit carbonate in Lithospermeae and its potential for paleoclimate research in the Mediterranean. *Glob. Planet. Change* **71**, 258–268.

Quade J., Shanying L., Stiner M., Clark A. E. and Mentzer S. (2014) Radiocarbon Dating, Mineralogy, and Isotopic Composition of Hackberry Endocarps from the Neolithic Site of: Asikli Höyük, Central Turkey. *Tree-Ring Res.* **70**, 17–25.

Stolwijk J. A. J. and Thimann K. V. (1957) On the Uptake of Carbon Dioxide and Bicarbonate by Roots, and Its Influence on Growth. 1. *Plant Physiol.* **32**, 513–520.

Viktor A. and Cramer M. D. (2005) The influence of root assimilated inorganic carbon on nitrogen acquisition/assimilation and carbon partitioning. *New Phytol.* **165**, 157–169.

Viktor A. and Cramer M. D. (2003) Variation in root-zone CO₂ concentration modifies isotopic fractionation of carbon and nitrogen in tomato seedlings. *New Phytol.* **157**, 45–54.

Vuorinen A. H., Vapaavuori E. M. and Lapinjoki S. (1989) Time-course of uptake of dissolved inorganic carbon through willow roots in light and in darkness. *Physiol. Plant.* **77**, 33–38.

Wang Y., Jahren A. H. and Amundson R. (1997) Potential for 14C Dating of Biogenic Carbonate in Hackberry (Celtis) Endocarps. *Quat. Res.* **47**, 337–343.

5. Curriculum Vita

Kazem Zamani

Dept. of Soil Science of Temperate Ecosystems
Georg-August University of Göttingen
37077 Göttingen, Germany
Phone: +49 551 39 12104
kzamani@gwdg.de
www.uni-goettingen.de/pgz



-
- 09-10.2016: Visiting student, University of Washington, Seattle, USA
- Determining formation temperatures of carbonate types from Nussloch paleosols-loess sequence with measuring clumped isotopes ($T_{\Delta 47}$)
- 06.2016: Summer school in Pieve Tesino, Trentino, Italy
- Workshops participation with focus on soil properties and soil processes in mountain ecosystems
 - Field trip, soil profile description and discussion about soil genesis processes and classification based on World Reference Base (WRB)
- Since April 2014:* Ph.D. candidate, Dept. of Soil Science of Temperate Ecosystems, University of Göttingen, Germany
Topic: Recrystallization of pedogenic and biogenic carbonates in soil: environmental controls, modelling and relevance for paleoenvironmental reconstructions
- Isotope labeling of soils and plants with ^{13}C and ^{14}C to trace the fate of organic and inorganic carbon in soil
 - ^{14}C labeling of carbonate-containing materials e.g. mollusk shells in soil to investigate the dynamics of recrystallization and consequences for dating and paleoenvironment reconstructions
- 2011-2014: Employed in non-academic professions (Writing research proposal for DFG; KU 1184/34-1)
- 2010-2011: Visiting researcher, Institute of Systematic Botany and Ecology, University of Ulm, Germany
- Investigating the effects of land-use and land-use change on soil quality parameters (physical, chemical and biological properties), soil CO_2 efflux as well as carbon sequestration
- 2009-2010: Research assistance, Department of Soil Science, University of Tehran, Iran
Topic: Effect of land-use change on soil carbon dynamics and soil quality
- 2006-2009: Lecturer and assistant teaching at University of Vali-e-Asr, Rafsanjan, Iran
- Courses for BSc. students: Fundamental of soil science, Soil genesis and classification, Soil quality and land evaluation

- 2003-2006: MSc. Student, Department of Soil Science, University of Tehran, Iran
 Master thesis: The study of formation mechanisms of petrocalcic horizons on *Fashand* alluvial deposits, North Central Iran
- Soil profiles description in the field, soil sampling for physical and chemical analyses, preparation and analyzing of soil thin sections (polarizing microscope), recognizing dominant soil formation mechanisms, classification of soils based on Soil Taxonomy and World Reference Base (WRB)
 - Extraction of soil clay fraction, pretreatments, analyzing with X-Ray instrument and description of X-Ray diffractograms
- 1999-2003: BSc. Student, Department of Soil Science, University of Guilan, Iran
 Bachelor thesis: Estimation of chloride concentration based on electrical conductivity measurements in some saline soils of *Amir-Abad*, Damghan, Iran
- Soil sampling in the field, analyzing electrical conductivity (EC) and Chloride concentration, presenting equation to estimate chloride concentration and toxicity in saline soils of the region based on an easily measurable parameter (i.e. EC)

Funded projects (assistance in writing):

- Recrystallization of pedogenic and biogenic carbonates in soil: environmental controls, modelling and relevance for paleoenvironmental reconstructions, German Research Foundation (DFG) (KU 1184/34-1)
- Carbonate clumped isotopes, German Academic Exchange Service (DAAD), PPP USA 1j ab 16, Application contract: 57211165
- Paleoenvironmental constraints from paleosols-loess sequences: evaluating clumped (Δ_{47}) isotopic records in biogenic and pedogenic carbonates, Quaternary Research Center, University of Washington

Grants and fellowships

- Research at University of Washington, Seattle, USA (01.09.-31.10.2016) provided by the German Academic Exchange Service (DAAD) (PPP mit USA 1j ab 16, Application contract: 57211165).
- Summer school in Pieve Tesino, Trentino, Italy (26-30 June 2016) granted by the COST Action ES1203 (EU Framework Programme)
- Congress Travel Grant to European Geosciences Union (EGU) General Assembly (17-22 April 2015), Vienna, Austria, donated by Georg-August University of Göttingen

Qualifications:

Languages: Persian (Mother language), English (good), German (good)

Computer skills: SigmaPlot and Statistica (statistic softwares), Photoshop, Initial knowledge of R and ArcGIS

Publications:

- Zamanian Kazem, Konstantin Pustovoytov and Yakov Kuzyakov, (2016) Cation exchange retards shell carbonate recrystallization: Consequences for dating and paleoenvironmental reconstructions, *Catena*, 142: 134-138
- Zamanian Kazem, Konstantin Pustovoytov and Yakov Kuzyakov, (2016) Pedogenic carbonates: Forms and formation processes, *Earth-Science Reviews*, 157: 1-17
- Zamanian Kazem, Konstantin Pustovoytov and Yakov Kuzyakov, (2016) Recrystallization of shell carbonate in soil: ^{14}C labeling, modeling and relevance for dating and paleo-reconstructions, *Geoderma*, 282: 87-95
- Zamanian Kazem, Konstantin Pustovoytov and Yakov Kuzyakov, (2017) Carbon sources in fruit carbonate of *Buglossoides arvensis* and consequences for ^{14}C dating, *Radiocarbon*, 59: 141-150

Conference participations

- Zamanian Kazem, Konstantin Pustovoytov and Yakov Kuzyakov, (2015) Recrystallization of biogenic carbonates in soils: consequences for paleo-reconstruction and carbon dating studies, European Geoscience Union (EGU), Vienna, Austria (Poster)
- Werth Martin, Kazem Zamanian, (2011), Ammonia efflux affects accuracy of CO₂ emission estimated by alkali-trap method, Jahrestagung der Deutschen Bodenkundlichen Gesellschaft, Berlin, Germany (Poster)
- Zamanian Kazem, Ahmad Heidari and Shahla Mahmoudi, (2009), Micromorphological and SEM evidences of calcified roots at the upper layer of petrocalcic horizon, 11th Iranian Soil Science Congress, Gorgan, Iran (Poster)
- Zamanian Kazem, Shahla Mahmoudi and Ahmad Heidari, (2008), Micromorphological evidences of residual petrocalcic horizon from arid region in Fashand watershed (North Central Iran), 13th ICSM (International Conference of Soil Micromorphology), Chengdu, China (Oral)
- Zamanian Kazem, Ahmad Heidari and Shahla Mahmoudi, (2008), Pedogenic barite in petrocalcic horizons in soils from Fashand region (North Central Iran), 13th ICSM, Chengdu, China (Oral)
- Zamanian Kazem, Shahla Mahmoudi and Ahmad Heidari, (2003), Investigation on the mechanisms of Petrocalcic horizon formation in soils of Fashand region, 9th Iranian Soil Science Congress, Karaj, Iran (oral)

6. Declaration

**Declaration by the doctoral candidate
at the Georg-August-Universität Göttingen**

(Surname, First Name): Zamani, Kazem

(Country / Postcode / Place): Büsgenweg 2, 37077 Göttingen

I intend to produce a dissertation on the topic of: "Recrystallization of pedogenic and biogenic carbonates in soil: Environmental controls, modelling and relevance for paleoenvironmental reconstructions and dating" at Georg-August-Universität Göttingen.

In this, I shall be supervised by Prof. Dr. Yakov Kuzyakov

I submit the following declaration:

1. The opportunity for the existing doctoral project was not made commercially available to me. Especially, I have not engaged any organization that seeks thesis advisers against a fee for the preparation of dissertations or performs my obligations with respect to examination components entirely or partly.
2. I have until now and shall in future accept the assistance of third parties only in a scope that is scientifically justifiable and compliant with the legal statutes of the examinations. I shall specifically complete all parts of the dissertation myself; I have neither, nor will I, accept unauthorized outside assistance either free of charge or subject to a fee.

Furthermore, I am aware of the fact that untruthfulness with respect to the above declaration repeals the admission to complete the doctoral studies and/or subsequently entitle termination of the doctoral process or withdrawal of the title attained."

.....
(Place and date)

.....
(Signature)



Georg-August-Universität Göttingen
Graduiertenschule Forst- und Agrarwissenschaften (GFA)

Recrystallization of pedogenic and biogenic carbonates in soil:

Environmental controls, modelling and relevance for
paleoenvironmental reconstructions and dating

Dissertation zur Erlangung des akademischen Grades

Doctor of Philosophy (Ph.D.)

der Fakultät für Agrarwissenschaften der Georg-August-Universität Göttingen

vorgelegt von

Kazem Zamaniān

geboren am Februar 1981 in Gonabad, Iran

Göttingen, May 2017